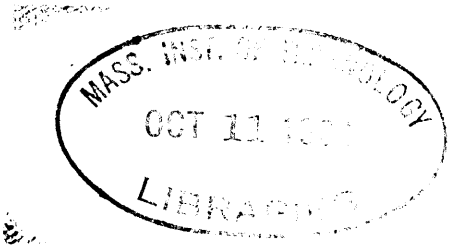

THE FRICTIONAL CHARACTERISTICS OF WESTERLY GRANITE

by

JAMES DOUGLAS BYERLEE

BSc. (Hon. Geol.) Queensland University
(1963)

SUBMITTED IN PARTIAL FULFILLMENT OF THE

REQUIREMENTS FOR THE DEGREE OF

DOCTOR OF PHILOSOPHY

at the

MASSACHUSETTS INSTITUTE OF TECHNOLOGY

June 1966

Signature of Author.....
Department of Geology and Geophysics,
May 13, 1966

Certified by.....
Thesis Supervisor

Accepted by.....
Chairman,
Departmental Committee on Graduate Students

ABSTRACT

Title: The Frictional Characteristics of Westerly Granite.

Author: James D. Byerlee.

Submitted to the Department of Geology and Geophysics May 13, 1966 in partial fulfillment of the requirements for the degree of Doctor of Philosophy at the Massachusetts Institute of Technology.

In contrast to metals, the static coefficient of friction, μ, of granite and quartz is strongly dependent on surface roughness. μ ranges from 0.2 for finely ground surfaces up to 0.6 or more for rough surfaces. The nature of the loose wear particles on the surface after sliding and the increase in the frictional force with normal load on surfaces with a fixed real area of contact suggests that brittle fracture rather than plasticity may be the controlling mechanism during frictional sliding of these and possibly other brittle materials. The effect of roughness reported here may explain the differences between μ of rocks and minerals which have been widely observed.

A theory of friction is presented which may be more applicable for geologic materials than the classic Bowden and Tabor theory. In the model, surfaces touch at the peaks of asperities, and sliding occurs when the asperities fail by brittle fracture. The coefficient of friction can be calculated from the strength of asperities of certain ideal shapes; for cone-shaped asperities μ is about 0.1 and for wedge-shaped asperities, μ is about 0.15, independent of the strength of the material. These values are close to those observed for polished surfaces of brittle minerals. If surface forces are present, the theory predicts that μ should decrease with load and that it should be higher in a vacuum than in air. Both these effects have been reported elsewhere. The effect of a fluid film between sliding surfaces is also predicted; μ should depend on the area of surfaces in contact. This effect has also been observed for sliding of quartz on quartz in the presence of water. At high confining pressure the contribution of the surface tension forces to μ are negligible. At very high loads the asperities become jammed together and the friction is a function of the strength of the material.

At a pressure of one kilobar μ for rocks sliding on shear surfaces is decreased by about ten percent if water is present. This is because the strength of brittle materials is dependent on the environment.

At high confining pressure μ for granite depends on the relative displacement of the surfaces. For ground surfaces μ reaches a maximum after about 0.1 cm and then decreases to nearly a constant value after 0.5 cm of sliding has occurred. Features on the surfaces after sliding suggest that the maximum μ is reached when intimate contact is first established. If this is correct then the initial μ for perfectly mated surfaces should be the same as the maximum μ for ground surfaces. Experimentally this was found to be correct. The decrease in μ from the maximum is caused by an accumulation of loose wear particles between the surfaces. μ decreases with an increase in the normal stress. This is because the interlocking irregularities on the surfaces have a finite shear strength when the normal stress is zero. Up to the highest pressures investigated movement between the sliding surfaces took place by violent stick-slip.

Results of the theoretical and both the low and high pressure experimental studies are correlated and applied to a number of geologic and geophysical problems. For sliding on fracture and possibly joint surfaces in granite, μ may be as high as 1.3 and as low as 0.1 for polished fault surfaces. For small shear displacements between the walls of Griffith cracks μ should be about 0.1, but for larger displacements μ may reach values as high as 1.0 or greater. Up to very high confining pressures it is easier to slide on old faults than to create new ones, so that in active tectonic regions movement within the crust should be confined to pre-existing faults. Stick-slip motion along a pre-existing fault may be a simple explanation for the seismic source mechanism of crustal earthquakes. The "brittle-ductile" transition pressure in rocks may simply be the pressure at which the frictional shear strength is equal to the fracture shear strength. In the Coulomb-Navier theory it is assumed that the strength of a rock is determined by μ and the cohesive strength. The theory does not hold for Westerly granite.

Thesis Supervisor: William F. Brace

Title: Associate Professor of Geology

TABLE OF CONTENTS

LIST OF FIGURES

LIST OF TABLES

INTRODUCTION

Friction plays an important role in the Coulomb-Navier criterion of rock fracture (Jaeger, 1962, p. 76), the modified Griffith theory of fracture (McClintock and Walsh, 1962), the Young's modulus of rocks (Walsh, 1965a), the Poisson's ratio of rocks (Walsh, 1965b), the indentation hardness of rocks (Brace, 1960) and the attenuation of seismic waves (Walsh, 1966).

In spite of the importance of friction we have a very poor understanding of just what determines the coefficient of friction in a particular geological situation. We can not predict within a factor of two the coefficient of friction on a fault, on a Griffith crack or on a grain boundary. It is not clear how pressure effects the coefficient of friction or how the coefficient of friction changes with displacement. No theory of friction is available other than that of Bowden and Tabor (1958) which is based on microscopic processes which do not seem reasonable for rocks.

One of the interesting results of previous work is that the coefficient of friction of rough rock surfaces at high confining pressure is about 0.8 (Jaeger, 1959), whereas it is between 0.1 and 0.2 for polished mineral surfaces at low loads (Horn and Deere, 1960). This is puzzling because rocks are polycrystalline aggregates of minerals.

There are two possible explanations for the apparent difference in friction between rocks and minerals. These are the effect of load and surface roughness. In this study both these possibilities have been investigated.

Part I is a description of the experiments carried out to study the effect of roughness on the friction of Westerly granite and quartz. Westerly granite was chosen because its other physical properties have been studied in detail (Paulding, 1965, Brace, 1965 and Brace, Orange and Madden, 1965). It was found that the friction of granite increases with roughness, but the friction of metals is almost independent of roughness (Rabinowicz, 1965, p. 97). This suggests that there may be some fundamental difference between the behavior of rocks and metals during frictional sliding. The obvious difference between the two classes of materials is that rocks are brittle whereas metals deform plastically. This observation

prompted a theoretical investigation of what effect this would have on friction. Part II is devoted to the development of a theory of brittle friction.

Part III is a description of the frictional behavior of Westerly granite under high confining pressure. At high pressure the friction was found to depend on relative displacement of the surfaces. This characteristic was studied in detail using ground surfaces of different roughnesses and perfectly mating surfaces. In addition, the fracture strength of Westerly granite and the friction for sliding on the newly created shear surface was determined up to a confining pressure of about 11 kb.

In Part IV the results from this study have been applied to several geologically important phenomena such as the mechanics of faulting, the apparent ductility of silicate rocks at high confining pressure and the earthquake source mechanism.

PART I

EFFECT OF SURFACE ROUGHNESS ON THE FRICTION OF GRANITE AND QUARTZ

Summary

In contrast to metals, the static coefficient of friction, μ, of granite and quartz is strongly dependent on surface roughness. μ ranges from 0.2 for finely ground surfaces up to 0.6 or more for rough surfaces. The nature of the loose wear particles on the surface after sliding and the increase in the frictional force with normal load on surfaces with a fixed real area of contact suggests that brittle fracture rather than plasticity may be the controlling mechanism during frictional sliding of these and possibly other brittle materials.

The effect of roughness reported here may explain the differences between μ of rocks and minerals which have been widely observed.

Introduction

The friction of brittle material differs in many respects from that of ductile material. For example, static coefficient of friction, μ, of most metals at room temperature is 1 (Bowden and Tabor, 1960, p. 145), whereas μ for finely ground surfaces of quartz or sapphire is around 0.1. Or, coefficient of friction of typical ductile materials is independent of load (Bowden and Tabor, 1958, p. 99), whereas for brittle materials it is markedly load dependent (Bowden and Tabor, 1964, p. 169). These differences in behavior suggest that other characteristics of frictional behavior of ductile materials might not pertain to brittle substances. Among these is the effect of surface roughness; again, for ductile materials, μ is nearly independent of surface roughness (Rabinowicz, 1965, p. 61).

A few exploratory studies have been reported in the literature of frictional behavior of rocks (Jaeger, 1959; Maurer, 1965; Raleigh and Paterson, 1965; Handin and Stearns, 1964), and single crystals of rock forming minerals (Penman, 1953; Tschebotarioff and Welch, 1948; Rae, 1963; Horn and Deere, 1962). Many of these materials are

brittle, that is, they fracture rather than flow plastically under conditions of the friction experiments. One of the interesting results of these studies is that coefficient of friction of rock surfaces is typically 0.6 to 1.0, whereas μ of minerals is 0.1 to 0.2. This is puzzling because rocks are polycrystalline aggregates of minerals. One possible explanation of this difference is the effect of surface roughness; in experiments with rocks, surfaces are typically ground, whereas polished surfaces of minerals or smooth cleavage surfaces are often selected for study. In order to test this possibility, experiments were designed to determine how friction of a brittle material is affected by roughness. Some results for granite and quartz are summarized in this note.

Experimental Procedure

Materials.

The rock selected for study was a rather typical although somewhat fine-grained granite, the chemical, mechanical and electrical properties of which have been extensively studied (Fairbairn et al 1951; Brace, 1965; Brace, Orange and Madden, 1965). The source was Westerly, R.I. The granite (Figure 1) had an average grain size of 0.75 mm and consisted of four phases: 35% microcline,

31% plagioclase, 28% quartz and 6% biotite. The first three are hard, brittle silicates; slip (and therefore plastic flow) probably can be produced in these materials but to judge from quartz, only under extremely high temperature and confining pressure (Griggs, Turner and Heard, 1960). Slip in these materials under room temperature and pressure is almost certainly ruled out. The fourth material, biotite, is a magnesian mica; slip in the basal plane can be produced at room temperature (Mugge, 1898).

The quartz used here came from a large single crystal from Minas Gerais, Brazil.

Apparatus

The measurements of friction were made in a device which incorporated an 8 inch Atlas bench lathe. The essential features of the device are indicated in Figure 2. The specimen, S, was a precisely ground cylinder. Two such specimens, each of the same material and roughness were placed end to end in an experiment and tangential force, F, was measured as normal force, N, was held constant. The specimens were gripped in specimen holders, SH, which were in turn held in the upper and lower arms, A. Specimen holders were clamped in such a way that the sliding surfaces of the specimens remained parallel. The

upper arm was attached rigidly to the bed plate and the lower moving arm to the carriage of the lathe. Normal force on the specimen was applied by raising the lower arm by a vertical slide attachment on the lathe carriage. Both arms were enclosed in a vacuum chamber, the flexibility for the movement of the lower arm being obtained by the use of bellows. All of the experiments were done in an atmosphere of dry air, obtained by evacuating the chamber and then admitting room air through a column of calcium sulphate.

A normal load range of 5 to 50 kg was available. Normal and tangential forces were measured by load cells built into the lower and upper arms. Constant sliding velocity of 0.02 mm/sec was maintained by the lathe screw drive.

Specimens were 16 mm in diameter and 25 mm long and were prepared from a large block of granite or quartz. Two types of surface were prepared for the friction measurements: (a) plane, ground surface and (b) more or less plane, totally interlocking surface.

The ground surfaces were produced on a reciprocating surface grinder; roughness was controlled by the grit size of the wheel and the horizontal and vertical feeds of the table. There was an upper limit to the roughness

of the surfaces that could be produced with the grinding wheels available and so a very rough surface was prepared by hand grinding on a plate glass. The flatness of the surfaces and the average asperity height was found with a Talysurf 4 profilometer. The out-of-flatness across the surface was held in all cases to a value less than the average asperity height. The grinding data and the roughness of the surfaces used in the experiments are given in Table 1.

Totally interlocking surfaces were prepared as follows. A cylindrical specimen (Figure 3a) was grooved circumferentially with a thin diamond saw (Figure 3b). The specimen was then broken through the groove by applying bending moments to the ends (Figure 3c). The two ends were then mounted in the machine in such a way that the two fracture surfaces mated perfectly (Figure 3d). The asperity height on a fracture surface such as this probably ranged up to about $\frac{1}{2}$ mm. Although the fracture surface was somewhat wavy, departure from a plane was not much greater than $\frac{1}{2}$ mm (Figure 4).

Observations

In all of the experiments, both with ground and with interlocking surfaces, frictional sliding was accompanied by distinct stick-slip. After the first stick-slip,

tangential force increased slightly for the finely ground surfaces and decreased somewhat for the rough and the interlocking surfaces. Only the force to cause first motion is recorded here because with subsequent motion there was damage to the surfaces and roughness changed. The surfaces contained a fine white debris after a friction experiment; the amount of debris and the size of the particles increased with the roughness. Under the microscope this debris, which could be dusted from the surface, was found to contain angular fragements of the quartz, feldspar and mica. The larger pieces could be readily identified and showed no evidence under polarized light of plastic flow but a minor amount of plastic deformation can not be completely ruled out. There was a wide range of grain size in this debris, which seemed in most respects identical with material which would be obtained by crushing the granite in a mortar and pestle. The wear particles were similar to those shown in Figure 22, Part III.

Three measurements of normal and tangential force were made at several values of normal force, N, on freshly ground surfaces. Results for two different area of contact are shown in Figure 5. As there appeared to be no dependence of μ on apparent area of contact, all the other measurements were made for an apparent area of 1.97 cm^2. Results for the different roughnesses are

shown in Figure 6: the mean of three measurements at each load is given.

Measurements of friction were made on cylinders of quartz, cut parallel with the c-axis, for one roughness (50 $\pm$ 10 micro inch). Results for various loads are shown in Figure 7.

For the totally interlocking surfaces (Figure 3) tangential force at a given normal force varied with apparent area of contact. Three areas were used and three measurements made at each load. The mean of the three measurements of force was reduced to <u>stress</u> and these values of normal and shearing stress are plotted in Figure 8. When reduced to stress the area dependence disappeared, and the points appeared to fall close to two lines; if we assume that ratio of shearing to normal stress gives coefficient of friction, μ , then for the interlocking surfaces,

$$\mu = 1.3 \qquad \text{if } \sigma_n < 0.06 \text{ kb}$$

$$\mu = 0.8 + 0.03/\sigma_n \qquad \text{if } 0.06 < \sigma_n < 0.15 \text{ kb}$$

where σ_n is normal stress (compression is positive).

Discussion

The results for ground surfaces of granite are summarized in Figure 8, which shows the relation of μ to roughness. μ increases from about 0.2 for surfaces of very low roughness to about 0.6 for the roughest surface. These results are not strictly comparable with the values for totally interlocking surfaces because of the differences in degree of interlocking, and ratio of asperity size to sample size, but μ for ground surfaces seem to be approaching the value of 0.8 which is the limiting value for the interlocking case.

Dependence of μ on roughness is also shown by quartz. The value of 0.5 found here for a rough surface (Figure 9) contrasts strikingly with the value of 0.1 to 0.2 typically found for polished surfaces (Horn and Deere, 1962; Penman, 1953; Tschebotarioff and Welch, 1948). Polished surfaces of single or polycrystalline calcite have a value of μ between 0.1 and 0.2 (Horn and Deere, 1962; Tschobarioff and Welch, 1948; Rae, 1963), but limestone, a polycrystalline calcite has values of 0.5 to 0.75 (Jaeger, 1959; Handin and Stearns, 1964; Rae, 1963) for rough surfaces. These observations suggest that this dependence on roughness is typical for brittle materials.

Very finely ground surfaces of metals do show a dependence on roughness but the effect is either very small or opposite to that found here. A typical result (Rabinowicz, 1965) is shown in Figure 10 for copper.

Thus, it seems fairly clear that metals behave quite differently than granite, quartz, calcite and perhaps other brittle material as well, with regards roughness. This suggests that there is a fundamental difference between the behavior of metals and brittle materials during sliding. The difference probably has to do with role the asperities play. Several observations suggest that the asperities are brittle in granite or quartz and that there is limited small-scale plasticity as assumed in the Bowden and Tabor model of sliding of metals. For one thing, the character of the wear particles with granite or quartz suggest that asperities have fractured. Also surfaces almost never adhere even after sliding under extremely high normal stress.

Behavior of the interlocking surfaces also suggests underlying differences between metals and granite or quartz. For surfaces with completely interlocking asperities, area of contact is independent of normal load. For metals, yield strength is usually assumed constant in friction models so that frictional force for complete

interlocking would be independent of normal force. The shear strength of brittle materials however is strongly dependent on confining pressure, so that here, frictional force ought to increase with normal load. This is clearly true for granite (Figure 8) beyond 0.06 kb. At lower normal stresses the surfaces lift over the interlocking irregularities but when the normal stress reaches 0.06 kb it is easier for the surfaces to slide by breaking through the asperities. Beyond this stress the slope of the straight line through the points represents the rate of change of the shear strength as the normal stress is increased. This behavior is put forward as further evidence that brittle fracture may be the controlling mechanism on the scale of the asperities during sliding of brittle materials.

FIGURE CAPTIONS

Figure

1 Photomicrograph of Westerly granite. Large crystals with lamella twinning are plagioclase, crystals with cross-hatched twinning are microcline, clear crystals are quartz, lathlike crystal in the center of the figure is biotite. Average grain size of the rock os 0.75 mm.

2 Low load friction apparatus. See text for explanation.

3 Method of preparing mated surfaces. See text for explanation.

4 Cross section of one half of a fracture surface represented schematically in Figure 3c,d. (Smallest scale division is 1 mm). Fracture surface shown between vertical bars.

5 Tangential force versus normal force for ground surfaces of Westerly granite. CLA roughness 63±15 microinch.

6 Tangential force versus normal force for ground surfaces of Westerly granite (five roughnesses).

7 Tangential force versus normal force for ground surfaces of quartz. CLA roughness 50±10 microinch.

8 Shear stress versus normal stress for mated surfaces of Westerly granite.

9 Coefficient of friction versus CLA roughness for ground surfaces of Westerly granite.

10 Coefficient of friction versus RMS roughness for surfaces of copper. (After Rabinowicz, 1965).

FIG. 1

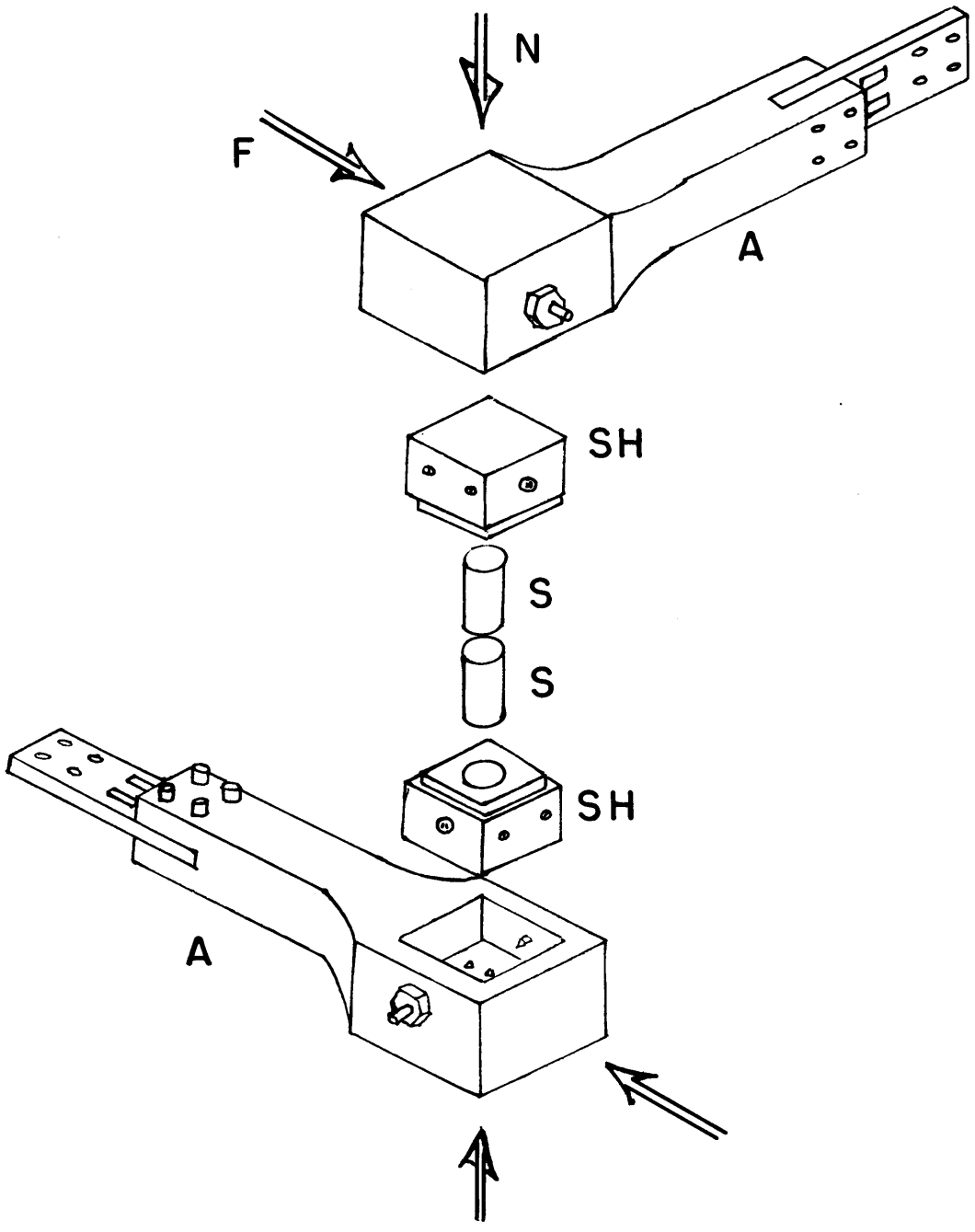

FIG. 2

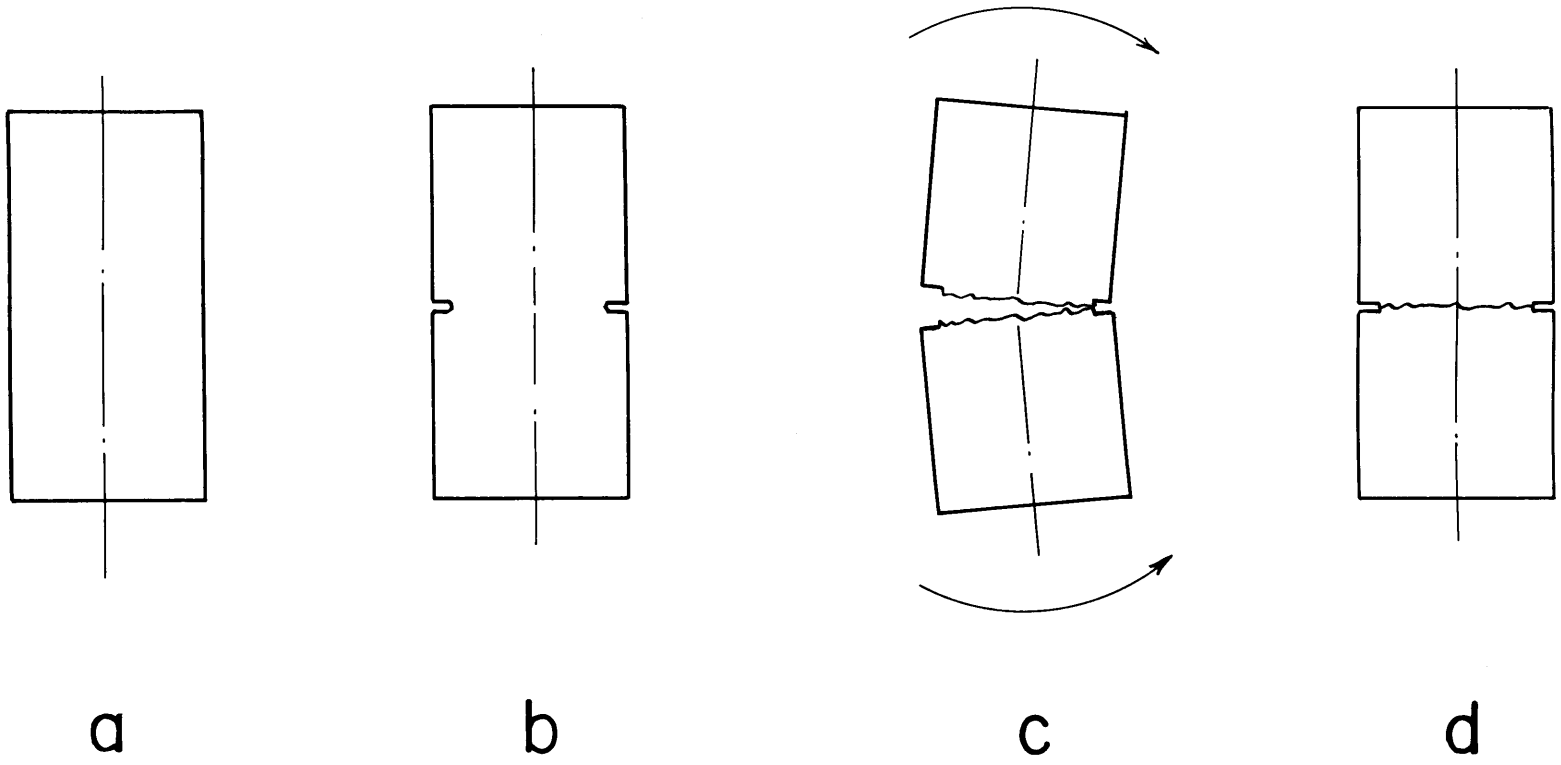

FIG.3

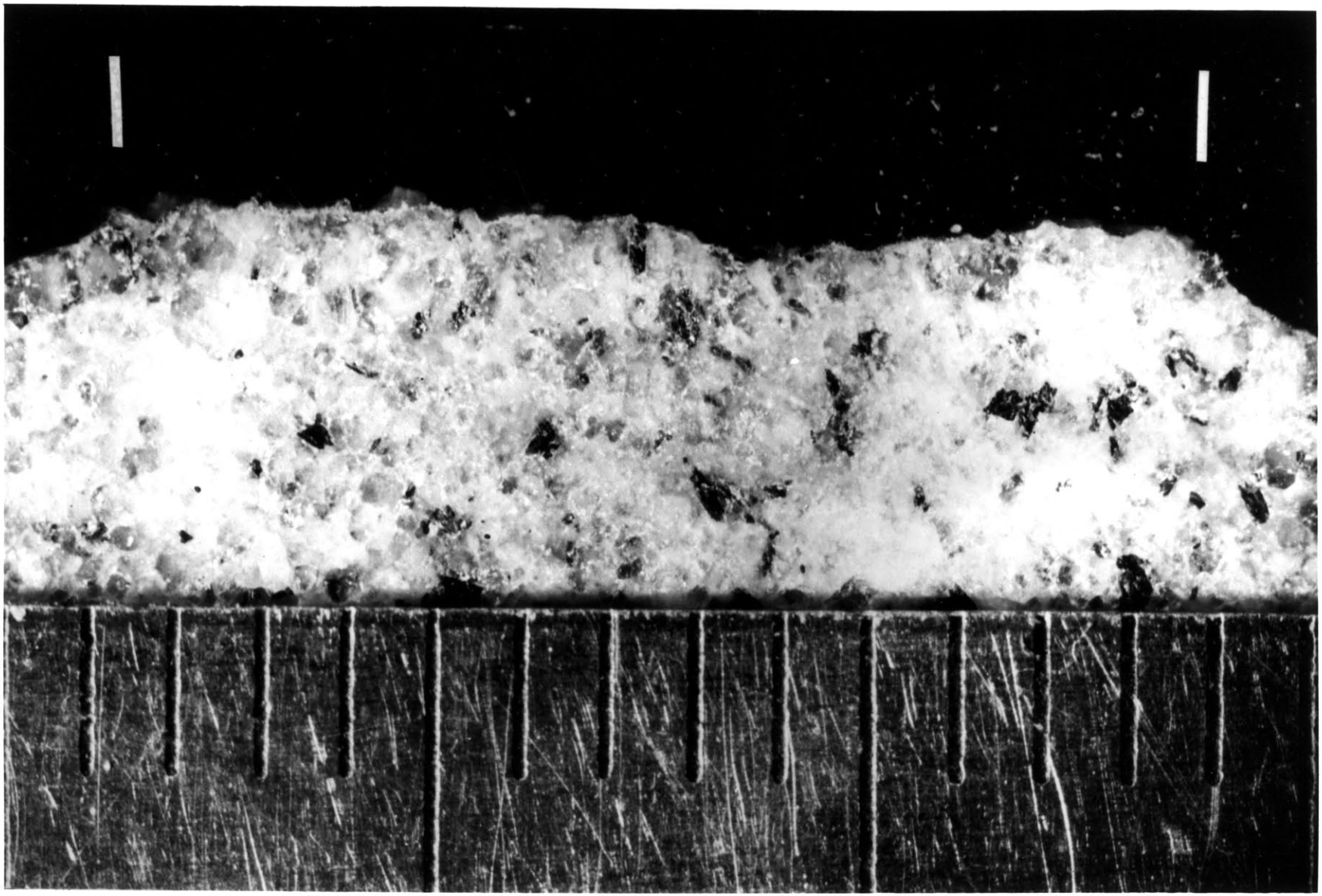

FIG. 4

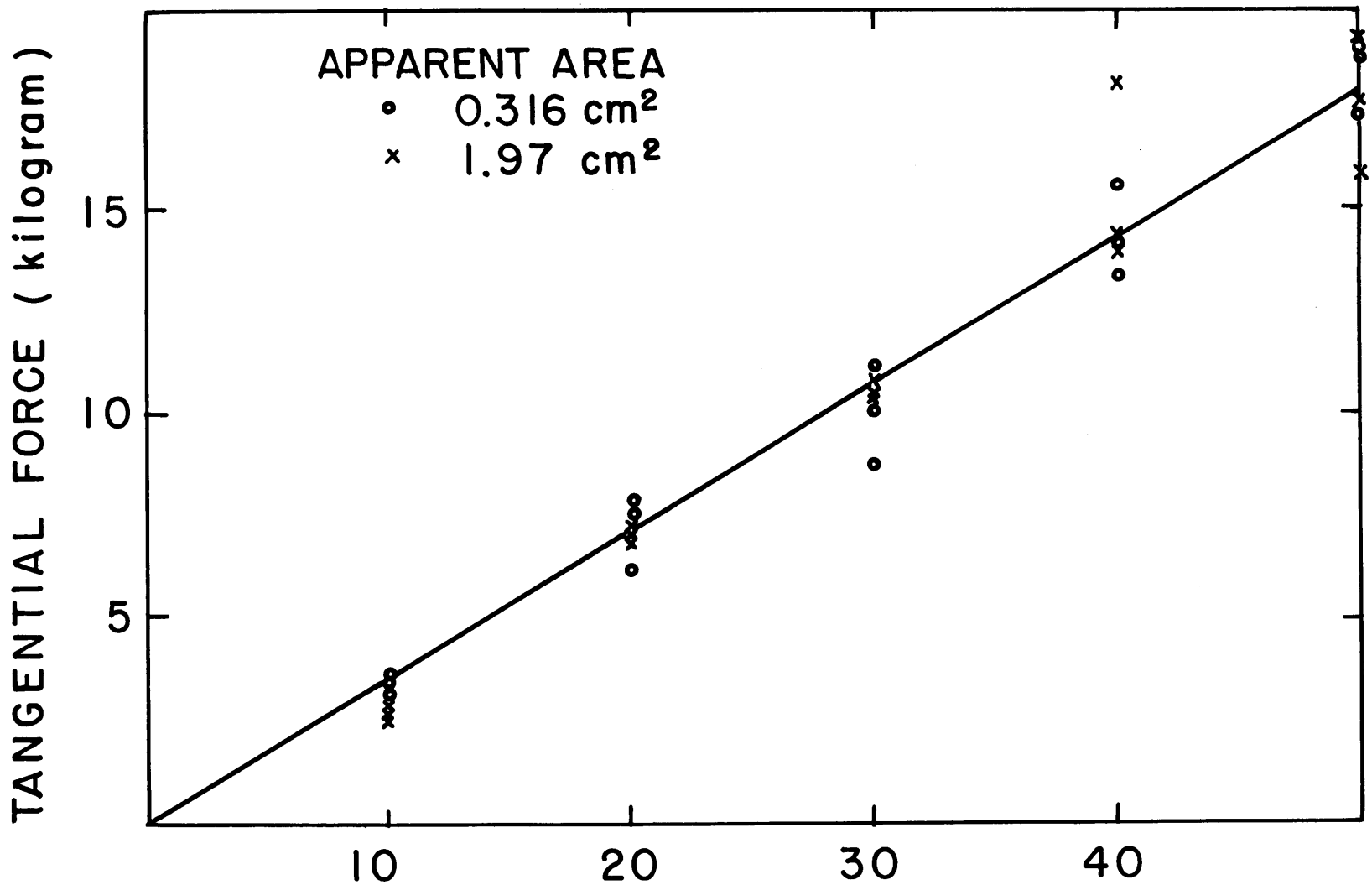
APPARENT AREA
o 0.316 cm²
x 1.97 cm²
TANGENTIAL FORCE (kilogram)
15
10
5
10
20
30
40
NORMAL FORCE (kilogram)

FIG. 5

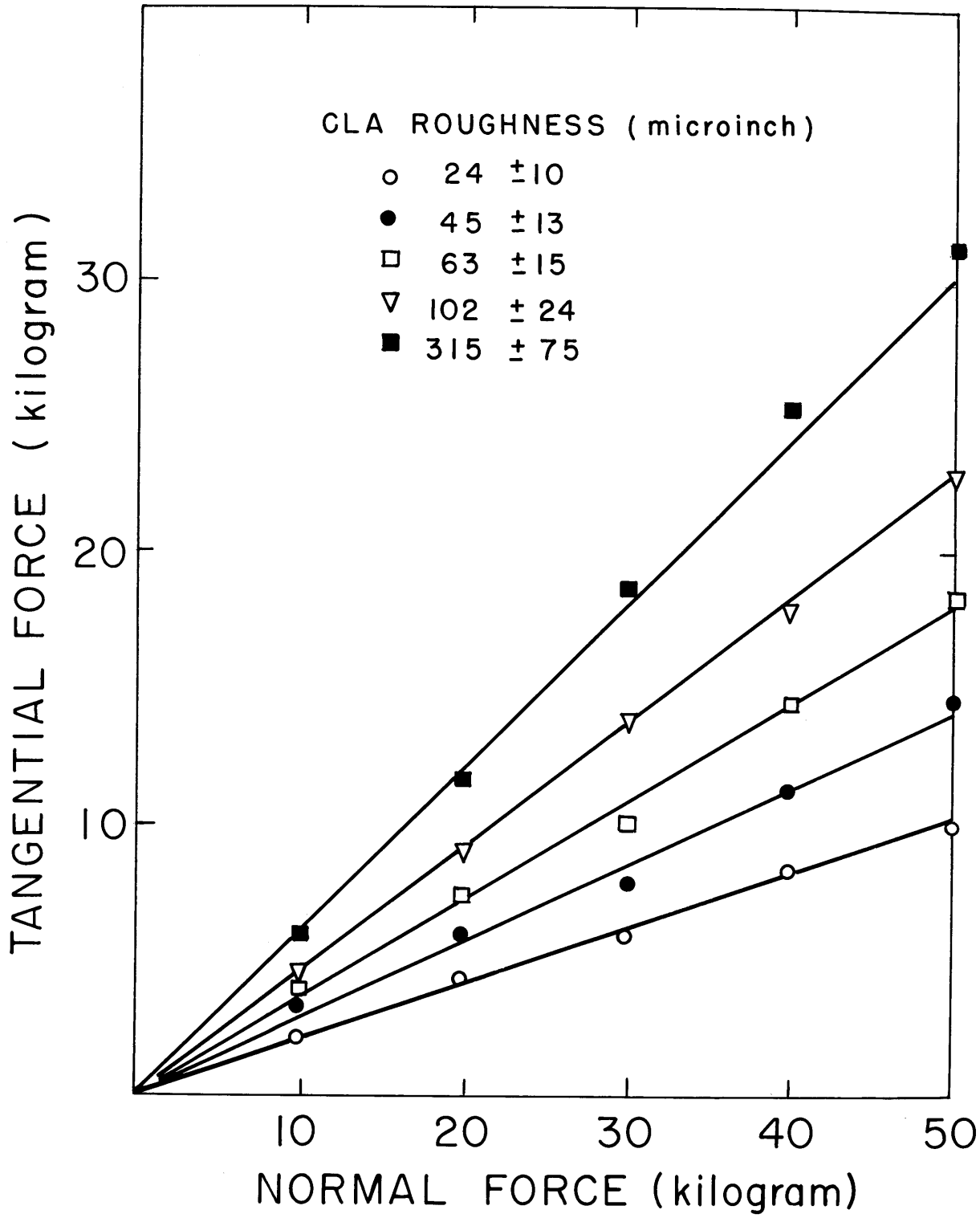
CLA ROUGHNESS (microinch)
24 ±10
45 ±13
63 ±15
102 ±24
315 ±75
TANGENTIAL FORCE (kilogram)
10
20
30
10
20
30
40
50
NORMAL FORCE (kilogram)

FIG. 6

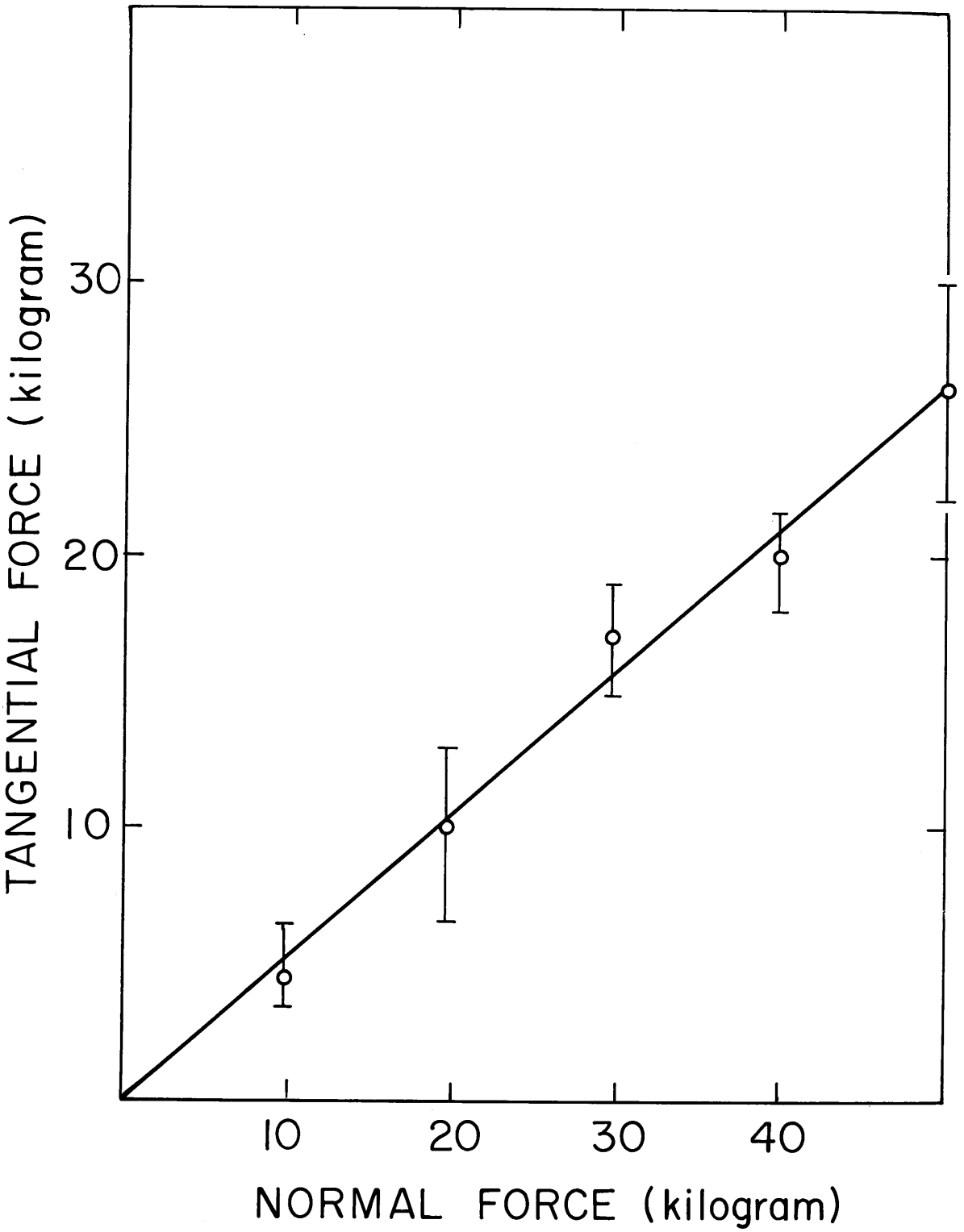
TANGENTIAL FORCE (kilogram)
30
20
10
10
20
30
40
NORMAL FORCE (kilogram)

FIG. 7

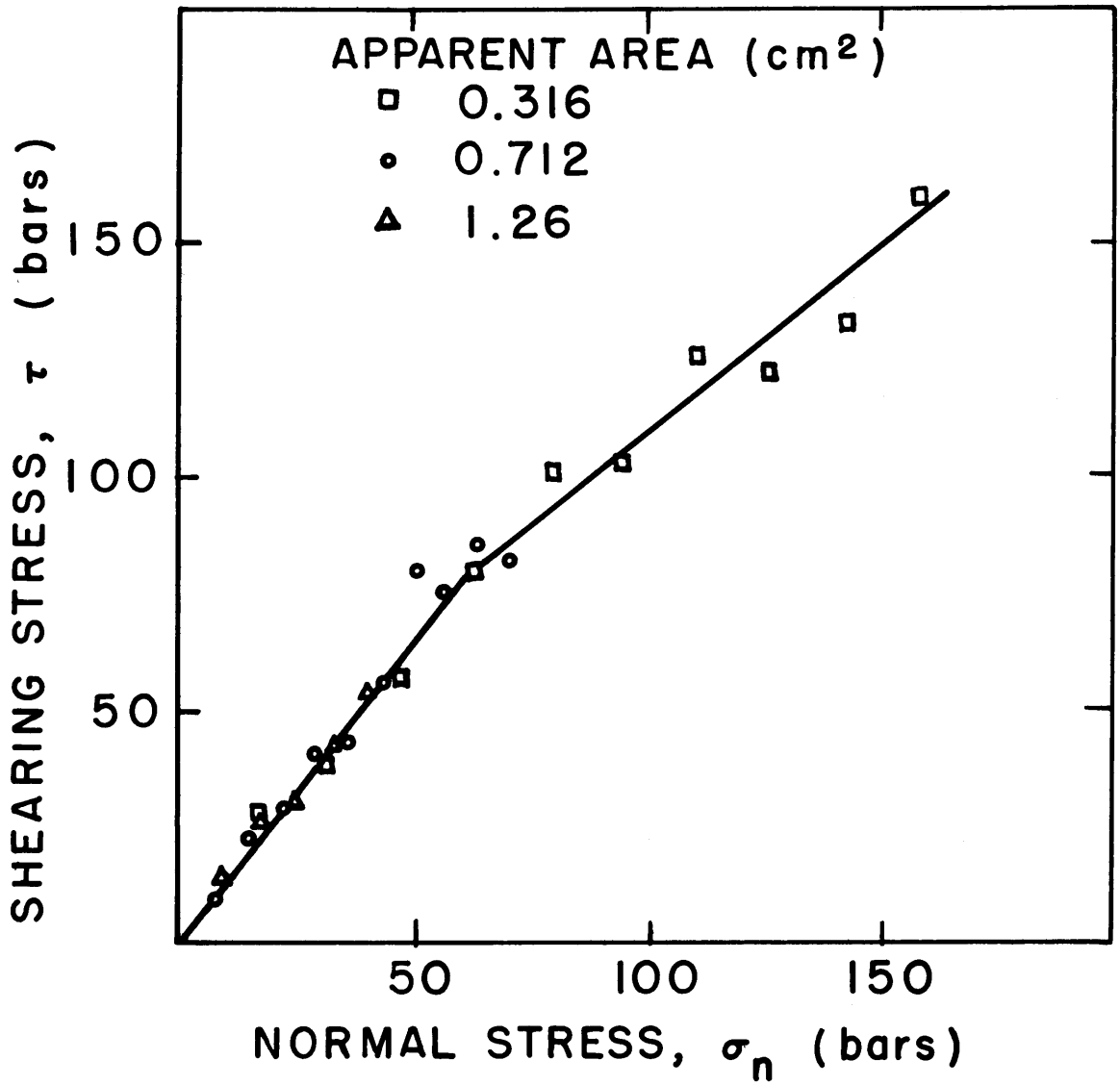
APPARENT AREA (cm²)
0.316
0.712
1.26
SHEARING STRESS, τ (bars)
150
100
50
50
100
150
NORMAL STRESS, σn (bars)

FIG. 8

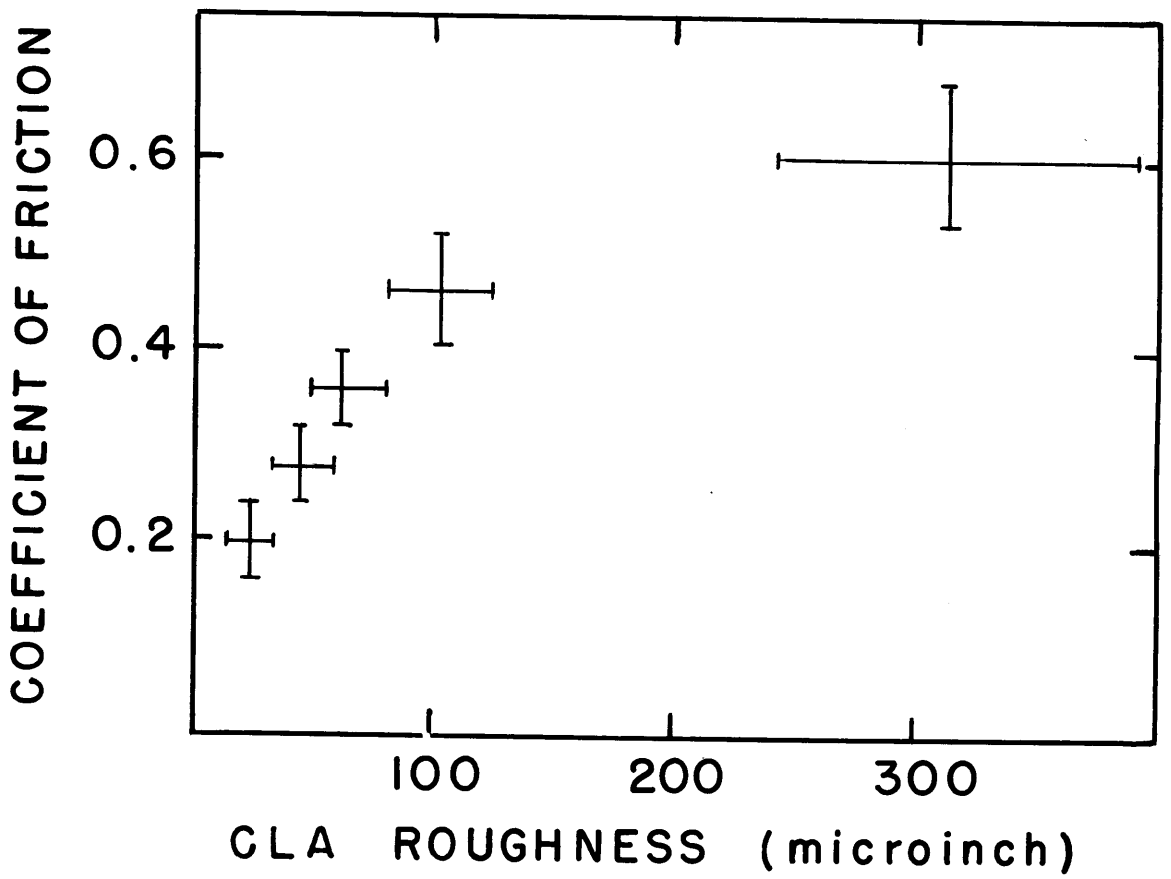
COEFFICIENT OF FRICTION
0.6
0.4
0.2
100
200
300
CLA ROUGHNESS (microinch)

FIG.9

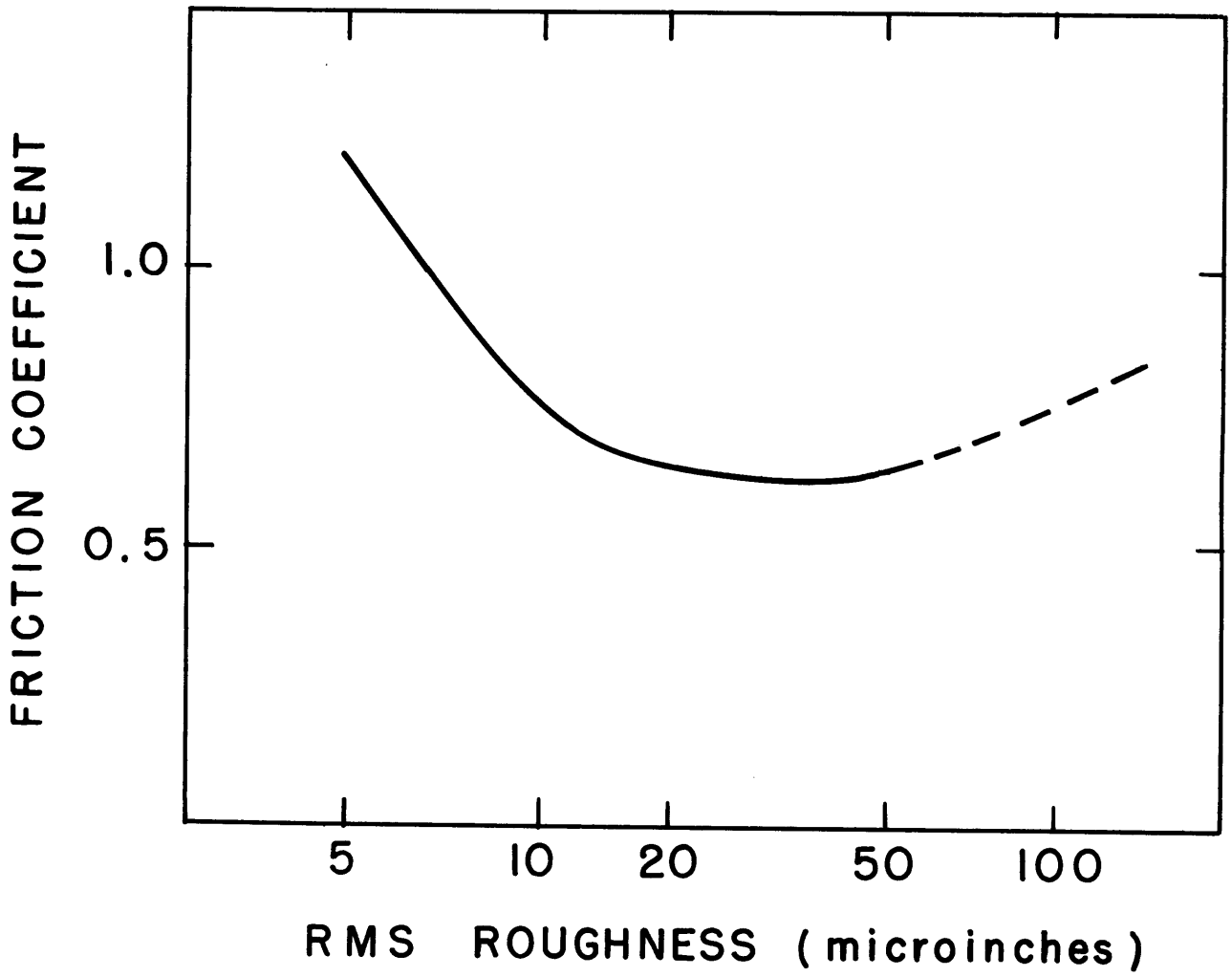
FRICTION COEFFICIENT
1.0
0.5
5
10
20
50
100
RMS ROUGHNESS (microinches)

FIG.10

Table 1

GRINDING DATA

Grit Size	Last Cut inches	Cross Feed inches	CLA Roughness microinches
400	.00025	.0075	26±10
220	.00050	.0075	45±13
100	.0010	.0075	63±15
24	.0020	.015	102±24
80	ground on plate glass		315±75

PART II

A THEORY OF BRITTLE FRICTION

Summary

A theory of friction is presented which may be more applicable for geologic materials than the classic Bowden and Tabor theory. In the model, surfaces touch at the peaks of asperities, and sliding occurs when the asperities fail by brittle fracture. The coefficient of friction can be calculated from the strength of asperities of certain ideal shapes; for cone-shaped asperities μ is about 0.1 and for wedge-shaped asperities, μ is about 0.15, independent of the strength of the material. These values are close to those observed for polished surfaces of brittle minerals.

If surface forces are present, the theory predicts that μ should decrease with load and that it should be higher in a vacuum than in air. Both these effects have been reported elsewhere. The effect of a fluid film between sliding surfaces is also predicted; μ should depend on the area of surfaces in contact. This effect has also been observed, for sliding of quartz on quartz in the presence of water. At high confining pressure the contribution of the surface tension forces to μ are negligible.

At very high loads the asperities become jammed together

and μ is a function of the strength of the material. At a pressure of one kilobar μ for rocks sliding on shear surfaces is decreased by about ten percent if water is present. This is because the strength of brittle materials is dependent on the environment.

Introduction

The most widely accepted theory of sliding friction is due to Bowden and Tabor (1942). According to this theory, the surface of a solid is made up of asperities; when two surfaces are placed in contact only the tips of asperities touch. Forces normal to the surfaces deform the asperities and they weld together at points of contact. Forces parallel with the surfaces are resisted by the shearing strength of these junctions.

The theory of Bowden and Tabor clearly requires material which can flow plastically and which welds under high contact pressure. The implicit assumption is also made that material near the tip of the asperity fails in shear. These requirements are probably met by a great many metals and by a number of the softer nonmetal single crystals, but for a great many materials of interest in geology, behavior of this sort seems unlikely. From a variety of evidence, applicability of Bowden and Tabor's theory to typical silicate minerals and, therefore, to rocks seems rather questionable.

This evidence is drawn from experimental studies of mechanical behavior of typical rock-forming minerals, from examination of wear particles formed during frictional sliding of rocks, and from the way in which coefficient of friction of brittle materials depends on factors like normal load and roughness.

Various studies have been made of the mechanical behavior of rocks containing typical silicate minerals such as quartz, feldspar, olivine, or pyroxene (Griggs, Turner and Heard, 1960). The characteristics of quartz have been particularly thoroughly investigated. At temperatures under about 500°C, true crystalline plasticity can almost be ruled out, even when ambient pressure is as high as 5 to 10 kilobars. The single characterizing feature of the deformation of these materials (which under these conditions have strengths which range up to 30 kilobars) is the brittleness. The deformed material is filled with cracks; it usually separates into fragments after an experiment. The tensile strength of even virgin material is a very small fraction of the strength in compression.

One might argue that behavior on the small scale of an asperity will not be the same as gross macroscopic behavior of samples several centimeters in dimension, particularly in view of the high local stresses likely to be found at

points of contact of asperities. One test of this possibility is offered by behavior of quartz during indentation (Brace, 1960). Indentation by a wedge-shaped indenter is not too different from deformation which a material might experience on a small scale when contact is made with an asperity. An indentation in quartz, under a load of 100 gm or less, for example, produces an average contact pressure of about 100 kilobars. Study of characteristics of the indentations and of the way in which hardness varied with composition and temperature, suggested that in spite of these extreme pressures (and resultant shearing stresses) the quartz had fractured rather than flowed plastically. Thus, the microscopic was consistent with the macroscopic behavior for quartz.

Although other silicate minerals have not been as thoroughly studied as quartz it is not likely that they are greatly different. Most of the common varieties consist of networks of silicon-oxygen tetrahedra; slip is difficult because strong silicon-oxygen bonds must be broken and because most of the minerals have low symmetry.

Marsh (1964a, 1964b) found permanent deformation in glass during indentation experiments. Glass has no crystal structure so deformation by the propagation of dislocations can be ruled out. Viscous flow of the material

at high stresses under the indenter may be possible. A feature of glass is that its compressive strength is far greater than its tensile strength. Under the combined stresses acting on the asperities on sliding surfaces brittle fracture is likely.

More direct evidence that frictional sliding of rocks involves brittle rather than ductile behavior is provided by examination of wear particles produced during sliding. In the present study, some material was dusted from the surface of Westerly granite following an experiment in which sliding was produced under a confining pressure of about 10 kilobars. The debris contained a wide range of sizes; all visible particles were angular and resembled material crushed in a mortar and pestle. The larger fragments were easily identifiable and showed no evidence of plastic flow. Although some flow of the mineral grains cannot be completely ruled out (in the mica grains primarily) brittle fracture was clearly predominant. The wear fragments were similar to those shown in Figure 22, Part III.

A final indication of a profound difference between frictional characteristics of geologic materials and most metals is given by the following comparisons; in each, behavior of brittle solids (glass, diamond, sapphire, quartz) is contrasted with that of ductile solids (most pure metals at room temperature, rock salt, ice, sulphur):

1. In air the coefficient of friction of polished surfaces of brittle materials such as quartz is approximately 0.15 (Horn and Deere, 1962), while for metals in air the coefficient of friction is approximately 1.0 or greater (Bowden and Tabor, 1958, p. 322). Large coefficient of friction has been reported for brittle materials (Bowden and Tabor, 1954, p. 126), but the values were found by using rough surfaces (See Item 5).
2. Lubricants with a low surface tension reduce the friction of metals (Bowden and Tabor, 1958, p. 324), but have little or no effect on the friction of brittle materials (Bowden and Tabor, 1958, p. 326).
3. The coefficient of friction of metals is independent of the normal load (Bowden and Tabor, 1958, p. 99), but for brittle materials it is load dependent (Bowden and Tabor, 1965, p. 169). A load dependence of friction can be obtained with metals (Bowden and Tabor, 1958, p. 99), but this is rather a special case of a thin layer of a soft metal underlain by a hard substrata. The area of contact is determined by the hard material and the shear strength by the soft material.

4. In single crystals of brittle materials a low wear rate direction is accompanied by a low coefficient of friction, but the reverse is true for metals (Flom, 1964).
5. The coefficient of friction of metals is almost independent of surface roughness (Rabinowicz, 1965, p. 62). But the friction coefficient of brittle materials is strongly dependent on roughness (Part I).

These observations suggest that there may be a fundamental difference in the behavior of brittle and ductile materials during sliding. In the following analysis, a theory of friction is presented which is based on the assumption that brittle fracture of asperities is the controlling mechanism during the frictional sliding of brittle materials.

Frictional Sliding of a Brittle Material.

We will assume with Bowden and Tabor that the surface of a mineral grain, even when polished, is made up of asperities, and that the resistance to sliding is determined by the strength of these asperities. We will depart from the Bowden and Tabor theory, however, and postulate

that the asperity is brittle, that is, it fails in a brittle manner, rather than by plastic shear. As the characterizing feature of a brittle material, we will take low tensile strength; in more precise terms, we will assume that the stress to produce brittle fracture of our material in tension is much less than the stress to cause plastic shear. Thus, we do not rule out material such as glass or sapphire, which may flow plastically under certain conditions; we simply suggest that under the combined stresses near the tip of the asperity a mineral like sapphire will more likely fail in a brittle tensile fracture than by shear.

As in the Bowden and Tabor theory we assume that the forces exerted by one surface on another are borne by the peaks of the asperities. In order to find how these forces are related we have to ask, how will an asperity fail brittlely when forces are applied at the peak. A unique relation can be found by analyzing certain ideal asperity shapes.

Analysis

As a first approximation, asperities are assumed to have the form of either (a) a wedge or (b) a cone. If n and f represent normal and tangential force which act on the apex of a wedge (Figure 11), then the stresses in the wedge are given from elasticity theory by

$$\sigma_{\theta\theta} = 0 \quad , \quad \sigma_{r\theta} = 0$$

$$\sigma_{rr} = \frac{1}{rL}\left[\frac{f \sin\theta}{(\alpha - \frac{1}{2}\sin 2\alpha)} - \frac{n \cos\theta}{(\alpha + \frac{1}{2}\sin 2\alpha)}\right] \tag{1}$$

where r is the distance from the apex, θ is the angle measured from the vertical and L is the thickness of the wedge (Timoshenko & Goodier, 1951).

Along the edge $\theta = \alpha$,

$$\sigma_{rr} = \frac{1}{rL}\left[\frac{f \sin\alpha}{(\alpha - \frac{1}{2}\sin 2\alpha)} - \frac{n \cos\alpha}{(\alpha + \frac{1}{2}\sin 2\alpha)}\right] \tag{2}$$

If the asperities break when σ_{rr} equals the tensile strength T of the material we have

$$T = \frac{1}{rL}\left[\frac{f \sin\alpha}{(\alpha - \frac{1}{2}\sin 2\alpha)} - \frac{n \cos\alpha}{(\alpha + \frac{1}{2}\sin 2\alpha)}\right] \tag{3}$$

Therefore

$$\frac{f}{n} = \cot\alpha\left[\frac{\alpha - \frac{1}{2}\sin 2\alpha}{\alpha + \frac{1}{2}\sin 2\alpha}\right] + \frac{TrL}{n}\left[\frac{\alpha - \frac{1}{2}\sin 2\alpha}{\sin\alpha}\right] \tag{4}$$

In the model it is assumed that the asperities break off at their tips so that r in equation (4) will approach zero and we will now have in the limit

$$\lim_{r \to 0} \frac{f}{n} = \cot\alpha \left[\frac{\alpha - \frac{1}{2} \sin 2\alpha}{\alpha + \frac{1}{2} \sin 2\alpha} \right]$$

The coefficient of friction μ is defined as the ratio of the total tangential force required to cause sliding to the total applied normal force. f and n in equation (5) are the forces on a single asperity. The total forces can be found by a summation over all the asperities supporting the load.

$$\mu_o = \frac{F}{N} = \frac{\sum_1^M f}{\sum_1^M n} \tag{6}$$

for a large number M of asperities we can replace the summation by an integral to give

$$\mu_o = \frac{1}{N} \int_0^M f \, dm \tag{7}$$

Substitution of equation (5) into equation (7) yields

$$\mu_o = \int_0^M \frac{n}{N} \cot\alpha \left[\frac{\alpha - \frac{1}{2} \sin 2\alpha}{\alpha + \frac{1}{2} \sin 2\alpha} \right] dm \tag{8}$$

If all angles of asperities between 0 and $\pi/2$ are equally probable and if on the average the load is shared equally by all angles of asperities then

$$\frac{ndm}{N} = \frac{d\alpha}{\pi/2} \tag{9}$$

and the coefficient of friction will be given by

$$\mu_o = \frac{1}{\pi/2} \int_0^{\pi/2} \cot\alpha \left[\frac{\alpha - \frac{1}{2}\sin 2\alpha}{\alpha + \frac{1}{2}\sin 2\alpha} \right] d\alpha \tag{10}$$

Numerical integration yields a value of

$$\mu_o = 0.15$$

We next assume that the asperities are cone-shaped rather than wedge-shaped. If n and f are the normal and tangential forces acting on the apex of a right circular cone of semi-apical angle α then the maximum tensile stress will be along the edge $\theta = \alpha$, on the f axis and is given by

$$\sigma_{rr} = \frac{f}{4\pi r^2}\left[\frac{20\sin\alpha}{(4+\cos\alpha)(1-\cos\alpha)^2}\right] \frac{-n}{4\pi r^2}\left[\frac{2(1-6\cos\alpha)}{(2+\cos\alpha+2\cos^2\alpha)(1-\cos\alpha)}\right] \tag{11}$$

where r is the distance from the apex (Michell, 1900)

If the asperities break when σ_{rr} equals the tensile strength T of the material we have

$$T = \frac{f}{4\pi r^2}\left[\frac{20 \sin\alpha}{(4+\cos\alpha)(1-\cos\alpha)^2}\right] - \frac{n}{4\pi r^2}\left[\frac{2(1 - 6\cos\alpha)}{(2+\cos\alpha+2\cos^2\alpha)(1-\cos\alpha)}\right] \quad (12)$$

therefore

$$\frac{f}{n} = \left[\frac{(6\cos\alpha-1)(4+\cos\alpha)(1-\cos\alpha)}{10\sin\alpha\,(2+\cos\alpha+2\cos^2\alpha)}\right] + T\,\frac{4\pi r^2}{n}\left[\frac{(4+\cos\alpha)(1-\cos^2\alpha)^2}{20\sin\alpha}\right] \quad (13)$$

By letting r approach 0 in equation 13 we have in the limit

$$\lim_{r\to 0}\frac{f}{n} = \left[\frac{(6\cos\alpha - 1)(4 + \cos\alpha)(1 - \cos\alpha)}{10\sin\alpha\,(2 + \cos\alpha + \cos^2\alpha)}\right] \quad (14)$$

If the angle of an asperity in contact is greater than 81° there is tension on the application of a normal force alone and the angle of the asperity will be reduced to a lower value. If all angles of asperities between 0 and 81° are equally probable we have as before by averaging over all the asperities in contact

$$\mu_o = \frac{F}{N} = \frac{1}{1.41}\int_0^{81^\circ}\left[\frac{(6\cos\alpha - 1)(4 + \cos\alpha)(1 - \cos\alpha)}{10\sin\alpha\,(2 + \cos\alpha + 2\cos^2\alpha)}\right]d\alpha \quad (15)$$

numerical integration yields a value of

$$\mu_o = 0.10$$

Observed sliding on rough and polished surfaces

In the model analyzed above, we assume that forces are applied near the apex of asperities. If there is appreciable interlocking of asperities, forces are applied down on the slopes of the asperities, so that the theory above will not hold. Two situations can be visualized for which interlocking should be negligible. If a rough surface is placed in contact with a smooth one, that is, one with much smaller asperities, then contact with the larger set will be at the peaks; these will probably fail first and will therefore determine the resistance to sliding. Some measurements for surfaces having these characteristics have been made. For example Tschebotarioff and Welch (1948) found that μ for a large number of quartz fragments set in plaster sliding on polished quartz surfaces was about 0.1. Approximately the same value of μ was found for calcite under the same condition. Experiments have been carried out here with hornblende sliding on sapphire using the low load friction apparatus described in Part I. The roughness of the sapphire was about 10 microinches and the hornblende was approximately

100 microinches. μ was found to range from 0.12 to 0.16.

The second situation likely to be close to the ideal one is the contact of two surfaces of the same roughness, which are flat to within the asperity height, and which barely make contact. These conditions will most easily be met by flat, polished or finely ground surfaces under light normal loads. Measurements on the friction of granite presented in Part I show that μ for finely ground surfaces is about 0.2 Probably the same conditions applied in the friction experiments carried out by Penman (1953) using quartz crystals with a large apparent area of contact. He found μ for quartz to be 0.19.

Values for the coefficient of friction of polished surfaces of brittle materials using a polished spherical rider or a diamond stylus at low loads also give low value of μ . These values are collected in Table 2.

It should be pointed out that at high loads using a sharply pointed stylus as a rider there would be tendency for the tip of the stylus to be jammed down between the asperities. The theory given above would not apply in this case.

The coefficient of friction of polished surfaces of brittle materials in Table 2 is seen to range from 0.05 to 0.2 which is close to the values predicted by the theory

above. It is interesting that μ for quartz and calcite are very close although these materials have greatly different strength. This independence of strength is also suggested by the theory (equation 10,15).

With appreciable interlocking, higher shearing resistance will be encountered and μ will increase above the values given by the theory. Experiments on granite were presented in Part I which demonstrate this. Surfaces were prepared which were completely interlocking; coefficient of friction depended rather strongly on normal pressure, but tended with high pressure to a value near 0.8. Finely ground surfaces of granite on the other hand, gave a μ of about 0.2. As roughness of a sequence of samples was increased at constant load, μ increased and seemed to approach the value for total interlocking. This probably reflected increase in interlocking with roughness. This is not unreasonable, for as asperity size increases for a sample of given apparent area of contact, the force carried by an individual asperity increases. This would jam the asperities together at the higher loads and increase interlocking. In the experiments of Bowden, Brooks and Hanwell (1964), they found that at high loads the friction of a diamond stylus sliding on diamond increased and the damage to the surfaces became severe. At the high load there would be a tendency for the stylus to be jammed down between the

asperities. This would give a greater degree of interlocking and the friction and damage to the surfaces should be high. In Part III it is shown that the friction of ground surfaces of granite is independent of the initial roughness. The average normal stress across the surfaces was between 1 and 5 kilobars. The load was probably high enough to jam the asperities together thus increasing the interlocking.

Thus, for situations which seem close to the ideal one observed μ is in good agreement with predicted value. The most important effect not yet amenable to analysis is interlocking, that is, geometrical situations in which forces are applied on the sides, rather than at the peaks of asperities. From experimental results this is seen to be a very important factor.

Roughness seems to be the most important factor that determines the coefficient of friction of brittle materials. This suggests that for single crystals of brittle minerals any direction of sliding which gives a high wear, because of some favorable orientation of cleavage planes, will be the direction in which the roughness of the surfaces increases during sliding. We would therefore expect the high wear direction to be associated with a high friction.

Effect of Adhesive Forces.

When two surfaces are brought close together there is an attractive force between them. In dry air the force is small (Bowden and Tabor, 1958, p. 303), but under a high vacuum it can be quite large. For example Smith and Gussenhoven (1965) found that the attractive force between polished quartz crystals was 14 kg/cm^2 when they were brought together under a vacuum of 10^{-6} Torr. The effect of these attractive forces on the friction of brittle materials is analyzed below.

If the material is brittle then the friction force is the force required to break off the tips of the asperities in contact. The magnitude of this friction force depends on the normal load N_t on the asperities and is given by

$$\frac{F}{N_t} = \mu_o \tag{16}$$

Figure 12 shows schematically two surfaces in contact. There is an attractive force $-N_a$ between the surfaces. This force is balanced by a compressive force $+N_a$ distributed over the asperities in contact. The total load carried by the asperities will be composed of two terms, the applied normal force N and the adhesive force N_a. Equation 16 now becomes

$$\frac{F}{N + N_a} = \mu_o \tag{17}$$

The measured coefficient of friction μ will be given by

$$\mu = \frac{F}{N} = \mu_o(1 + \frac{N_a}{N}) \tag{18}$$

We will assume that the adhesive force is caused by Van der Waals forces. Following Bowden and Tabor (1965, p. 424) we assume that the force $-n_a$ per unit area is given by

$$-n_a = \frac{\alpha}{(y + r_o)^3} \tag{19}$$

where y is the separation of the surfaces, r_o is the distance of closest approach and α is a constant which remains to be determined. The surface energy γ per unit area of the material is equal to one half of the work done in separating the surfaces from their distance of closest approach to infinity. The factor one half is introduced because two free surfaces are produced in the process. We now have

$$\begin{aligned} \gamma &= \tfrac{1}{2}\int_{r_o}^{\infty} n_a dy \\ &= \tfrac{1}{2}\int_{r_o}^{\infty} \frac{\alpha}{(y + r_o)^3}\, dy \\ &= -\frac{\alpha}{16 r_o^2} \end{aligned} \tag{20}$$

Substitution of equation 20 into equation 19 yields

$$-n_a = \frac{-16r_o^2\gamma}{(y + r_o)^3} \tag{21}$$

The total adhesive force is now given by

$$-N_a = \frac{-16r_o^2\gamma A}{(y + r_o)^3} \tag{22}$$

where A is the total area over which the forces act. Equation 18 now becomes

$$\mu = \mu_o \left[1 + \frac{16r_o^2\gamma A}{(y + r_o)^3 N}\right] \tag{23}$$

when a normal force is applied to the asperities they will deform elastically and the surfaces will approach each other by an amount δ which is given by

$$\delta = K_1(N + N_a)^{2/3} \qquad \text{(Lubkin,1960)} \tag{24}$$

where K_1 is a constant which will depend on the shape, number of asperities in contact and the elastic constants of the material. The equation is valid for the contact of spheres and solids of revolution. This equation is probably a reasonable approximation for the deformation of asperities.

If y_o is the separation of the surfaces when the asperities first come into contact then y in equation 23 is given by

$$y = y_o - \delta$$

$$= y_o - K_1(N + N_a)^{2/3} \qquad (25)$$

Substitution of equation 25 into equation 23 yields

$$\mu = \mu_o + \frac{\mu_o 16 r_o^2 \gamma A}{N\left[y_o + r_o - K_1(N + N_a)^{2/3}\right]^3} \qquad (26)$$

If y_o the separation of the surfaces is not a constant but varies from point to point over the surfaces then equation 26 will be an integral equation given by

$$\mu = \mu_o + \mu_o \int_o^A \frac{16 r_o \gamma dA}{N\left[y_o + r_o - K_1(N + N_a)^{2/3}\right]^3} \qquad (27)$$

The problem is made even more complex because N_a can not be explicitly evaluated in terms of N.

The equation does however tell us something about the frictional behavior of brittle materials.

The first thing we notice is that the friction should increase with an increase in the surface energy of the material. The surface energy of a material is higher in a

vacuum than it is in air. This is because in air the surfaces are covered with an adsorbed layer of water or oxygen but in a high vacuum this layer is removed (Bowden and Tabor, 1965, p. 416). We would therefore expect that the friction would increase in a vacuum. Equation 22 also predicts that the friction would decrease with an increase in the applied normal load.

Experimentally both these effects have been observed. For example Bowden and Young (1951) found that the friction of diamond both in vacuum and in air decreased with an increase in the normal load but the friction in a vacuum was much higher.

Effect of Surface Tension

It has been observed experimentally that when two surfaces are placed together in the presence of a liquid there is a force between them caused by the surface tension of the fluid (Bowden and Tabor, 1958, Chapter 15). How this force will effect the friction of brittle materials is given below.

The total normal force N_t between the surfaces will be composed of two terms, the applied normal force N, and N_s the force due to the surface tension of the liquid.

Following the same reasoning as given in the previous section we arrive at the equation

$$\mu = \mu_o(1 + \frac{N_s}{N}) \tag{28}$$

The surface tension force is caused by the pressure inside the liquid being lower than it is outside. The difference in pressure is given by

$$P = \alpha/r \tag{29}$$

where α is the surface tension of the liquid and r is the radius of curvature of the meniscus. The force between the surfaces will be

$$N_s = \alpha A/r \tag{30}$$

where A is the area of the surfaces surrounded by the liquid-air interface. The radius of curvature r of the meniscus, Figure 13, is given by

$$r = \frac{d}{2 \cos \theta} \tag{31}$$

where d is the separation of the surfaces and θ is the contact angle of the solid-liquid interface. We now have

$$N_s = \frac{2 \alpha A \cos\theta}{d} \tag{32}$$

At zero normal load the separation of the surfaces will be of the order of twice the asperity height h. As

in the previous section we assume that when a normal load is applied, the asperities deform elastically and the surfaces will approach each other by an amount ζ , given by

$$\zeta = K_1(N + N_s)^{2/3} \qquad \text{(Lubkin 1960)} \qquad (33)$$

We now have

$$d = 2h - K_1(N + N_s)^{2/3} \qquad (34)$$

substitution of equation 34 in equation 32 yields

$$N_s = \frac{2\alpha A \cos\theta}{2h - K_1(N + N_s)^{2/3}} \qquad (35)$$

substitution of equation 35 in equation 28 yields

$$\mu = \mu_o + \frac{\mu_o \, 2\alpha A \cos\theta}{N\left[2h - K_1(N + N_s)^{2/3}\right]} \qquad (36)$$

If the surfaces are flooded with water the meniscus around the edges will be destroyed but during sliding the continuity of the liquid film will be disrupted and a water-air or water-water vapor interface will be established over portion of the surfaces in contact. The area enclosed by the meniscus (A in equation 36) may be difficult to evaluate but in a qualitative sense it would be expected that the larger the apparent area of contact the larger

will be the surface tension forces and hence the large will be the measured coefficient of friction.

This may explain why Penman (1953) found that μ for large flat surfaces of quartz increased from 0.19 in air to 0.6 in water, but the Norwegian Geotechnical Institute (1959) found that μ for quartz with a very small area of contact was virtually unaffected by the presence of water.

It can be seen from equation 36 that at very high normal loads the friction approaches a constant value μ_o. Therefore under pressures of geological interest surface tension of the fluid should have little or no effect on μ. However there is another effect that may be considerable. That is the dependence of strength of brittle materials on the environment. At low loads μ is independent of the strength of the material but at very high loads this is not the case. The asperities become jammed together and even with zero normal load across the surfaces the interlocking irregularities have a finite shear strength.

It is shown in Part III that at high confining pressures μ is given by

$$\mu = A + B/\sigma_n \qquad (37)$$

where B is the shear strength of the interlocking asperities at zero normal stress and A is the rate of

change of shear strength as the normal stress σ_n is increased.

It has been found by Colback and Wiid (1965) that the shear strength of rocks is reduced by a constant amount independent of confining pressure in the presence of liquids. Therefore B in equation 37 should be smaller in the presence of a fluid. This means that at a given normal stress across the surfaces μ should be less if water is present. Experimentally this has been found to be the case. For example Jaeger (1959) found that at a confining pressure of 1 kb, μ for dry sandstone was 0.52 but for wet sandstone it was 0.47. For dry granitic gneiss μ was 0.71 but it was 0.61 when the rock was wet.

Conclusions

Most workers in the field of friction have assumed that brittle materials deform plastically during frictional sliding regardless of the fact that materials such as quartz can only be made to fail plastically under rather special conditions of high temperatures and extremely high confining pressures which would not ordinarily be obtained during frictional experiments. It is difficult to explain the differences between the frictional characteristics of metals and brittle materials and still adhere to the belief that all materials behave plastically during sliding.

The low friction coefficient of polished surfaces of brittle materials is predicted almost exactly if we assume that the tips of the asperities in contact fail by brittle fracture. The theory in this section predicts that for polished surfaces the friction should be independent of the strength of the material and this agrees with the experimental results. If tips of the asperities must be broken off for sliding to occur it would not be expected that lubricants would have any effect on the coefficient of friction of brittle materials. The increase in friction at low loads is a natural consequence if we take into account the surface forces. The increase in friction under a high vacuum is explained by the increase in the surface energy of the material. The increase in friction of brittle materials in the presence of fluids can be explained by considering the surface tension forces that are known to exist. If the area of the surfaces in contact is small the surface tension forces will be negligible. This may explain why Bowden and Tabor (1965, p. 171) found that the friction of a diamond stylus sliding on diamond was unaffected by the presence of mineral oil or fatty acids.

The theory has not been developed to the stage where the friction can be predicted as a function of roughness. A possible explanation for the observed increase of

friction with rough surfaces of brittle materials is that with rough surfaces in contact the asperities jam together rather than being supported on their tips. The increase in friction with roughness may explain why in single crystals of brittle materials a high wear rate direction is associated with a high coefficient of friction. At a confining pressure of one kilobar μ for rocks sliding on shear surfaces is decreased by about ten percent if water is present. This can be explained by the fact that the strength of brittle materials is dependent on the environment.

FIGURE CAPTIONS

Figure

11 Theoretical model of an asperity.

12 Ideal model for adhesive forces between surfaces in contact.
Van der Waal's forces - n_a exert an attractive force between the surfaces.
In the model the separation of the surfaces over which the Van der Waal's forces act is y. These forces are balanced by a compressive force $+n_a$ distributed over the asperities in contact.

13 Ideal model for surface tension forces between two surfaces on contact.
In the model the distance of separation of the two surfaces is d, the radius of curvature of the meniscus of the fluid between the surfaces is r, and the contact angle of the fluid is θ.

Theoretical model for brittle friction

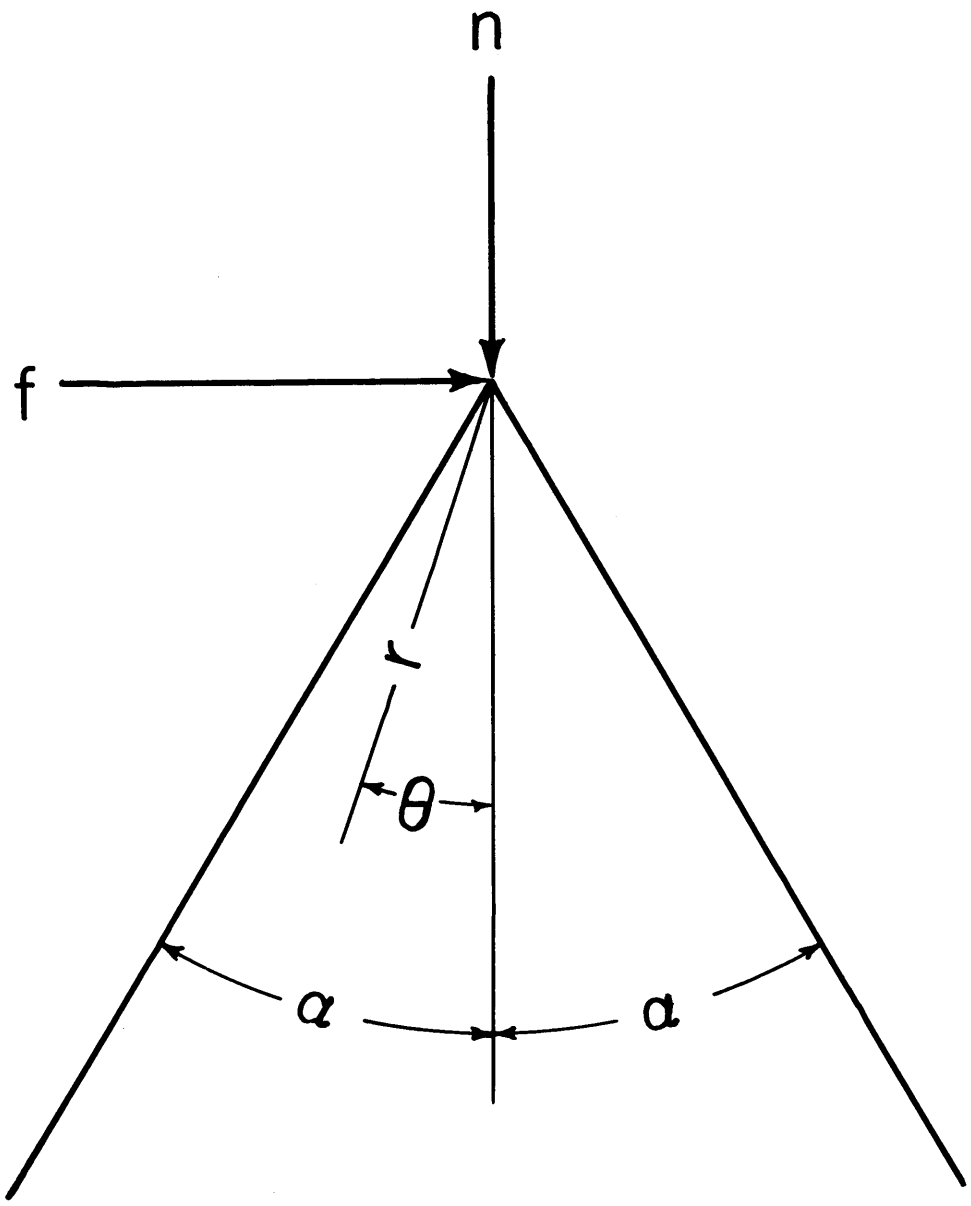

FIG.11

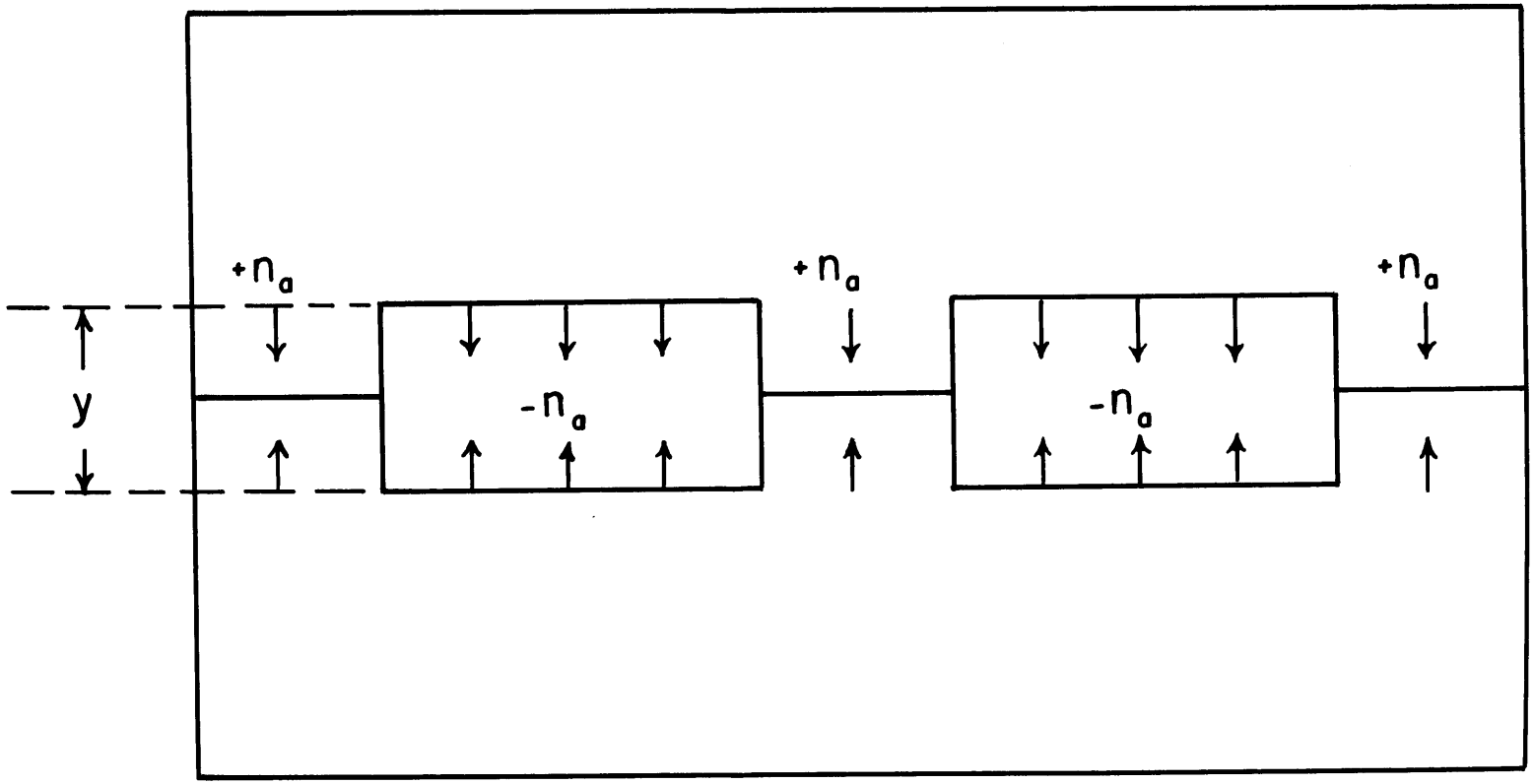

FIG.12

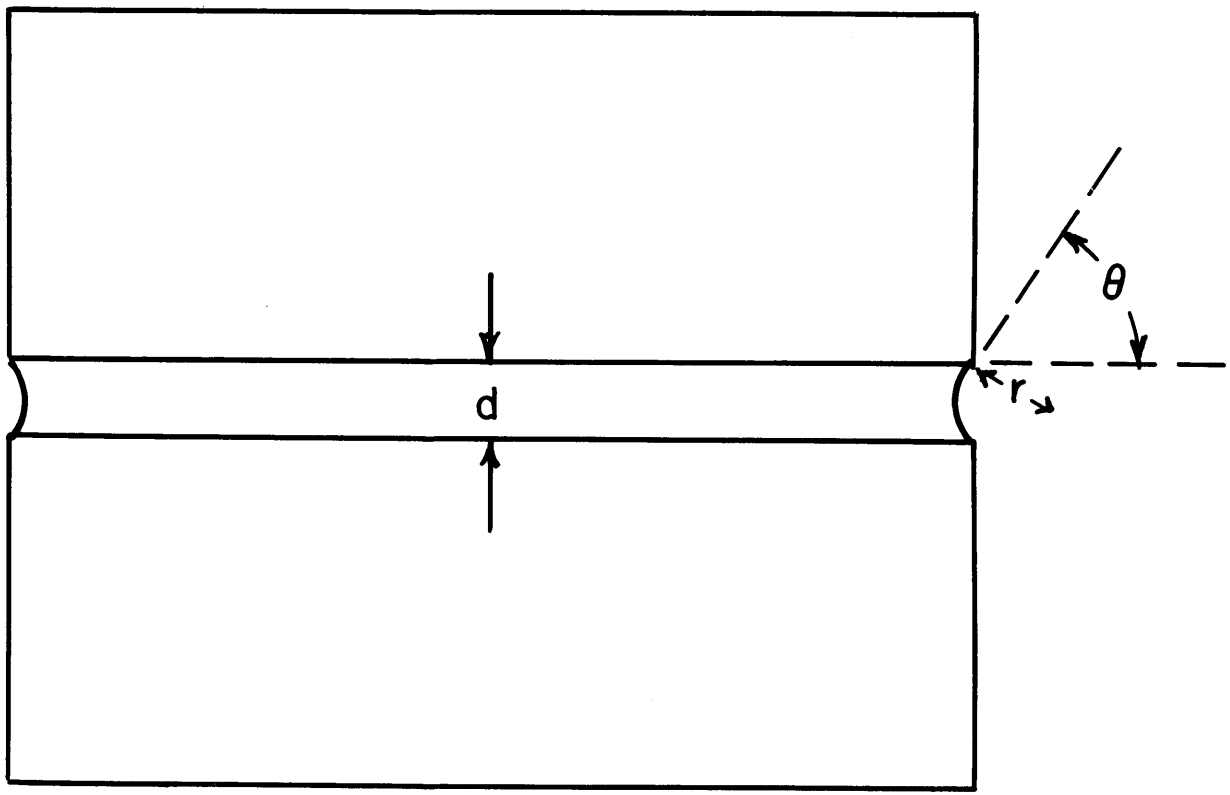

FIG.13

Table 2

COEFFICIENT OF FRICTION FOR POLISHED SURFACES OF BRITTLE MATERIALS

(in air at room temperature)

Surface	Rider	Coefficient of friction	Source
Diamond	Diamond Stylus	0.04-0.15	Seal (1958)
Diamond	Diamond Stylus	0.05-0.15	Bowden,Brooks,Hanwell(1964)
Sapphire	Sapphire Sphere	0.07	Riesz, Weber (1964)
Quartz	Quartz Sphere	0.11-0.14	Horn, Deere (1962)
Quartz	Quartz Plate	0.19	Penman (1953)
Quartz	Quartz fragments	0.106	Tschebotarioff,Welch(1948)
Microcline	Microcline Sphere	0.11-0.12	Horn, Deere (1962)
Calcite	Calcite Sphere	0.14	Horn, Deere (1962)
Calcite	Calcite fragments	0.107	Tschebotarioff,Welch(1948)
Calcite	Quartz fragments	0.098	Tschebotarioff,Welch(1948)

PART III

FRICTIONAL BEHAVIOR OF WESTERLY GRANITE UNDER HIGH CONFINING PRESSURE

Summary

At high confining pressure μ for granite depends on the relative displacement of the surfaces. For ground surfaces μ reaches a maximum after about 0.1 cm and then decreases to nearly a constant value after 0.5 cm of sliding has occurred. Features on the surfaces after sliding suggest that the maximum μ is reached when intimate contact is first established. If this is correct then the initial μ for perfectly mated surfaces should be the same as the maximum μ for ground surfaces. Experimentally this was found to be correct. The decrease in μ from the maximum is caused by an accumulation of loose wear particles between the surfaces.

μ decreases with an increase in the normal stress. This is because the interlocking irregularities on the surfaces have a finite shear strength when the normal stress is zero. Up to the highest pressures investigated movement between the sliding surfaces took place by violent stick-slip.

Introduction

Table 3 gives the coefficients of friction of rocks that have appeared in the literature. The most striking features are that μ, the coefficient of friction, can range from 0.2 and 2.0 and that there is no significant variation between rock types. Thus, for example, μ of granite is close to that of marble although strength and mineralogy of these rocks is very different. In the first chapter it was established that μ of Westerly granite was strongly dependent on the surface roughness. This was also shown by Jaeger (1959), who found that the friction for sliding on ground surfaces of quartz prophyry was less than the friction on shear failure surfaces, over a confining pressure range of 200 to 1000 bars. These observations suggest that roughness may also be the important factor that determines the coefficient of friction of rocks at pressures of geological interest.

In the present section, the dependence of friction on roughness has been systematically investigated for Westerly granite up to a confining pressure of 2.6 kb. During sliding the surfaces are modified by wear and the friction changes with the amount of relative displacement between the surfaces. This characteristic has been studied

in detail.

In addition to studying the fundamental processes involved in the frictional sliding of rocks, experiments were designed to test the Coulomb-Navier criterion of rock fracture and Orowan's theory for the ductility of brittle materials.

In the Coulomb-Navier theory of rock fracture it is assumed that the compressive strength is determined by the cohesive strength and the coefficient of friction for sliding along the fracture surface. The theory has no rational basis (Brace, 1964; Orowan, 1965) but it is firmly entrenched in the minds of many workers in the field of rock mechanics. Experiments were carried out to critically test the theory. This was done in the following way. The shear fracture strength of virgin and fractured samples of Westerly granite was determined up to a confining pressure of 10 kb. If the Coulomb-Navier theory is correct then the difference between the two values at any given normal stress should be independent of the normal stress across the surfaces.

Orowan (1960) suggested that at sufficiently high confining pressure the axial stress required to create a fracture surface in a rock may be equal to the axial stress required to cause sliding on the newly created surface. If

this is so then the stress-strain curve would have the characteristics of a ductile material, that is, the rock would deform without loss of strength. Experiments were carried out in this study in order to test this possibility. The confining pressure at which the stress-strain curves for Westerly granite had ductile characteristics was compared with the confining pressure at which the axial stress required to create a fracture surface was equal to the axial stress required to cause sliding on a fracture surface.

Experimental Procedure

General

One type of experiment, shown schematically in Figure 14 was carried out on three different types of surface. G has a ground surface, F has a fracture surface, and V is a virgin rock with the fracture surface after failure indicated by the dotted line. The experiments were carried out in two different types of apparatus, one which operated to 5 kb pressure and the other to 10 kb. An axial force was applied to the cylindrical specimens under a confining pressure. The axial force was recorded as a function of the axial displacement as movement occurred on the surfaces.

The average axial stress σ_3 in the rock supporting the load is given by

$$\sigma_3 = \left[F - \sigma_1 (A_p - A_r)\right] / A_r \qquad (38)$$

where A_p is the area of the piston and A_r is the area of the rock supporting the load. The force F was corrected for friction in the same manner as described by Brace (1964) and Paulding (1965).

As sliding occurs, the area of contact along the sliding surface changes. The cross sectional area, A_r, supporting the load after an axial displacement ϵ is given by

$$A_r = 2\left[\frac{\pi r^2}{2} - \frac{\epsilon \tan\alpha}{2}\left(r^2 - \left(\frac{\epsilon \tan\alpha}{2}\right)^2\right)^{\frac{1}{2}} + r^2 \sin^{-1}\left(\frac{\epsilon \tan\alpha}{2r}\right)\right] \qquad (39)$$

where r is the radius of the cylinder, and α is the angle the sliding surface makes with the axis of the cylinder.

The average normal stress σ_n and the average shear stress τ on the plane of the sliding surfaces is given by

$$\sigma_n = \left(\frac{\sigma_3 + \sigma_1}{2}\right) - \left(\frac{\sigma_3 + \sigma_1}{2}\right)\cos 2\alpha \qquad (40)$$

$$\tau = \left(\frac{\sigma_3 - \sigma_1}{2}\right)\sin 2\alpha \qquad (41)$$

The coefficient of friction μ is then

$$\mu = \tau / \sigma_n \qquad (42)$$

Sample Preparation

The specimens used to study the frictional sliding of ground surfaces were cylinders 1.5 inches long and 0.625 inches in diameter, cut at an angle of 45° to the axis. The saw cuts were ground to the required roughness on a surface grinder. The specimens (Figure 15a) were enclosed in an annealed copper tube with a wall thickness of 0.005 inches and then subjected to a hydrostatic pressure of about 1 kb. This insured that the sliding surfaces were in close contact and gave some mechanical strength to the sample. The ends of the specimen were ground parallel and jacketed in a gum rubber tube with a wall thickness of 0.125 inches. The ends were sealed with a wire clamp against hardened steel end plugs. Figure 15a shows the jacketed sample.

To study the frictional characteristics of Westerly granite with completely interlocking asperities, a 4"x4"x6" block of granite was broken under tension by applying a bending moment to the sample as shown in Figure 16a. The fracture surfaces were coated with Eccobond cement (Emerson and Cummings Company, Canton, Mass.), and the two blocks fitted back together so that the fracture surfaces mated

perfectly. A force was applied to the block normal to the fracture with an arbor press to extrude all but a minute amount of the cement from between the two surfaces. After the cement had hardened, cores, oriented such that the fracture was at an angle of approximately 30° to the axis, were cut and ground to the required size with a cylindrical grinder. Two sample configurations were used in the experiments carried out in the 5 kb apparatus. One was a straight cylinder 0.625 inches in diameter and 1.5 inches long, shown in Figure 16b. The other, as shown in Figure 3c, was a 0.625 inch diameter cylinder 2 inches long with a central section 1.25 inches long reduced to a diameter of 0.437 inches. The radius of curvature of the fillets at the end of the reduced section was made 0.125 inches, in order to reduce the stress concentrations. The fractured specimens were separated after soaking them in Eccostrip (Emerson and Cummings Company, Canton, Mass.) for 24 hours to break down the cement. The cement was then carefully removed from the surfaces. To remove the Eccostrip from the rock, the specimens were placed in running water for 72 hours, then dried out in a vacuum oven at 100°C, and finally placed in acetone for 72 hours. This also ensured that the cutting oil used in the grinding process was removed from within the pores of the rock.

Next, the fractured cylinders were enclosed in a thin-walled copper cylinder. After the ends were ground parallel, the cylinders were jacketed in a gum rubber tube in the same way as the cylinders with ground surfaces as described above. The samples with reduced central section (Figure 15b) were placed together with the central section covered with heat-shrinkable plastic tube which gave a small mechanical strength to the sample. The ends of the sample were then ground parallel on a surface grinder. Annealed copper caps with a wall thickness of 0.005 inches were placed on the ends of the specimen and soldered to a 0.005 inch thick cylinder which covered the sides of the heads and were crimped over portion of the reduced central section of the specimen. The specimens were finally jacketed in a 0.5 inch diameter gum rubber tube with the ends clamped to the copper end caps. The jacketed sample is shown in Figure 15b. With a copper jacket only a small amount of relative displacement between the sliding surfaces can be obtained before the jacket breaks and allows the confining pressure medium to enter the rock. This problem was eliminated by the use of gum rubber as the jacketing material.

A number of experiments, V in Figure 14 were carried out on straight cylinders and cylinders with a reduced central section to determine the fracture strength of the

block of Westerly granite used in the frictional experiments. Cores were cut from the block of granite with a similar orientation, ground to the same geometry and jacketed in the same way as the fractured specimens described above (Figure 15). Before jacketing, the specimens were soaked in acetone for 72 hours to ensure that the cutting oil used as a coolant in the grinding process was completely removed from the pores of the rock.

The specimens of fractured and virgin granite used in the 10 kb apparatus experiments were cylinders 1.25 inches long and 0.5 inches in diameter prepared in the same way as the fractured and unfractured cylindrical specimens used in the 5 kb apparatus experiments. At high confining pressures gum rubber passes through a glassy transition (Paterson, 1964) and fails by brittle fracture after only a small amount of strain. It was therefore necessary to use a material that does not become brittle at high confining pressures as the jacketing material. Polyurethane tubing (Globe Rubber Company, Quincy, Mass.) with an internal diameter of 0.5" and a wall thickness of 3/16" was found to be satisfactory.

Apparatus and Procedure

The pressure vessel (Figure 17) was described by Brace (1964). The axial force applied to the piston was

measured externally by a load cell and the confining pressure by a manganin coil situated inside the pressure vessel. The initial movement between the frictional surfaces was detected with a strain gauge extensometer attached to the piston. The load cell, manganin coil and extensometer were connected to bridge circuits the ouput of which were fed into a Mosely model 136 XY recorder.

The amount of axial movement was measured by recording at the moment of each violent stick slip motion the displacement of the piston with a dial gauge.

In the 10 kb apparatus which had essentially the same design as that shown in Figure 17, the sample was attached by a clamp to a hardened steel plug situated in the upper end of the pressure vessel. As the piston was advanced the confining pressure in the vessel increased until contact was made with the lower end of the specimen. The pressure was measured with a manganin coil in the high pressure fluid line outside the vessel. To adjust the pressure to the required value, fluid was bled from the vessel. The axial force on the specimen was increased by advancing the piston and the magnitude of the force exerted on the piston was measured with four strain gauges attached to the piston. A correction was made to all the measurements to allow for

the force expended in overcoming friction at the cylinder walls. The displacement of the piston was measured with a 7 DCDT-500 Transducer (Hewlett Packard Company, Sanborn Division, Waltham, Mass.). Output from the strain gauge bridge circuit, manganin coil bridge circuit and the transducer was displayed on a Mosely XY-recorder.

Data from a typical friction experiment carried out with the 5 kb apparatus as recorded by the XY-recorder, are shown in Figure 18. The abscissa is axial force and, depending on the trace, the ordinate is the confining pressure or axial displacement of the piston. The force-axial displacement curve is shown as a dashed line in Figure 18. The confining pressure was increased from zero to 2 kb along the path OA. The increase in the axial force is due to the pressure exerted on the base of the piston by the fluid in the vessel. The position of the trace was then adjusted to the point B by inserting known resistances into one arm of the respective bridge circuits. The extensometer and dial gauge were then adjusted until they made contact with the end of the ram. As the axial force was increased the force-deflection curve initially traced out a straight line the slope of which is a measure of the elastic modulus of the rock. At the point C there was sliding on the ground surfaces, which produced a sudden change in slope of the

force-displacement curve. The point D gives the force and confining pressure at which movement commenced. At the point E there was a violent stick slip motion between the ground surfaces, the axial force suddenly decreased and, because of the small volume of the pressure vessel, the confining pressure increased as the piston advanced. The axial force and confining pressure were then decreased to the point B by bleeding off oil from the pressure vessel and the ram. The position of the force-confining pressure curve was then adjusted to the point F by decreasing the resistance in the manganin coil bridge circuit by a known amount. The extensometer was then disconnected and the experiment continued in the same manner to produce stick-slip at the points H, I, J, etc. The axial displacement of the piston due to the sliding between the two frictional surfaces at each stick-slip was found by subtracting the elastic strain of the rock under the applied force at the moment of slip, found from the extrapolated linear portion of the force deflection curve, from the reading of the dial gauge at the moment of each stick-slip.

Accuracy of measurements, calculated stresses and the coefficient of friction

The overall accuracy of the force and confining

pressure measurements in both the 10 kb and 5 kb experiments was approximately ± 1%. This included the uncertainties in the friction on the piston and the inaccuracies in the XY-recorder. Axial displacement of the piston could be measured to within 0.005 inches. The error in measuring the angle which the sliding surfaces make with the axis of the specimens is about ± 1° for the fractured and virgin specimen and ± 0.5° for the ground surfaces.

In the 10 kb vessel the piston was 1.5 inches and the specimen 0.5 inches in diameter, so that an appreciable percentage of the force measured with the load cell balanced the pressure of the fluid acting on the base of the piston and the overall accuracy of the axial stress calculated from the axial force and the confining pressure had a theoretical value of ± 7%. In the 5 kb vessel the piston was 1 inch and the specimens were 0.625 inches in diameter so that the calculated axial stress was somewhat better, the theoretical value being ± 2%.

The calculation of the normal and shear stresses on the sliding plane for the fracture of virgin rock, the initial sliding for perfectly mating surfaces and the maximum friction for ground surfaces involves an error in the measurement of the angle which the sliding surfaces makes with the axis of the specimen. The theoretical accuracy of both the normal

and shear stresses in the 5 kb experiments is ± 3.5% and in the 10 kb experiments it is ± 9.5% for the fractured and virgin specimens. All the experiments with the ground surfaces were carried out using the 5 kb apparatus and the theoretical accuracy of the normal and shear stresses at the maximum in friction is about ± 3%.

The calculation of the coefficient of friction after a large amount of relative displacement between the sliding surfaces involves the additional uncertainty in the measurement of the axial displacement. The theoretical error in μ after about 0.5 cm of sliding has a value of approximately ± 9%.

Experimental Results

Experiments were carried out which gave data that enabled the coefficient of friction to be determined as a function of displacement on ground surfaces of Westerly granite with average asperity heights of 24±10, 63±15, 102±24 microinch over a confining pressure range of 0.7 to 2.6 kb and on a fracture surface with completely interlocking asperities over a confining pressure range of 1.1 to 10.1 kb.

In addition a number of experiments were performed without measuring the axial displacement but the data were sufficient to determine the coefficient of friction at the

first slip for Westerly granite with completely mating surfaces.

The compressive strength of Westerly granite was determined up to a confining pressure of 10.86 kb. Stress-strain curves of unfractured samples of Westerly granite were obtained at confining pressures of about 6.6 and 10.1 kb.

Ground Surfaces

The shear stress required to initiate movement between ground surfaces with a high normal stress across the sliding plane are plotted in Figure 19. The large scatter in the results is due to the uncertainty in estimating the stress at which movement first starts. The finely ground surfaces tend to have lower values, but the low accuracy of the results do not permit any quantitative conclusions to be reached as to the effect of surface roughness on the coefficient of friction at high normal loads.

Numerical data on the change in friction with the distance of sliding on ground surfaces are listed in Table 4. The coefficient of friction changes in a striking manner and is illustrated in Figure 20 which shows the results from the experiments carried out at a confining pressure of 0.7 kb.

There is initially a rapid increase in the friction with a maximum being reached after approximately 0.1 cm of sliding. Between 0.1 and 0.4 cm of movement between the surfaces, the friction decreases. For distances of sliding greater than 0.4 cm the variation in the coefficient of friction is slight but the accuracy of the results do not permit any definite conclusions to be reached. The friction could either remain constant or decrease continuously with movement between the surfaces.

The experiments were repeated at different confining pressures up to 2.6 kb and all the results (Table 4) showed the same characteristics.

A number of experiments were carried out in which the individual experiments were terminated at different points along the friction displacement curve. Examination of the surfaces (Figure 21) revealed that within the first 0.1 cm of displacement, damage to the surfaces was confined to isolated regions. When the displacement corresponding to the maximum in friction was reached, there was minor damage over the whole of the surface, as indicated by a fine layer of crushed material. This suggested that the maximum in the coefficient of friction corresponded to the point when contact was first made over the whole surface area.

Beyond the maximum, the layer of comminuted material on

the surfaces increased in thickness and the friction coefficient measured in this region was that required to shear through a layer of loose particles on a substrata of solid material. Some of the comminuted material was removed from the surface and examined under a microscope. It was found to be composed of finely crushed grains of the rock, the particles showed optical continuity and had sharp angular edges similar to that which would be expected in the grains failed by brittle fracture. The grain size ranges from approximately 0.1 mm in diameter down to grains which could be barely resolved with the microscope (Figure 22).

It was found that the maximum value of the coefficient of friction decreased with increase in the confining pressure of the experiment. Physically the important parameter is the normal stress across the sliding plane and in Figure 23 the shear stress is plotted against normal stress at the maximum in friction for all the experiments on ground surfaces. The dashed line on the diagram represents the equation

$$\tau = 0.5 + 0.6\sigma_n \qquad (43)$$

where τ and σ_n represent the shear and normal stresses measured in kilobars. The significance of this line is discussed in the next section.

The coefficient of friction μ for points falling on

this line is given by

$$\mu = 0.6 + 0.5/\sigma_n \qquad (44)$$

Interlocking Surfaces

The change in friction with displacement for interlocking surfaces was measured in a number of experiments and the results are listed in Table 5. Data from a typical experiment are plotted in Figure 24 and the results show that the friction decreases rapidly from an initially high value to a constant value of approximately 0.6 after about 0.1 cms of sliding has occurred. Finely ground powder was found over the whole of the surfaces after sliding.

A number of experiments with interlocking surfaces were carried out without measuring the change in friction with displacement but the results were sufficient to calculate the initial high value of friction and are listed in Table 6. In Figure 25 the shear stress at which sliding commenced is plotted against the normal stress across the sliding surface. The results fall about the straight line

$$\tau = 0.5 + 0.6\sigma_n \qquad (45)$$

and the coefficient of friction μ is given by

$$\mu = 0.6 + 0.5/\sigma_n \quad \text{if } 2 < \sigma_n < 17 \text{ kb} \qquad (46)$$

Behavior of unfractured granite

The fracture strength and fracture angle, α , of Westerly granite was determined up to a confining pressure of 10.86 kb and the numerical results are listed in Table 7. In Figure 26 the fracture strength is plotted against confining pressure, the solid circles are the results from straight cylinders while the open circles are the results from samples with a reduced central section.

One feature of the experiment is the absence of any appreciable effect of the configuration of the specimen on the fracture strength under a confining pressure. A significant feature of the results is the nonlinear increase in the fracture strength with confining pressure and similar results were obtained by Mogi (in press) and by Brace, Paulding and Scholz (in press) on Westerly granite with a similar grain size.

The shear and normal stresses at fracture across the shear plane were calculated and are plotted in Figure 27.

Experiments were carried out on Westerly granite in which the sliding was continued after fracture. The stresses were calculated by correcting for the change in the cross sectional area and these values together with the percent axial strain and the differential stress in the specimen before and after slip are listed in Table 8. In

Figure 28 and 29 the differential stress is plotted against the percent axial shortening at confining pressures of 6.6 kb and 10.1 kb respectively.

Discussion of Experimental Results

Introduction

Figure 30 shows schematically the stress-strain envelopes for the three types of surfaces studied; an envelope is obtained by eliminating the stick-slip parts of the observed stress-strain curves. G is an initially ground surface, F is a fracture surface which initially had perfect interlocking of the irregularities on the surfaces, and V is a virgin rock which after fracture slid on the newly created shear surface. The schematic diagram represents the results that would be obtained if the sliding surfaces were all inclined at the same angles to the axis of the specimen. Curves for 3 different pressures P_1, P_2, and P_3 are given.

With ground surfaces the differential stress required to cause sliding increases with the amount of relative displacement between the surfaces until a maximum is reached after about 0.1 cm. The friction then decreases to a constant value after approximately 0.5 cm of movement has occurred. The difference between the maximum and final value of the

differential stress decreases with an increase in the confining pressure of the experiment.

The differential stress required to cause sliding on surfaces that initially had complete interlocking of the irregularities falls after a small amount of displacement between the surfaces. The stress required to initiate movement is the same as the maximum stress for ground surfaces. This is shown in Figure 23. The line which is the best fit to the points in Figure 25 for interlocking surfaces falls very close to the maximum in friction for ground surfaces.

For a virgin rock below a confining pressure of 10 kb the differential stress at fracture is greater than the initial stress for sliding on either perfectly mating surfaces (F) or the maximum stress for sliding on ground surfaces (G).

After about 0.5 cm of sliding has occurred the stress required to cause further movement is the same for the initially virgin rock, interlocking or ground surfaces.

At a confining pressure of about 10 kb the stress required to cause sliding is a constant independent of the amount of relative displacement between the surfaces.

Stick-slip

In all the experiments it was found that the frictional sliding of Westerly granite was accompanied by violent jerky

motion. This phenomenon is commonly known as stick-slip and a few words of explanation of this behavior seem necessary.

Stick-slip occurs if the frictional force is not a constant but decreases with displacement between the surfaces (Rabinowicz, 1965, p. 94).

Figure 31 shows schematically how the friction experiments were carried out in this study. The specimen with the surface ground at an angle to the axis is situated in the lower chamber under a confining pressure P. An axial force is applied to the specimen by advancing the piston. K is the stiffness of the loading system which is represented by a spring in the diagram.

Figure 32 shows a hypothetical plot of the axial force required to cause sliding on the surfaces as a function of the axial displacement in the specimen. Sliding will proceed without stick-slip until the point B is reached. Beyond B if the stiffness of the spring is K_2 the force in the spring is greater than the force required to cause movement and the sliding surface will accelerate. The acceleration will continue until the point C is reached when the force in the spring equals the friction force. The area A has the dimensions of force times displacement and represents the excess kinetic energy of the moving system if damping is negligible. For displacements beyond

C the friction force is greater than the force in the spring and the moving surface decelerates until the surface comes to rest at the point D when the area above the straight line equals the area below. The force in the spring is now well below the friction force and the surfaces will remain stationary until the spring force is increased to the point E and sliding will recommence. Stick-slip will reoccur whenever the force displacement curve has a greater slope than the force-displacement function of the loading system.

If the moving system is damped so that the kinetic energy during slip is decreased then the magnitude of the force drop during slip will be less. Elimination of stick-slip is possible if the slope of the force-displacement function K_1 in Figure 31 is greater than the slope of the friction force-displacement curve. This has been verified experimentally by Rabinowicz (1959).

There are two main conditions under which stick-slip occurs with metals. One is the sliding of clean like metals in which the junctions in the contact area coalesce to form super junctions and this gives rise to severe fluctuations in the friction force (Rabinowicz, 1959). The other case is when the surfaces are partially coated with lubricant. The fluctuations in friction arise because the sliding surface traverses alternate regions covered by

the lubricant and regions from which the lubricant is absent.

Under normal circumstances, however, stick-slip does not occur with metals but with brittle materials stick-slip is almost universal. Bridgman (1935, 1936, 1937, 1946) found that in the shearing of metals at very high normal stresses the shearing took place smoothly, but brittle materials invariably sheared with a jerky movement. This occurred up to normal stress of 50 kb which was the highest stress investigated by Bridgman. This suggests that there may be some fundamental differences between the frictional behavior of metals and brittle materials. For metals the shear force required to cause sliding is dependent on the true area of contact. The area of contact will be constant during sliding if the normal load remains the same. Therefore the frictional force will be independent of the displacement and stick-slip will not occur.

With brittle materials however, if the frictional force is determined by the force required to break through the interlocking irregularities there will be a sudden drop in the friction as fracture occurs. The friction force will rise when the irregularities on the surfaces interlock once more. This variation in the friction with displacement will give rise to stick-slip.

Figure 33 shows the differential stress required to cause sliding on a ground surface as a function of the percent axial shortening of the specimen. Stick-slip motion occurred in the regions shown by the dotted lines. The magnitude of the stress drop during slip is variable. An explanation for this phenomenon is given below.

Figure 34 shows the hypothetical plot of the friction force against displacement for sliding on a ground surface. The minor fluctuations are caused by the sudden drop in friction when the interlocking asperities on the surfaces fail by brittle fracture. Superimposed on this minor variation there is a gross change in friction with displacement. This is caused by changes in the contact area and the amount of wear particles on the surfaces. This phenomena will be discussed in detail in the next section. The straight lines with the slope of K represent the force-displacement function of the loading system. In the region where the mean friction force increases, the stress drops during slip should be small. Large stress drops would be expected in the region where the mean friction decreases. There should be moderate stress drops when the mean friction force is constant. This would be an explanation for the variation in the magnitude of the stress drops with displacement for ground surfaces.

Change in Friction with Displacement

One striking feature of the experimental results (see Figure 20 for example) is the change in friction on ground surfaces with the distance of sliding. It was found that within the first 0.1 cm of sliding (see 11/100, figure 21), the damage to the surfaces was confined to isolated regions. This indicates that contact was initially made over only a small portion of the surfaces. This would occur if the surfaces were not perfectly flat when they were originally placed together. After about 0.1 cm of sliding had occurred it was found that there was a fine layer of frushed material covering the whole of the surfaces (see 12/100, figure 21). This suggested that during the first 0.1 cm of sliding the out-of-flatness across the surfaces was eliminated by wear until intimate contact was established. When examined under a microscope the crushed material on the surface was found to be extremely fine and the depth of this layer of loose material appeared to be much smaller than the height of the irregularities on the surfaces. If this is correct then the amount of material to be sheared through for sliding to occur will not differ very much from what it would be for perfectly mating surfaces. The friction for ground surfaces after about 0.1 cm of sliding should be about the same as the initial friction for perfectly mating surfaces.

The points in Figure 23 are the maximum friction for ground surfaces and they scatter about the dashed line which is the best fit for the initial friction for interlocking surfaces (Figure 25).

The physical processes involved in sliding when contact between the surfaces is confined to isolated regions are no different from the physical processes when contact is made over the whole of the surfaces. The interlocking irregularities must be sheared through in order for sliding to take place. If the area of true contact is small the force required to shear the asperities is less than it would be if the true contact area is large. Analytically this can be described in the following way.

The friction stress for perfectly mated surfaces is given by the equation

$$\tau = 0.5 + 0.6\sigma_n \qquad (47)$$

The stresses τ and σ_n are the average stresses over the real area, A, of the surfaces in contact. If interlocking is confined to isolated regions on the surfaces, then real area is less than apparent area of contact, A_a. The apparent stresses, τ_a and σ_{na} become

$$\tau_a = \frac{A}{A_a}\tau \qquad (48)$$

$$\sigma_{na} = \frac{A}{A_a} \sigma_n \tag{49}$$

Substitution of equations 48 and 49 into equation 47 yields

$$\tau_a = 0.5 \frac{A}{A_a} + 0.6\sigma_{na} \tag{50}$$

If A is less than A_a then the frictional shear stress will be smaller than it would be if the apparent area of contact was equal to the true area of contact.

Beyond about 0.1 cm of sliding on ground surfaces the friction decreases. Examination of the surfaces revealed that in this region the layer of loose wear particles on the surfaces increased in thickness and after about 0.5 cm of sliding, the surfaces were completely coated with a fine friable white powder. In this region the particles may roll and this is most probably the reason for the reduction in friction.

FIGURE CAPTIONS

Figure

14 Schematic diagram of friction experiments G has a ground surface, F has a fracture surface, V is a virgin rock with the shear surface after fracture indicated by the dashed line.

15 Method of jacketing specimens.

16 Method of preparing mated surfaces.

17 5 kb pressure vessel.

18 Typical record of friction experiment data.

19 Initial friction for ground surfaces (3 roughnesses).

20 Friction *versus* displacement for ground surfaces.

21 Ground surfaces after sliding. (Scale is in cm) Upper left to lower right progressively greater amount of relative displacement between the surfaces. Tests Nos.(11, 12, 13, 14, 15, 16)/100.

22 Wear particles on surfaces after sliding. Largest particles approximately 0.1 mm in diameter.

23 Shear stress *versus* normal stress for maximum friction on ground surfaces.

24 Friction *versus* displacement for mated surfaces.

25 Shear stress *versus* normal stress for initial friction on mated surfaces.

26 Axial stress *versus* confining pressure at fracture.

27 Shear stress *versus* normal stress at fracture.

28 Differential stress *versus* percent axial strain (confining pressure 6.6 kb).

Figure

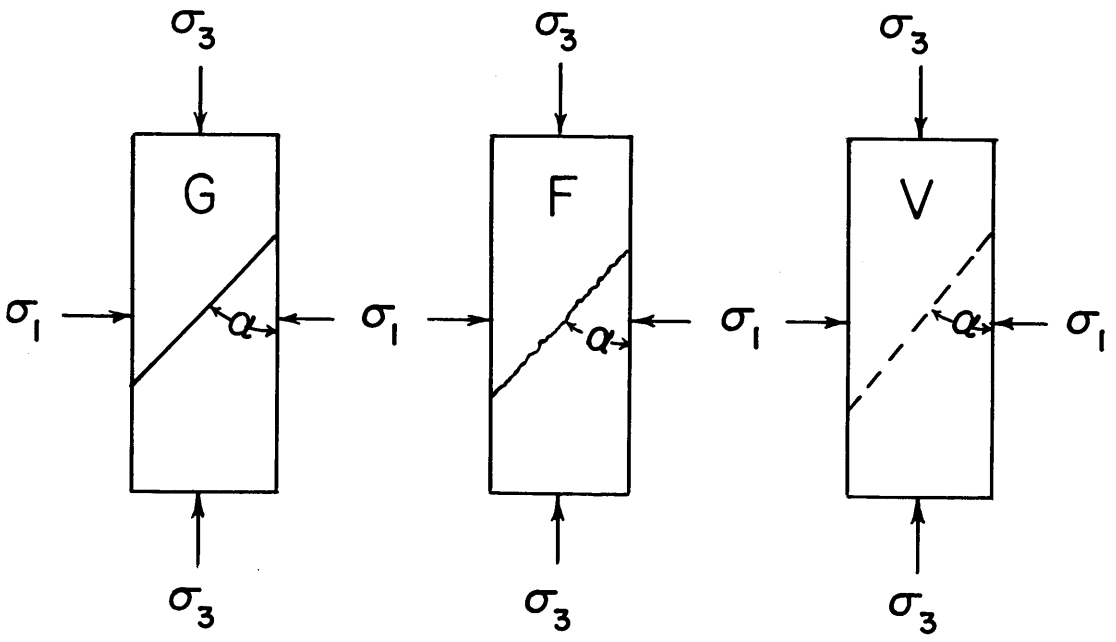

$$\sigma_n = \left(\frac{\sigma_3 + \sigma_1}{2}\right) - \left(\frac{\sigma_3 - \sigma_1}{2}\right) \cos 2\alpha$$

$$\tau = \left(\frac{\sigma_3 - \sigma_1}{2}\right) \sin 2\alpha$$

$$\mu = \tau / \sigma_n$$

FIG.14

JACKETING PROCEDURE

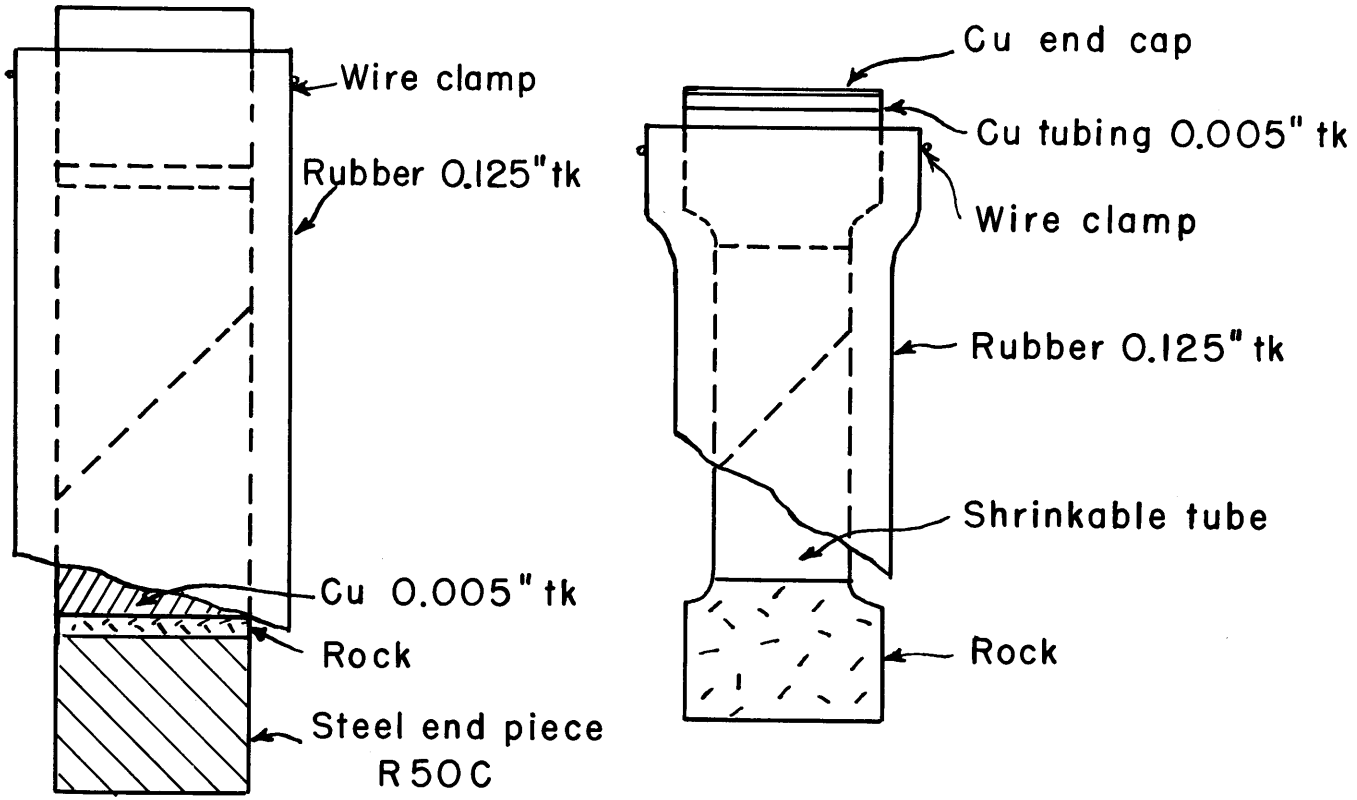

FIG.15

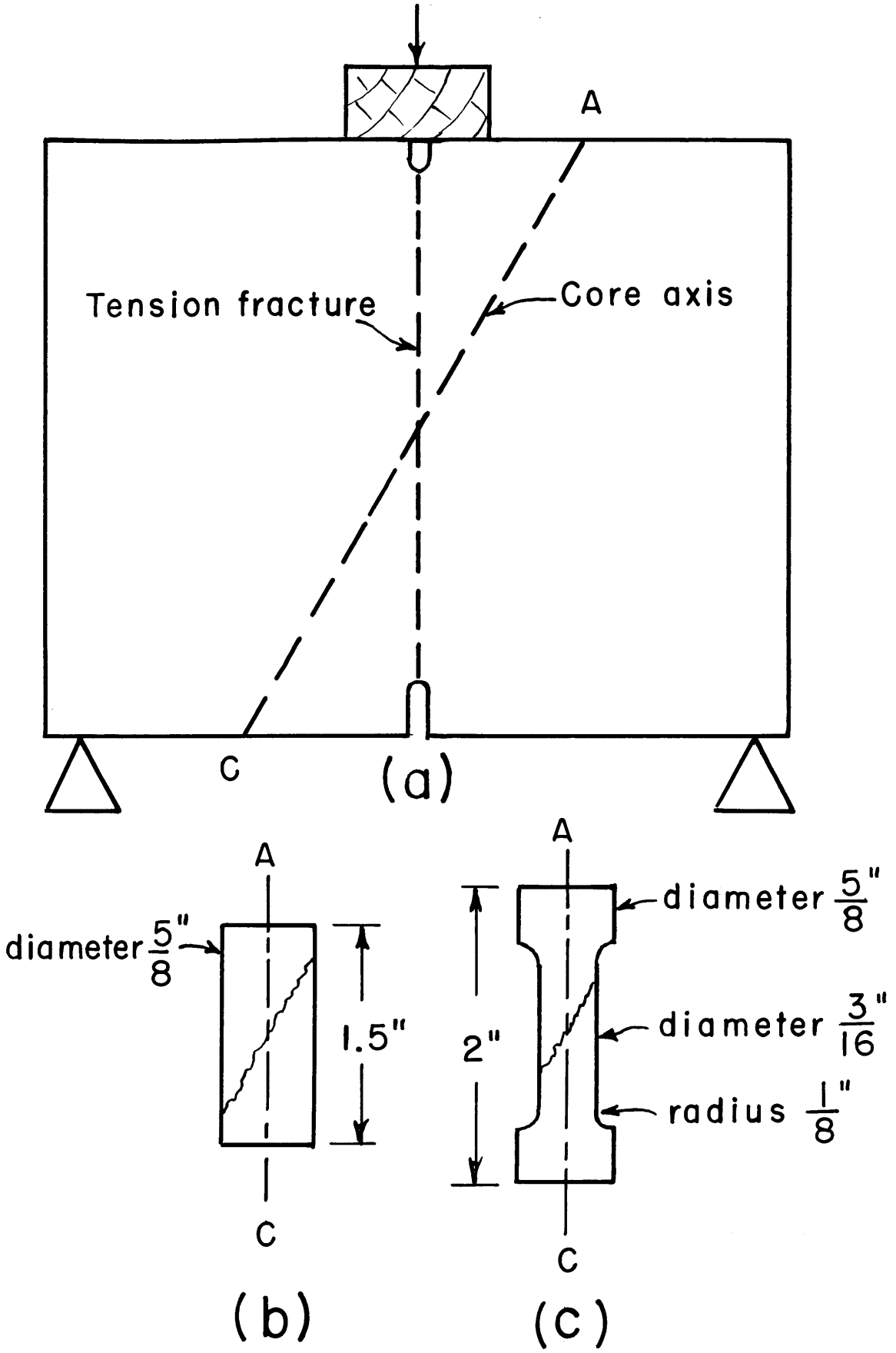
A
Tension fracture
Core axis
C
(a)
A
diameter 5/8"
1.5"
C
(b)
A
diameter 5/8"
2"
diameter 3/16"
radius 1/8"
C
(c)

FIG.16

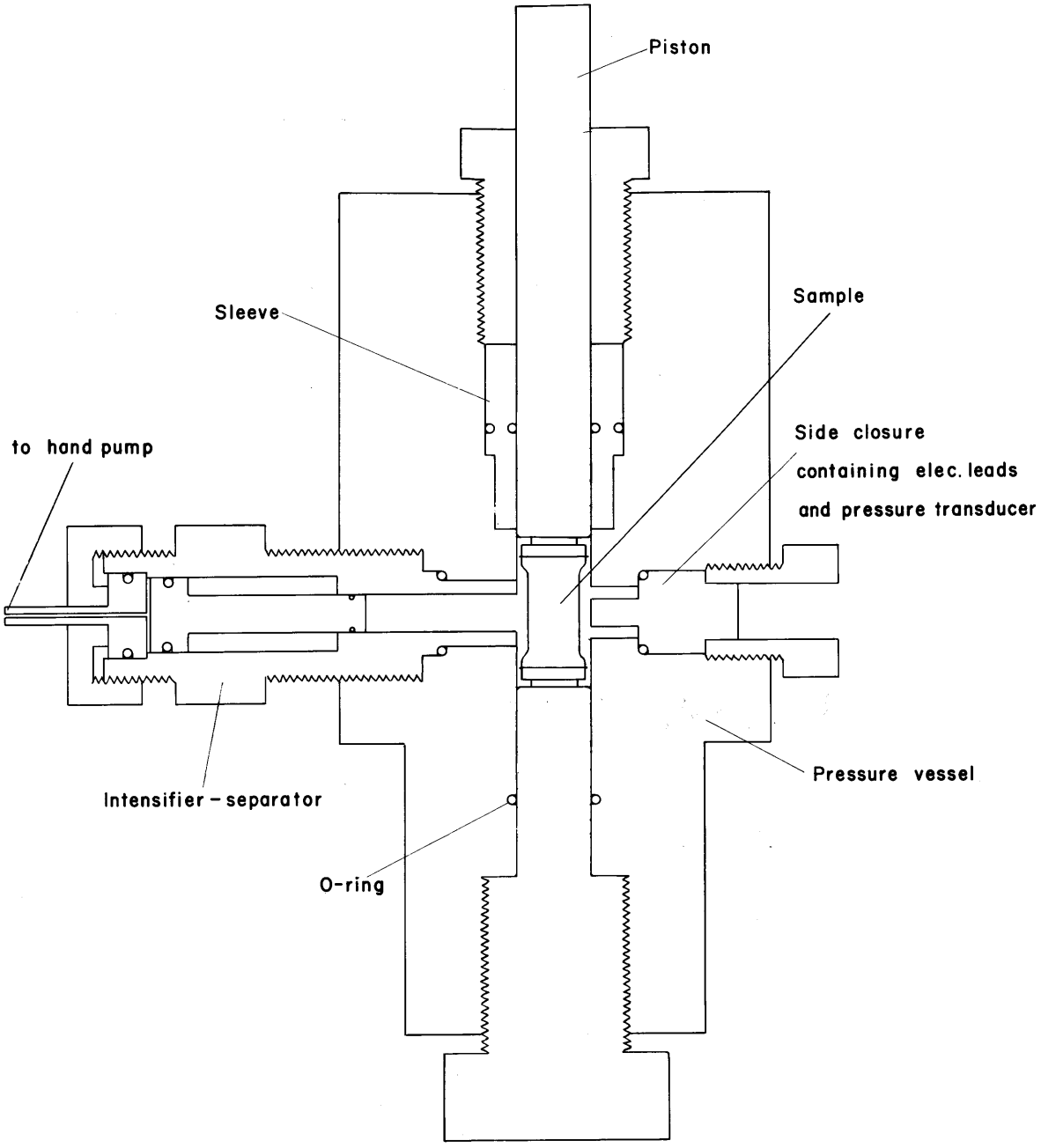
Piston
Sleeve
Sample
to hand pump
Side closure
containing elec. leads
and pressure transducer
Intensifier – separator
Pressure vessel
O-ring

FIG.17

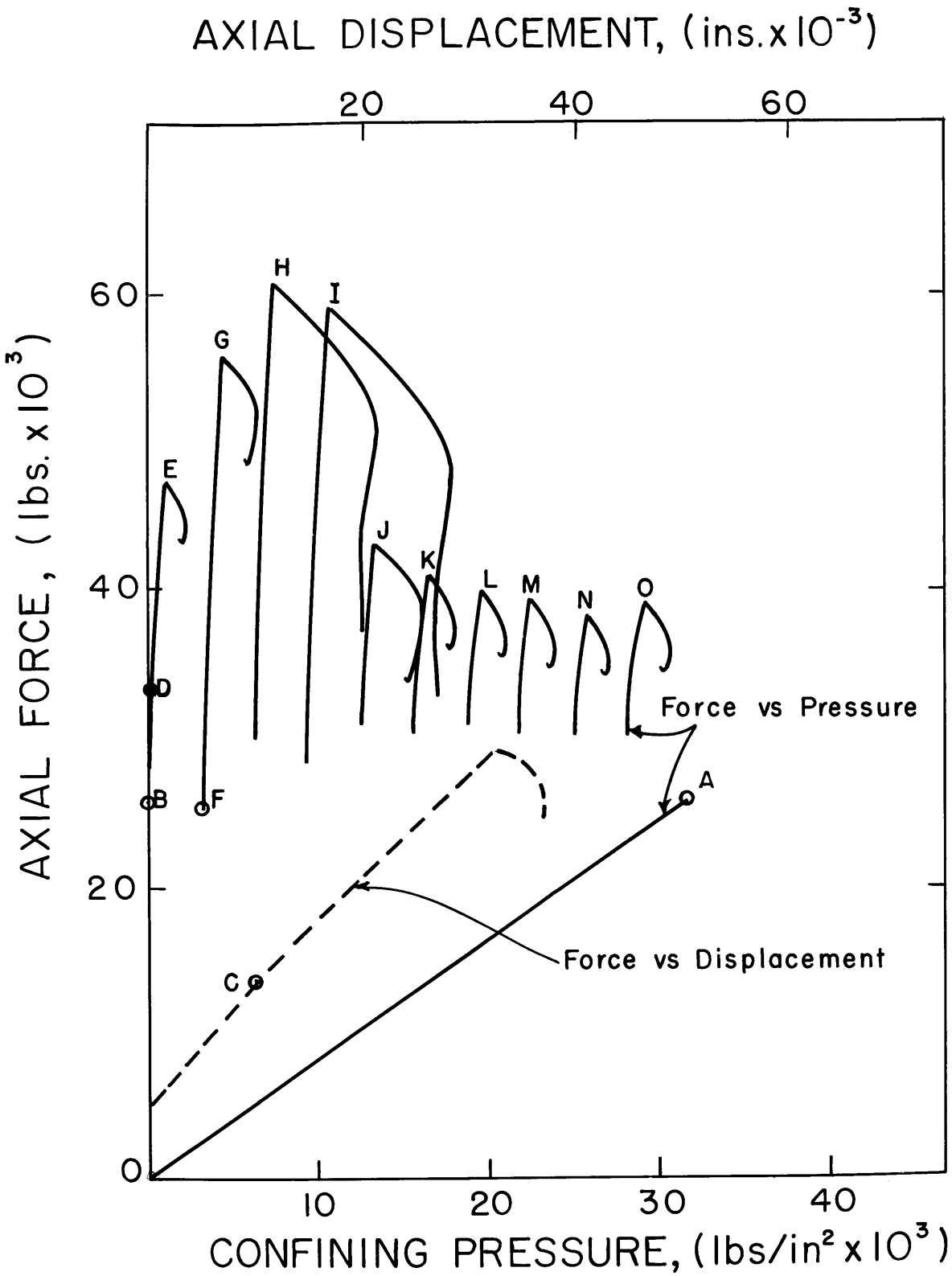
AXIAL DISPLACEMENT, (ins.x10⁻³)
20
40
60
AXIAL FORCE, (lbs.x10³)
60
40
20
0
H
I
G
E
J
K
L
M
N
O
D
B
F
A
C
Force vs Pressure
Force vs Displacement
10
20
30
40
CONFINING PRESSURE, (lbs/in² x10³)

FIG. 18

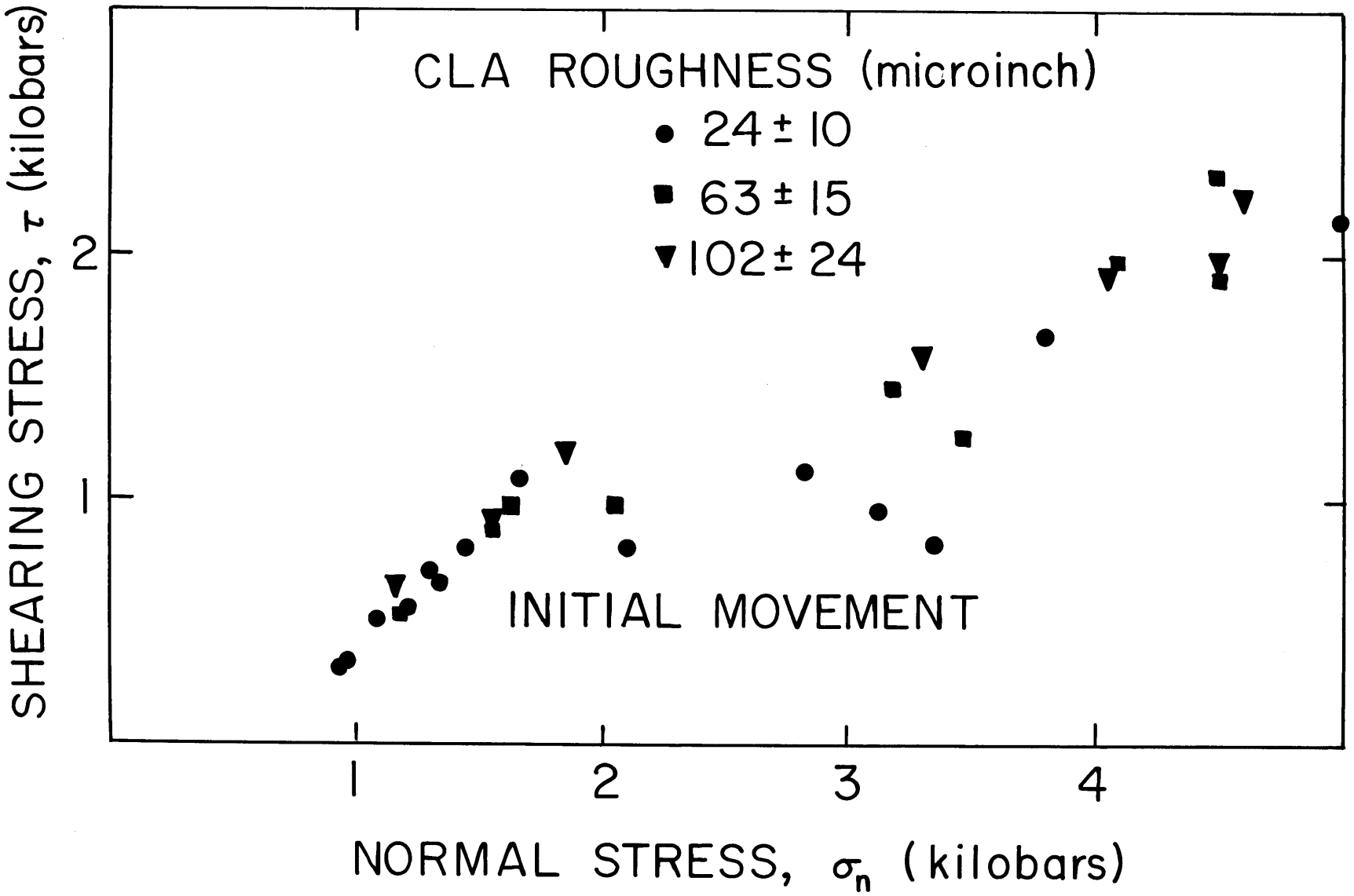
CLA ROUGHNESS (microinch)
• 24 ± 10
■ 63 ± 15
▼ 102 ± 24
INITIAL MOVEMENT
SHEARING STRESS, τ (kilobars)
NORMAL STRESS, σn (kilobars)
1
2
3
4

FIG. 19

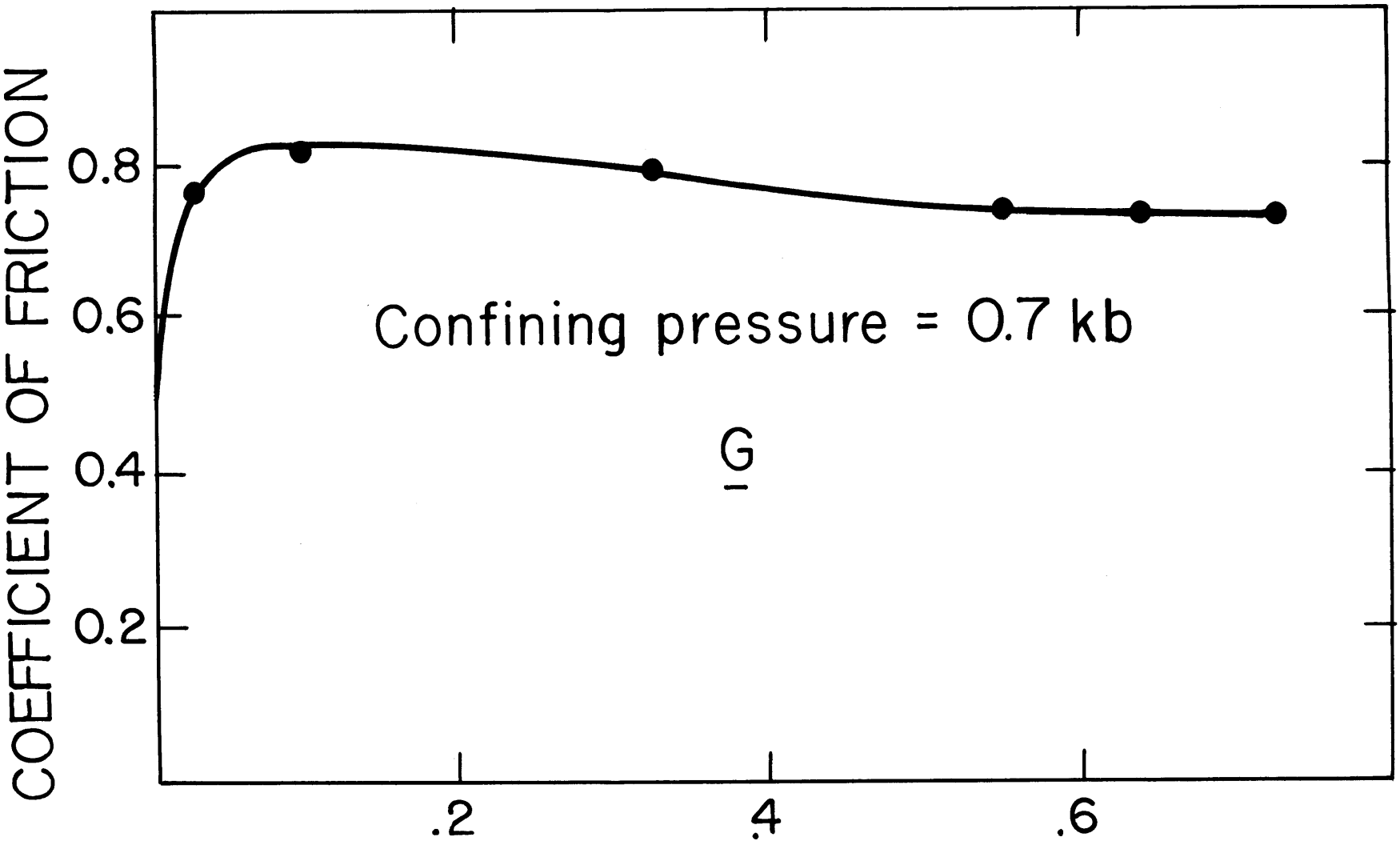
COEFFICIENT OF FRICTION
0.8
0.6
0.4
0.2
Confining pressure = 0.7 kb
G
.2
.4
.6
DISPLACEMENT ON SURFACE (cm)

FIG. 20

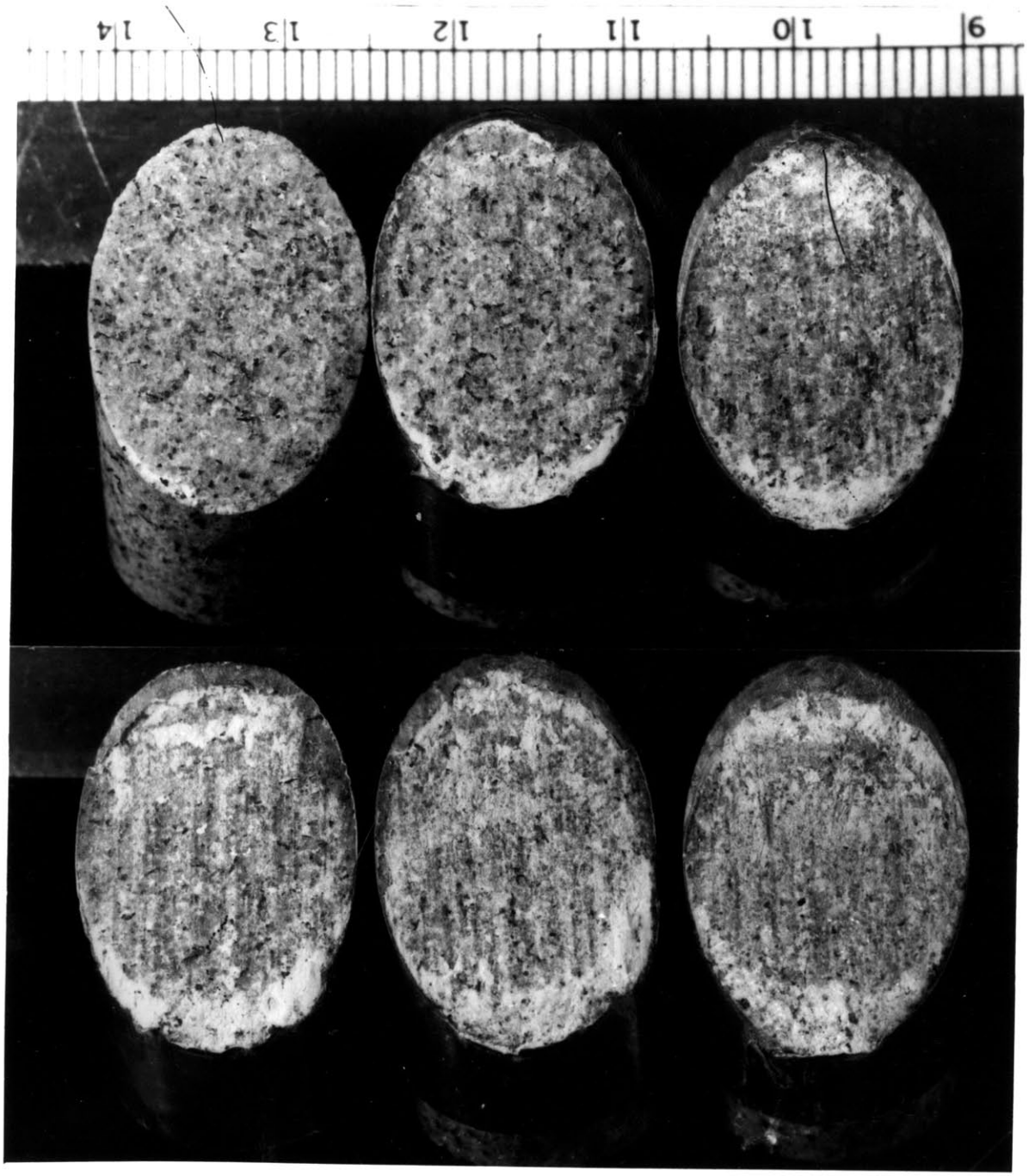

FIG.21

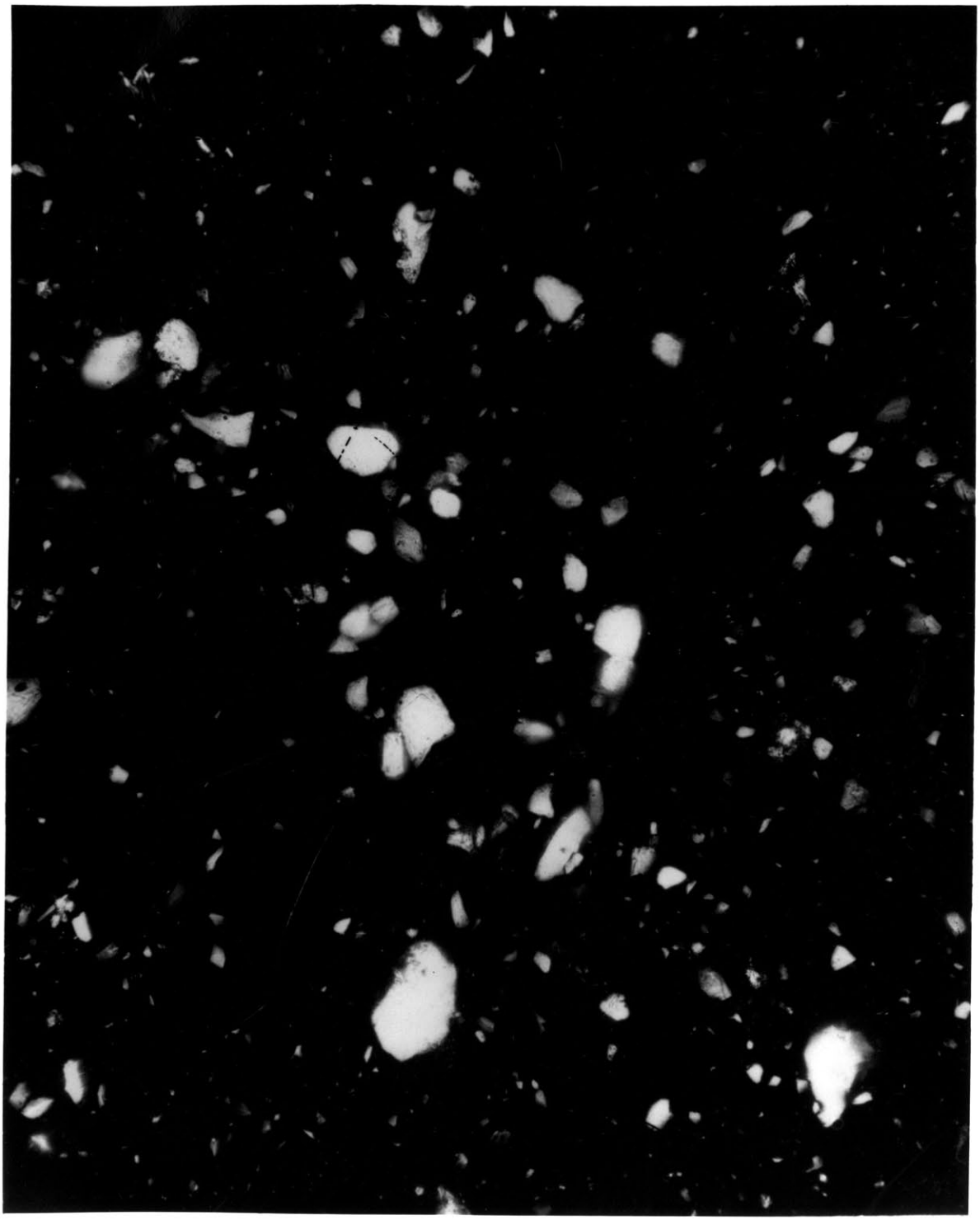

FIG. 22

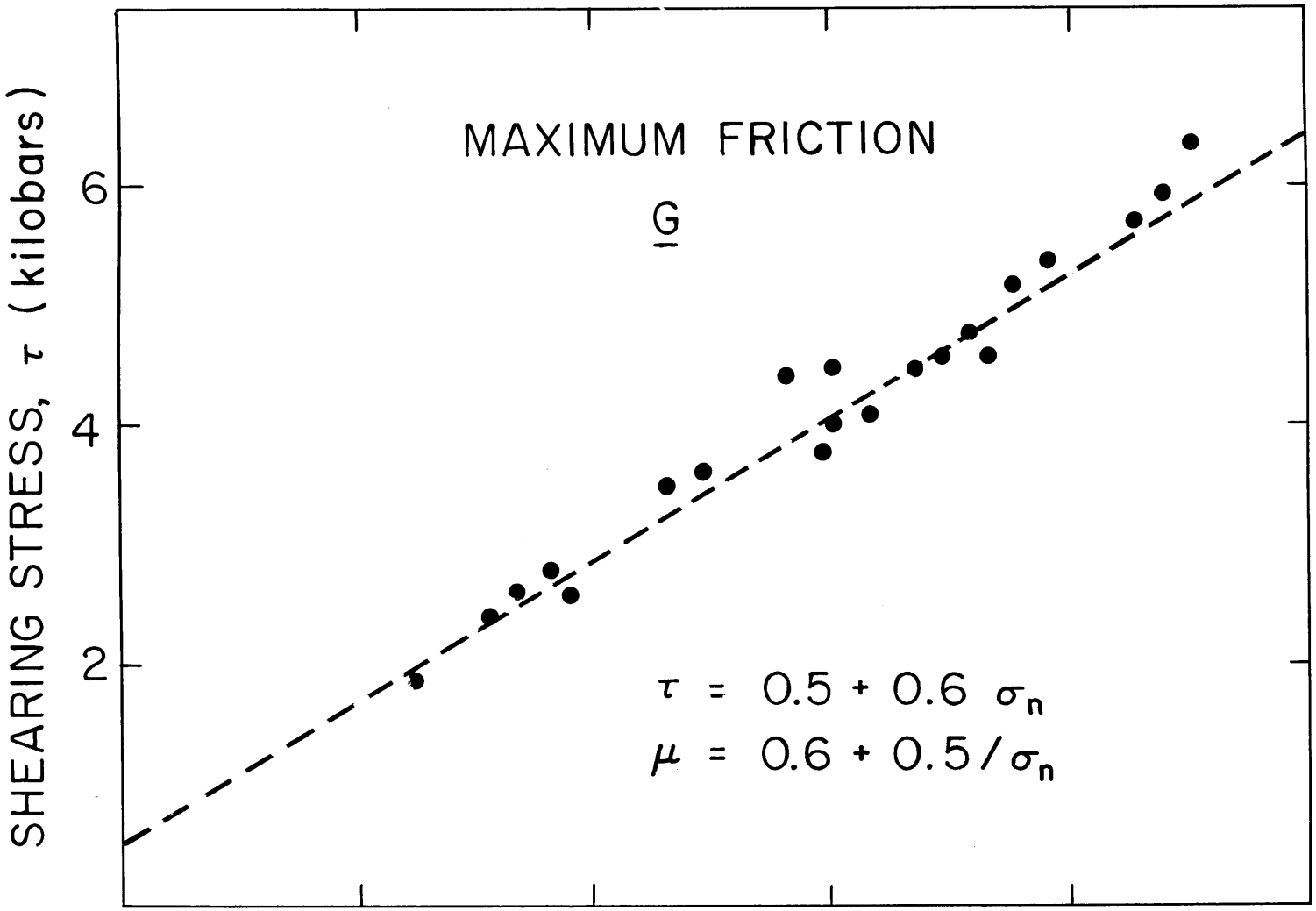
MAXIMUM FRICTION
G
SHEARING STRESS, τ (kilobars)
NORMAL STRESS, σn (kilobars)
τ = 0.5 + 0.6 σn
μ = 0.6 + 0.5/σn
2
4
6
8

FIG.23

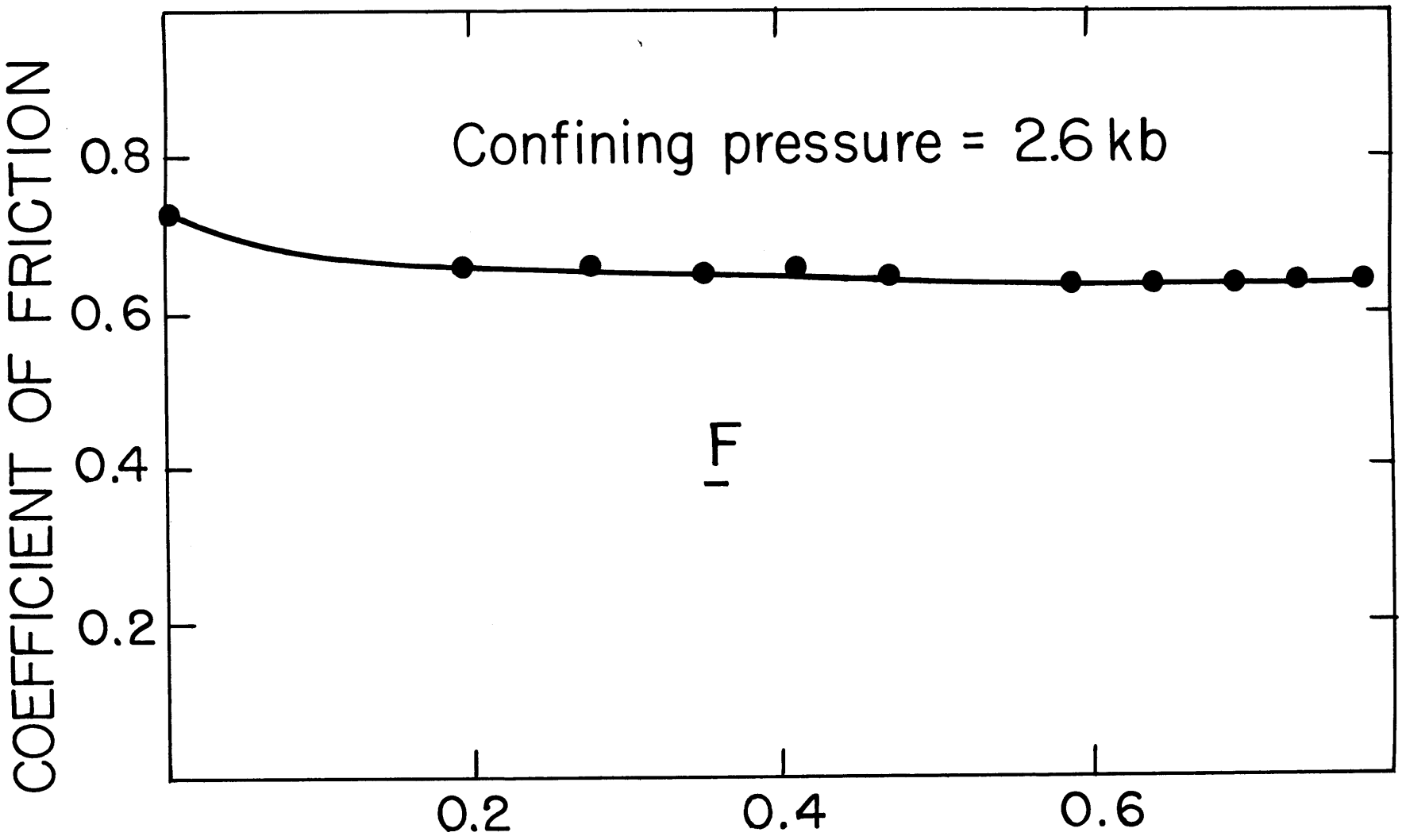
Confining pressure = 2.6 kb
F
COEFFICIENT OF FRICTION
0.8
0.6
0.4
0.2
0.2
0.4
0.6
DISPLACEMENT ON SURFACE (cm)

FIG.24

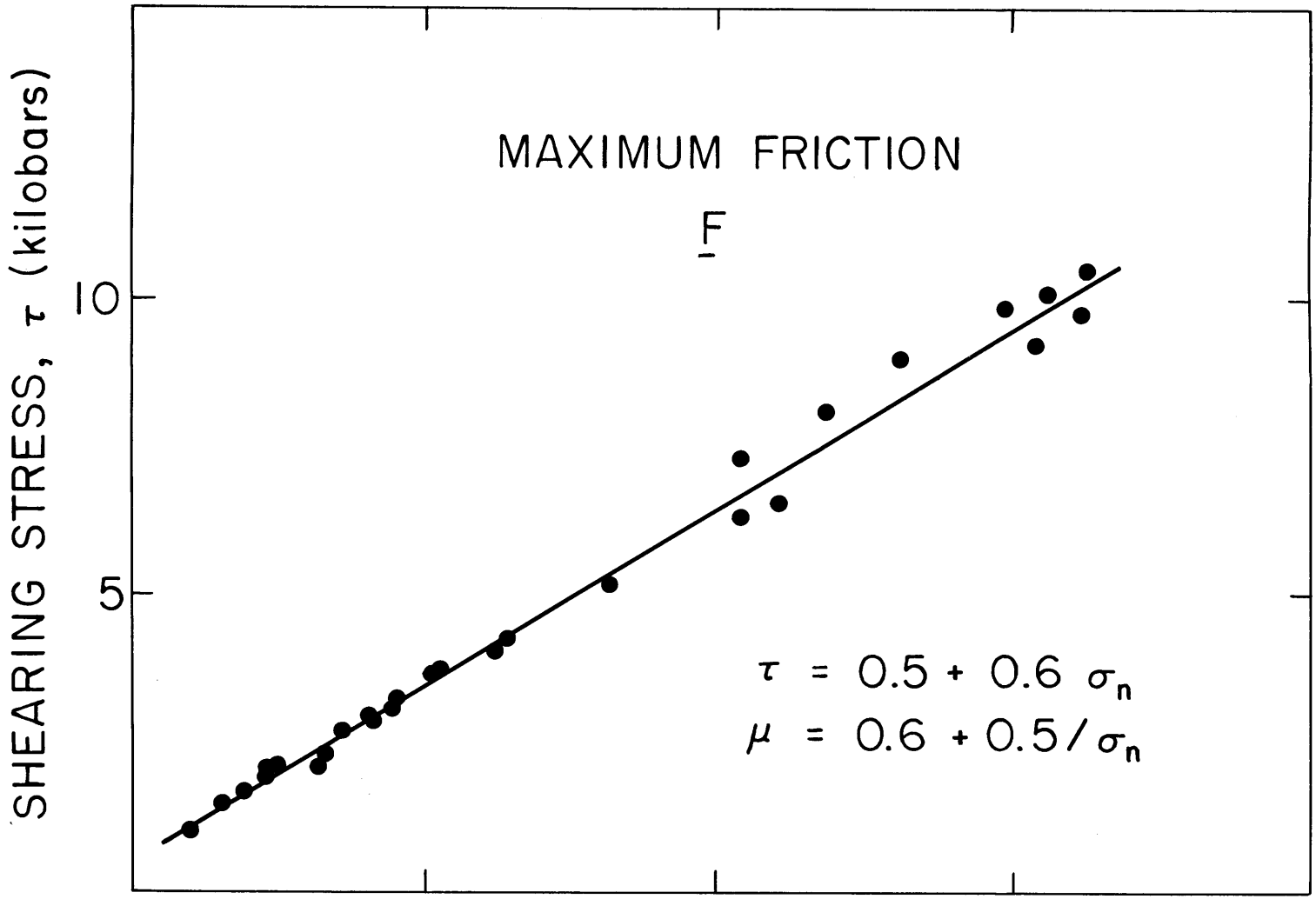
MAXIMUM FRICTION
F
SHEARING STRESS, τ (kilobars)
10
5
τ = 0.5 + 0.6 σn
μ = 0.6 + 0.5/σn
5
10
15
NORMAL STRESS, σn (kilobars)

FIG.25

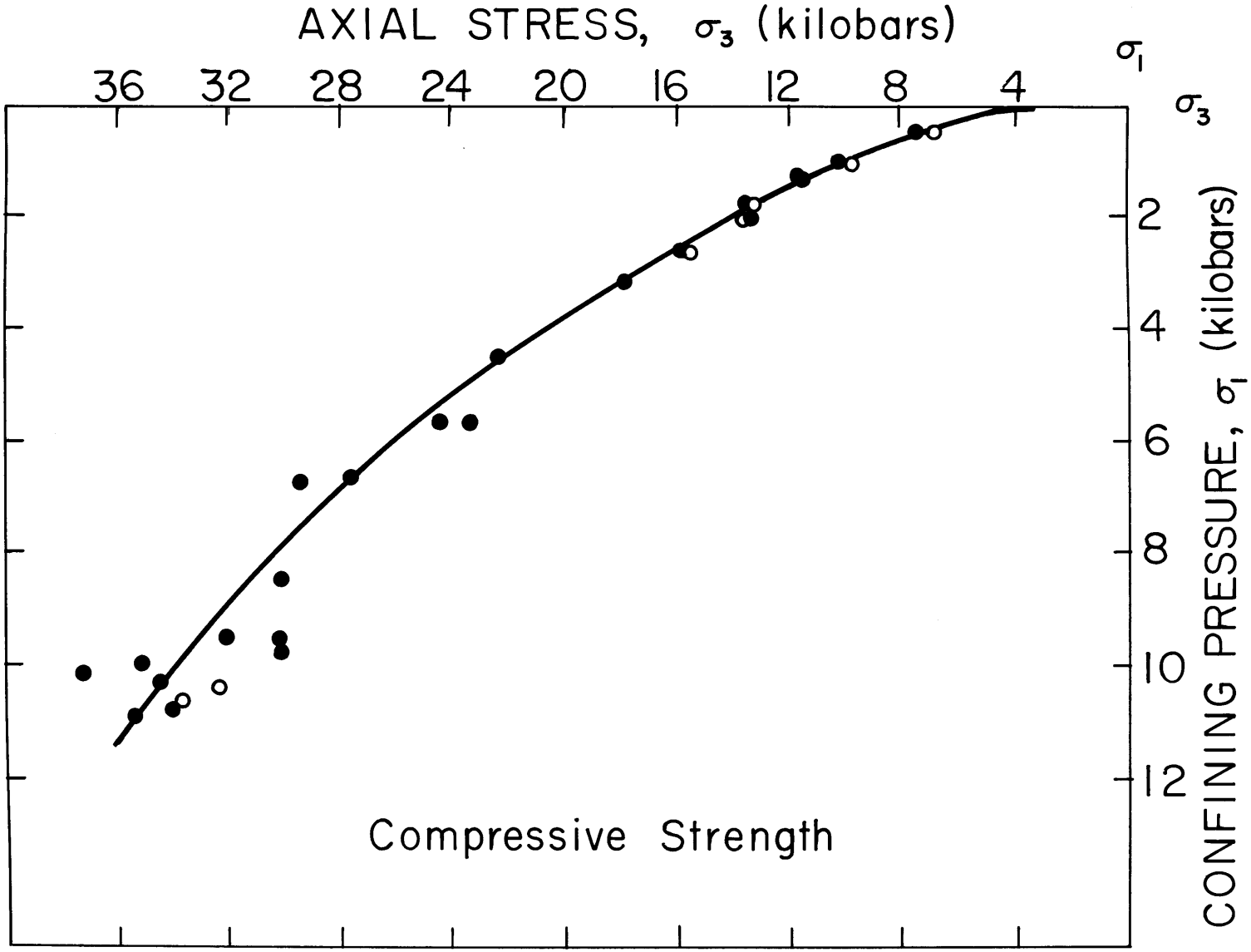
AXIAL STRESS, σ_3 (kilobars)
36
32
28
24
20
16
12
8
4
σ_1
σ_3
2
4
6
8
10
12
CONFINING PRESSURE, σ_1 (kilobars)
Compressive Strength

FIG.26

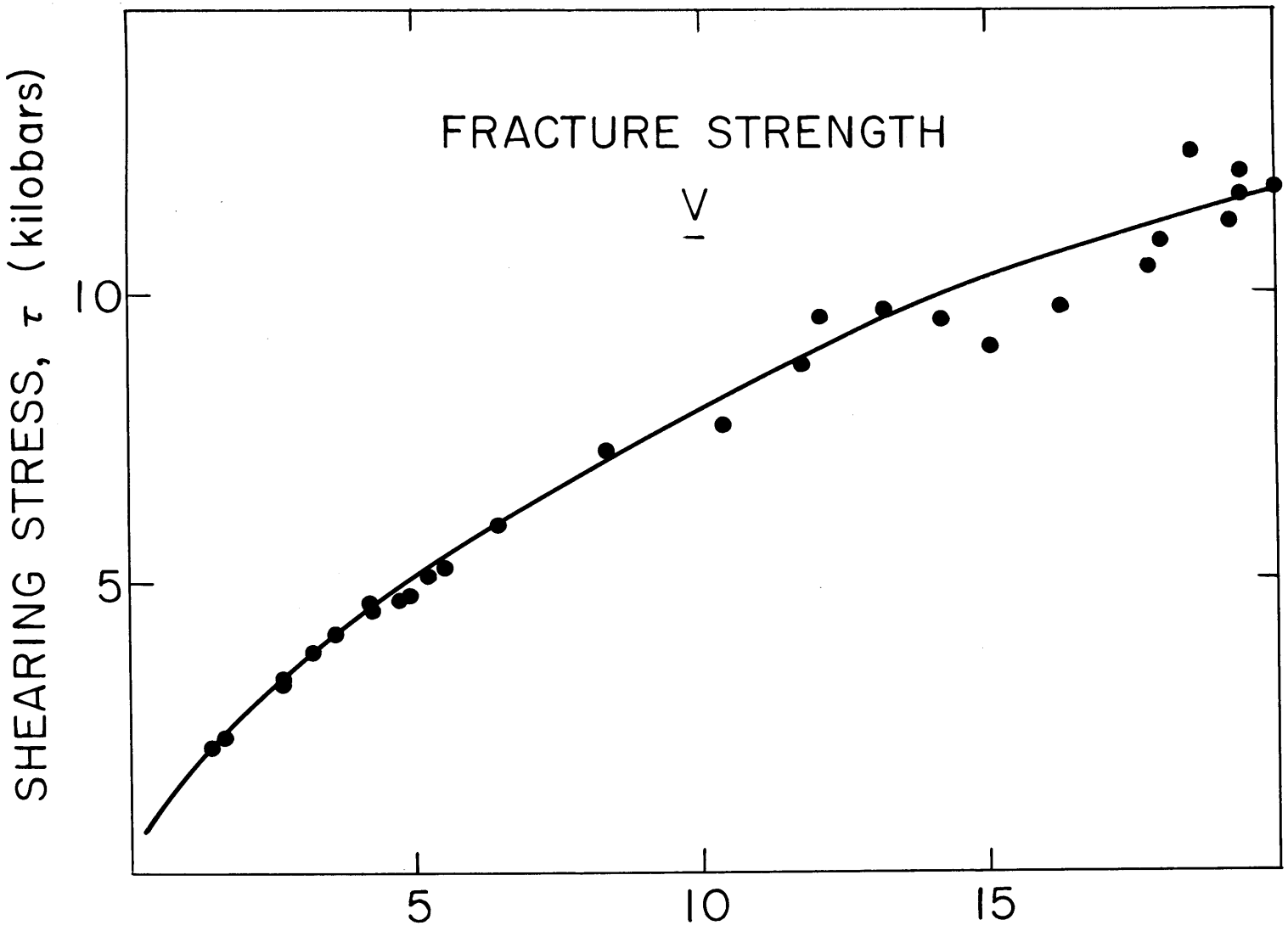
FRACTURE STRENGTH
V
SHEARING STRESS, τ (kilobars)
10
5
5
10
15
NORMAL STRESS, σn (kilobars)

FIG.27

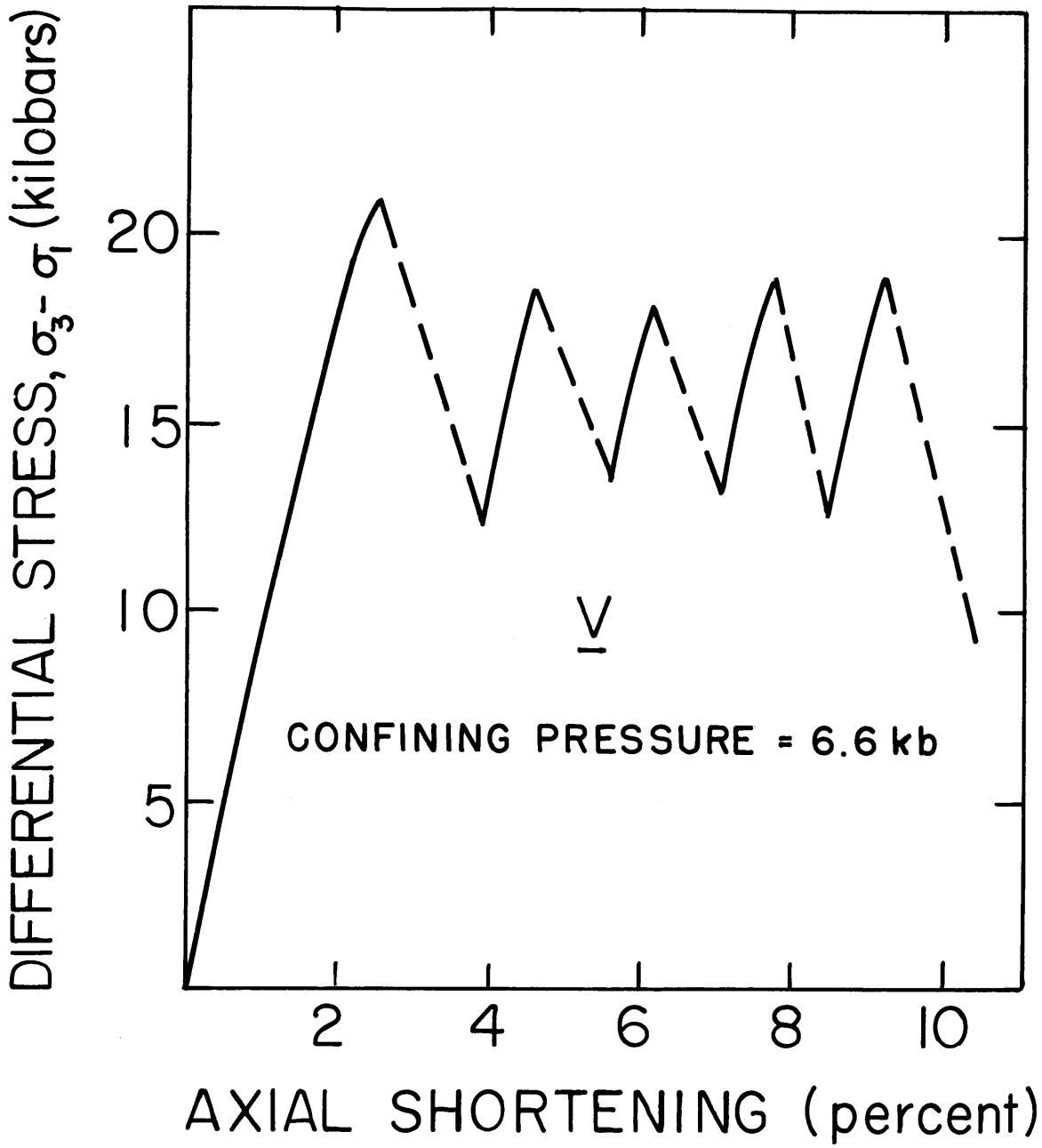
DIFFERENTIAL STRESS, $\sigma_3 - \sigma_1$ (kilobars)
20
15
10
5
V
CONFINING PRESSURE = 6.6 kb
2
4
6
8
10
AXIAL SHORTENING (percent)

FIG.28

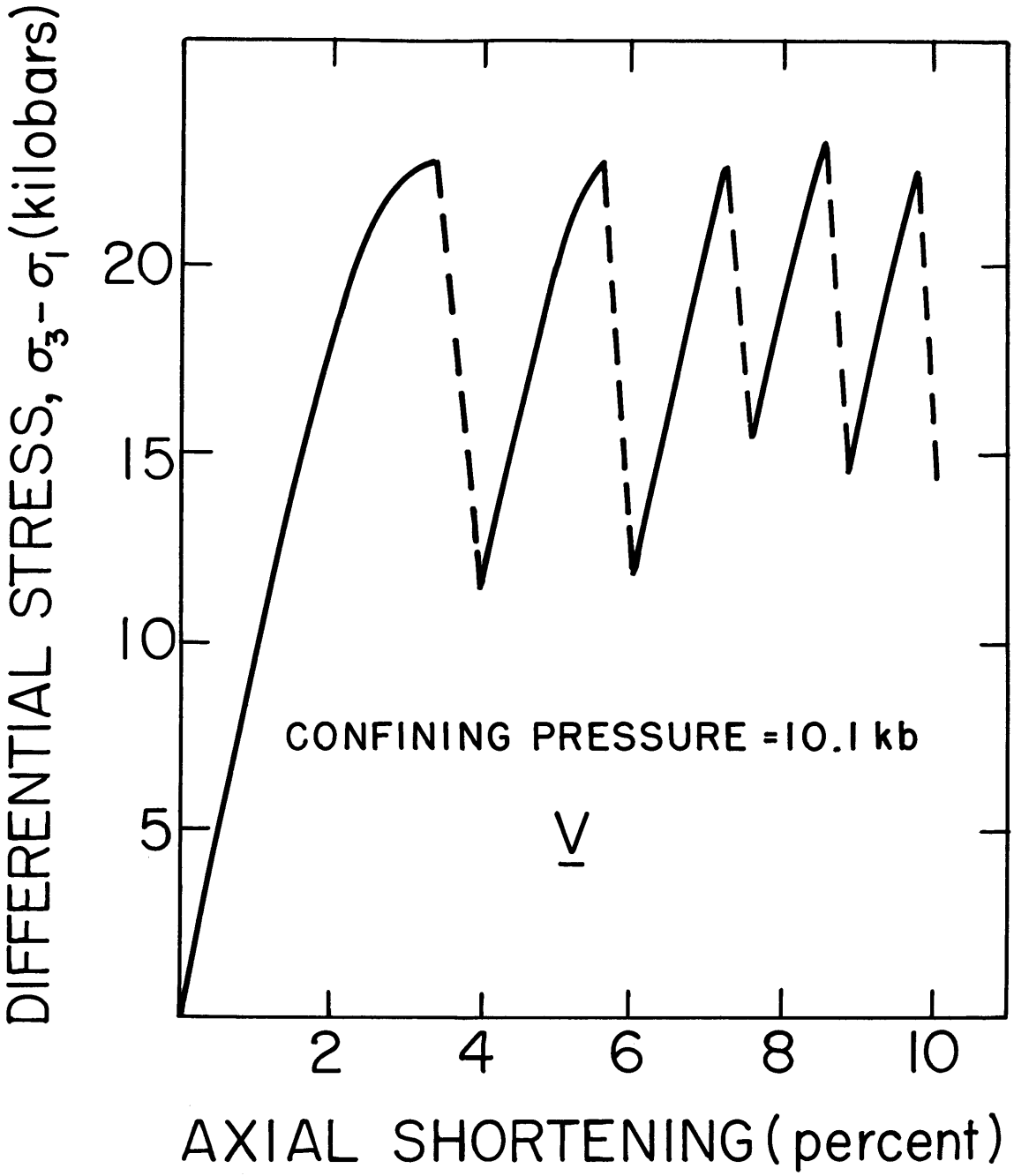
DIFFERENTIAL STRESS, $\sigma_3 - \sigma_1$ (kilobars)
20
15
10
5
CONFINING PRESSURE = 10.1 kb
V
2
4
6
8
10
AXIAL SHORTENING (percent)

FIG. 29

$P_3 > P_2 > P_1$

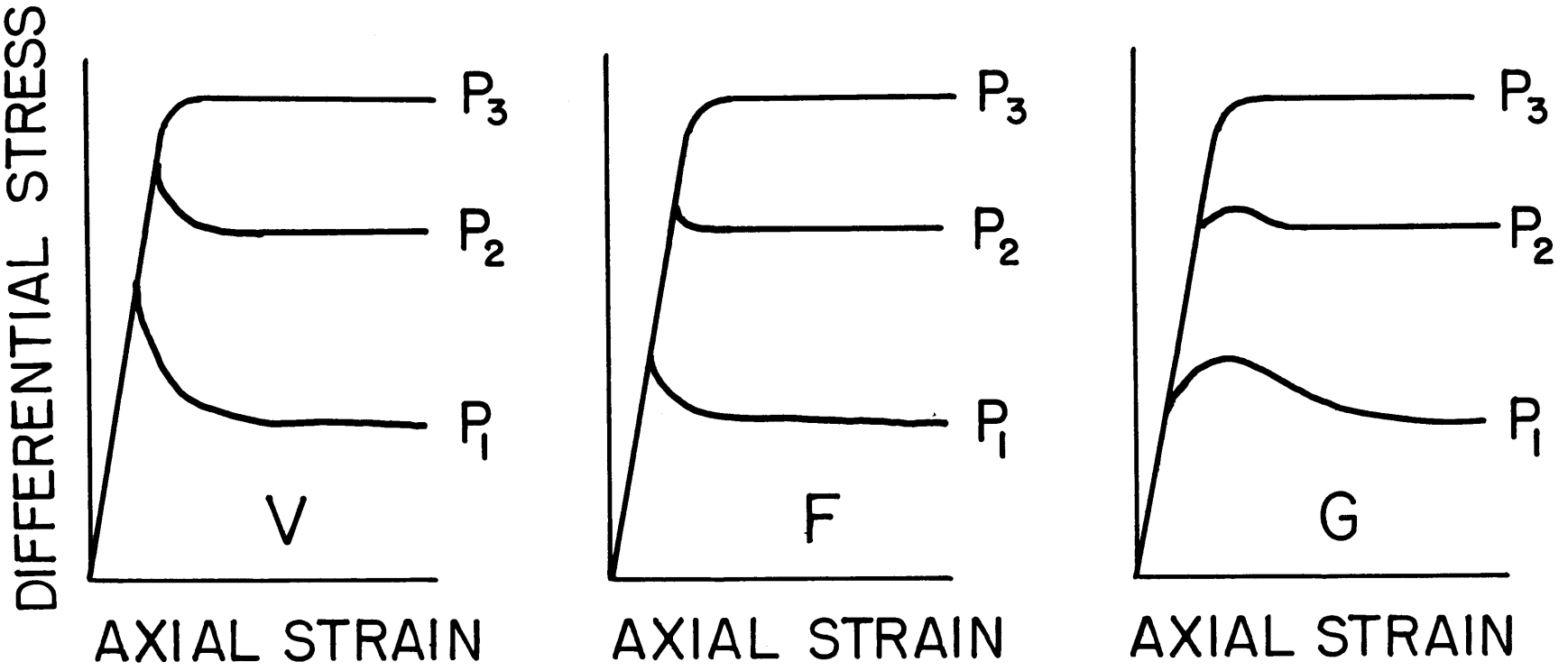

FIG.30

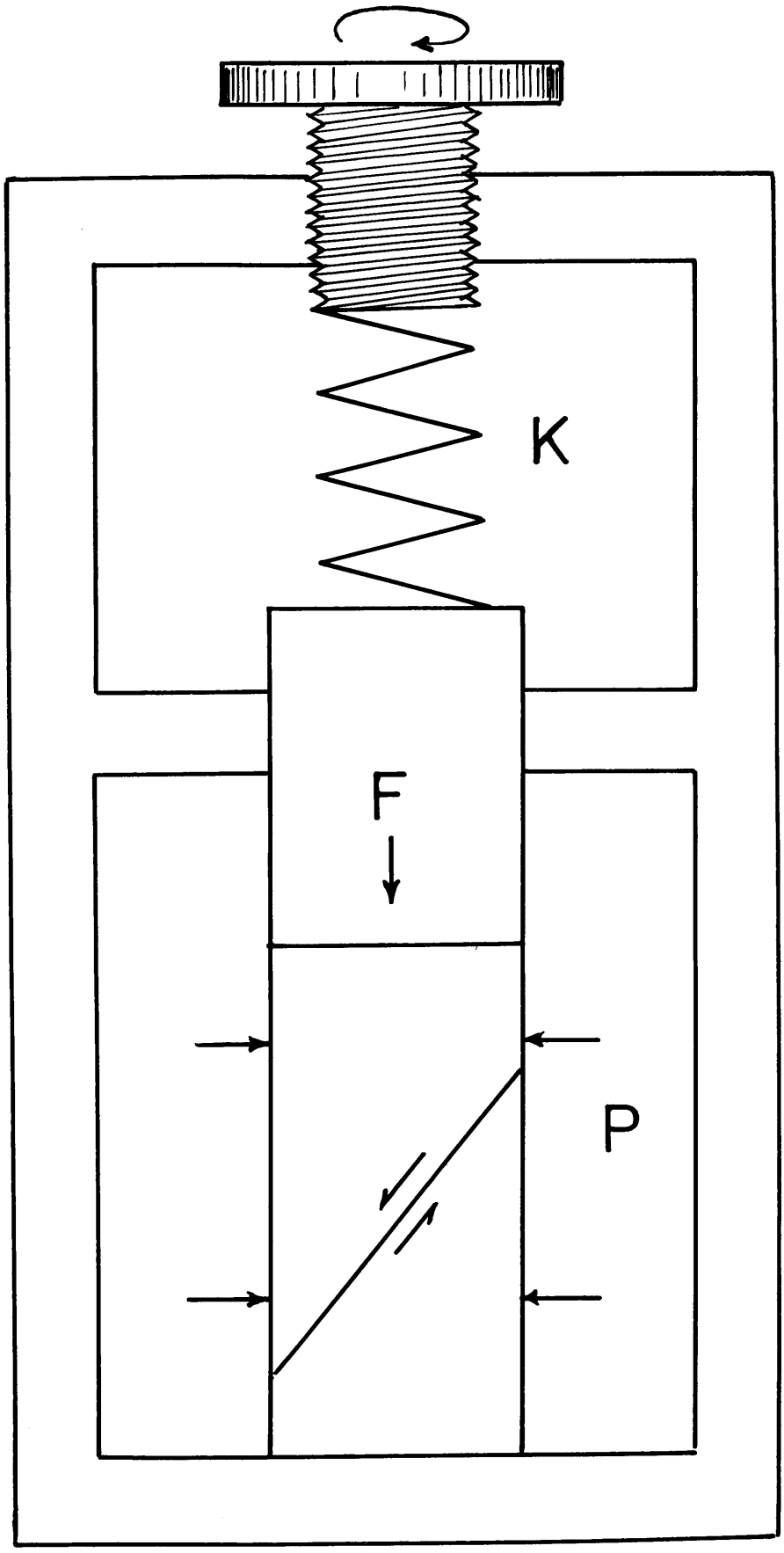

FIG.31

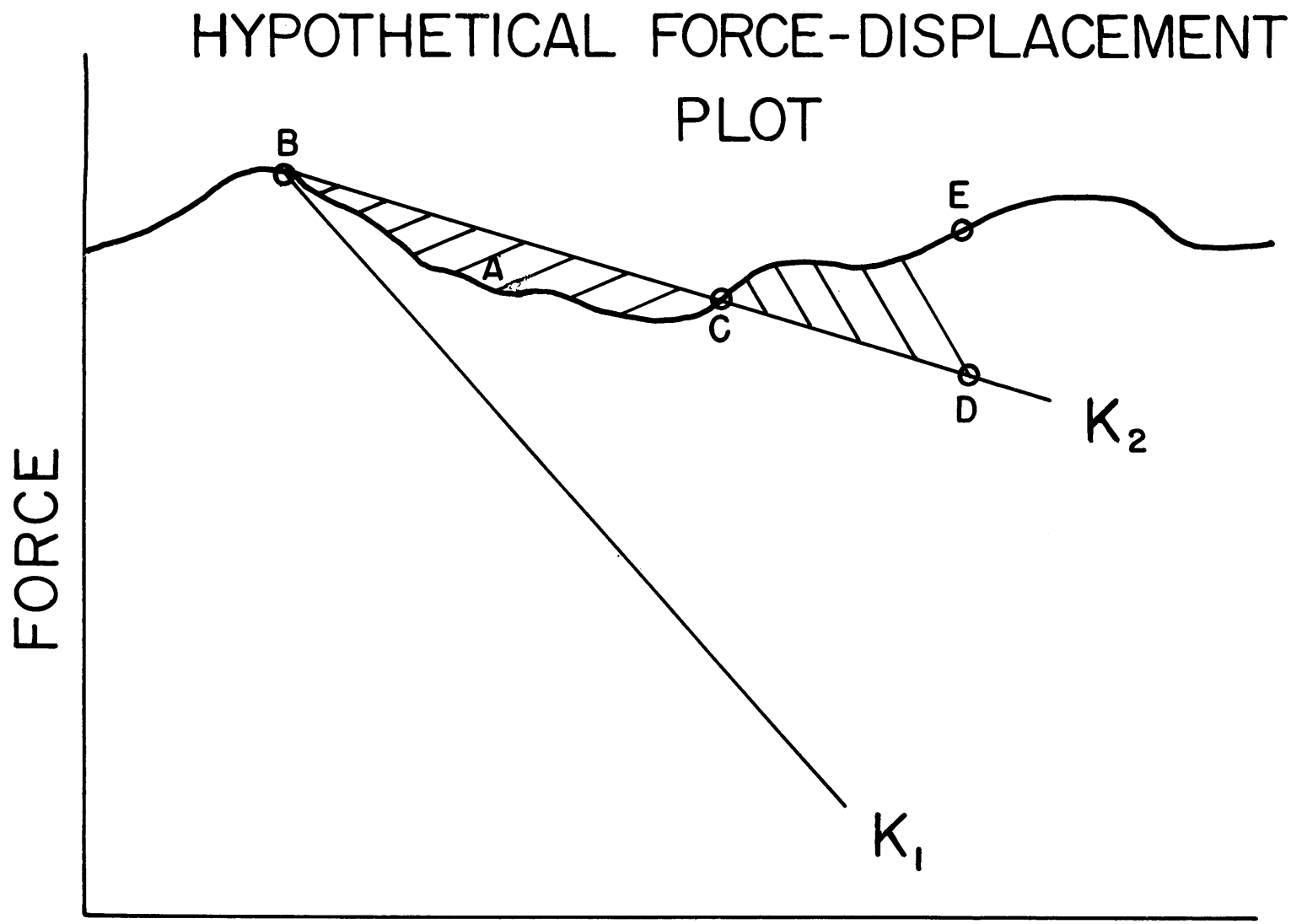
HYPOTHETICAL FORCE-DISPLACEMENT PLOT
B
A
C
D
E
K_2
K_1
FORCE
DISPLACEMENT

FIG 32

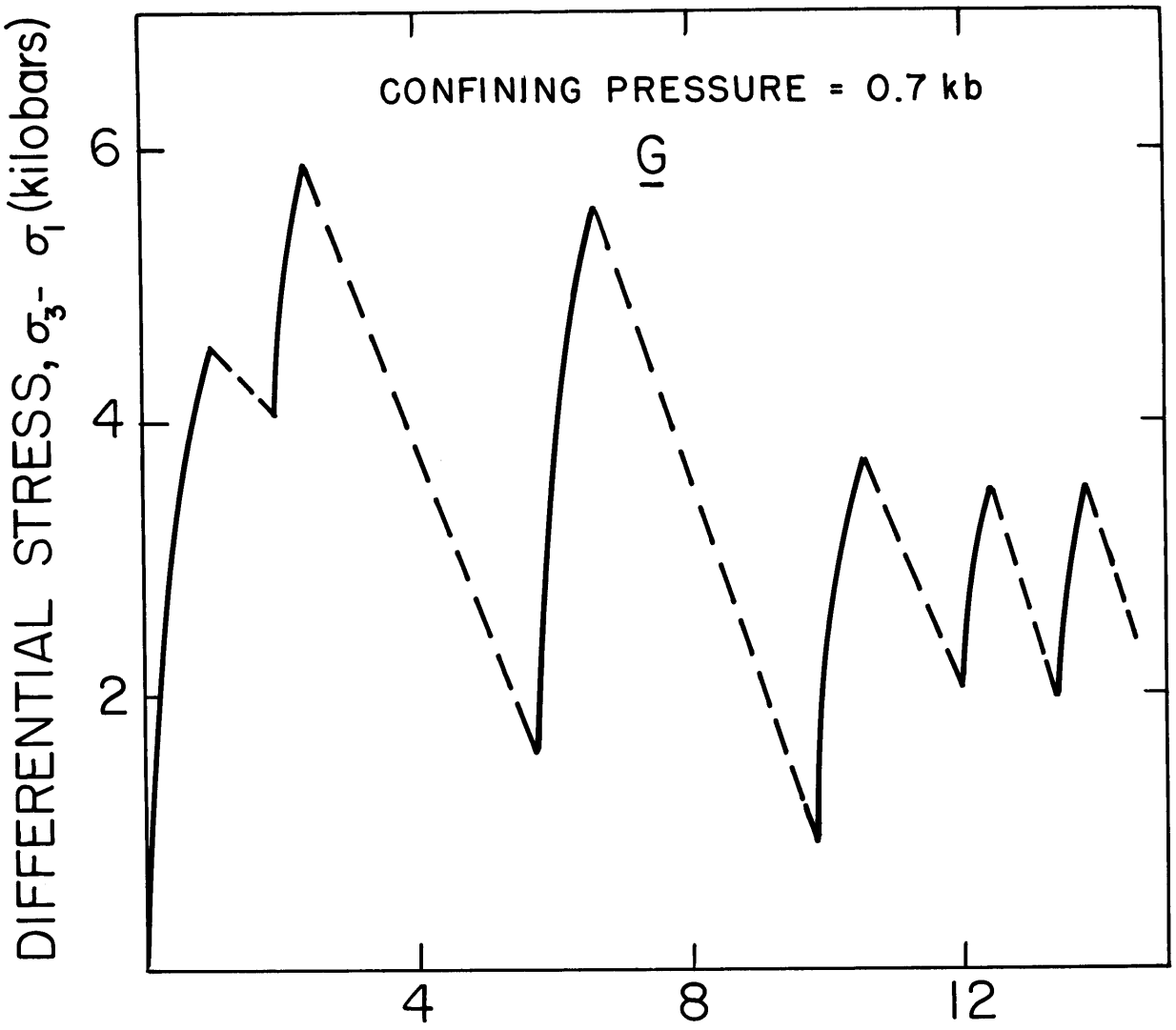
CONFINING PRESSURE = 0.7 kb
G
DIFFERENTIAL STRESS, σ_3- σ_1 (kilobars)
6
4
2
4
8
12
AXIAL SHORTENING (percent)

FIG. 33

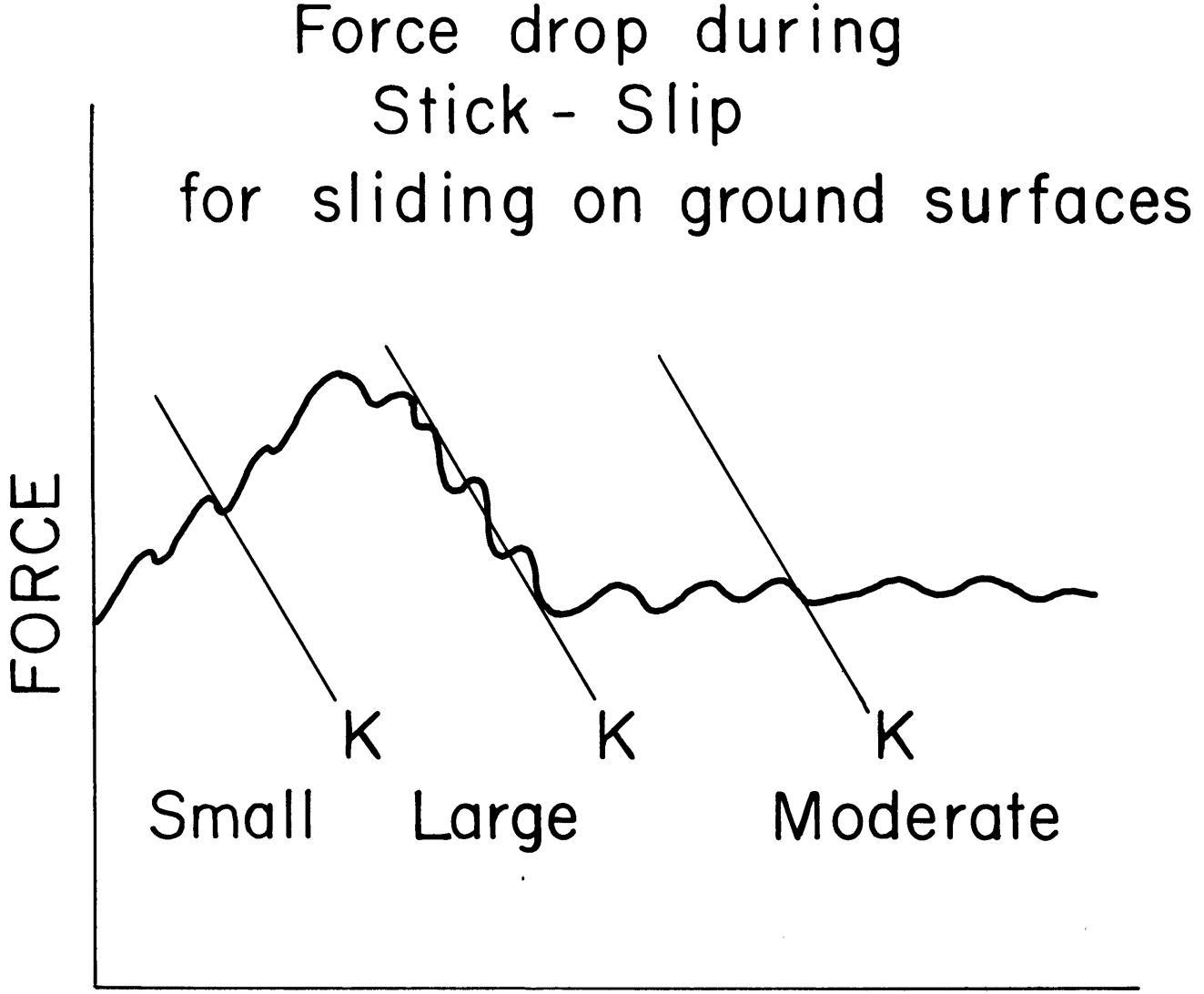
Force drop during
Stick - Slip
for sliding on ground surfaces
FORCE
K
K
K
Small
Large
Moderate
DISPLACEMENT

FIG.34

Table 3

COEFFICIENT OF FRICTION FOR ROCKS

Rock	Type of Surface	Confining Pressure bars	Normal Stress bars	Coefficient of friction
Shale (Seminole)	(1) Natural Shear		34.5	0.7
			138	0.4
Sandstone (Berea)	(1) Natural Shear		69	1.6
			207	1.25
Sandstone (Rush Springs)	(1) Natural Shear		138	1.5
			1034	0.9
Sandstone (Hawksbury)	(2) Natural Shear	200		0.52
		1000		
Sandstone(Wet) (Hawksbury)	(2) Natural Shear	200		0.47
		1000		
Sandstone (Tennessee)	(3) Saw Cut	250		0.76
		2000		0.66
Limestone (Chico)	(1) Natural Shear		69	2.0
			275	
Limestone (Indiana)	(1) Natural Shear		69	1.4
			275	0.7

Table 3 continued

Rock	Type of Surface	Confining Pressure bars	Normal Stress bars	Coefficient of friction
Limestone (Solenhofen)	(3) Saw Cut	250 2000		0.67 0.52
Marble (Carthage)	(2) Natural Shear		138 552	1.8 1.1
Marble (Wombeyan)	(2) Natural Shear	200 1000		0.62
Dolomite (Knox)	(3) Saw Cut	250 2000		0.60 0.48
Dolomite (Blair)	(3) Saw Cut	250 2000		0.55
Dolomite (Beekmantown)	(1) Natural Shear		138 827	1.8 0.8
Gneiss (Granitic)	(2) Natural Shear	200 1000		0.71
Gneiss (Wet) (Granitic)	(2) Natural Shear	200 1000		0.61
Granite (Georgia)	(1) Natural Shear		138 698	1.3 0.7
Porphyry (Quartz)	(2) Ground	200 1000		0.61 0.52

Table 3 continued

Rock	Type of Surface	Confining Pressure bars	Normal Stress bars	Coefficient of friction
Porphyry (Quartz)	(2) Natural Shear	200 1000		0.86
Basalt (Knippa)	(1) Natural Shear		138 698	1.7 0.8
Serpentinite (Antigorite)	(4) Natural Shear	200 5000		0.91 0.68
Serpentinite (Fidalgo)	(4) Natural Shear	1000 5000		0.75 0.4

(1) Maurer (1965)

(2) Jaeger (1959)

(3) Handin & Stearns (personal communication)

(4) Raleigh & Paterson (1965)

Table 4

STRESSES AND COEFFICIENT OF FRICTION FOR SLIDING ON GROUND SURFACES

(Stresses corrected for change in area)

Relative displacement cm	σ_1 kb	σ_3 kb	τ kb	σ_n kb	μ
Test No. 3/24 $\alpha = 45^\circ$					
0.005	1.70	5.46	1.88	3.58	0.52
0.05	1.79	8.88	3.55	5.33	0.66
0.21	2.08	10.50	4.21	6.29	0.67
0.42	2.43	9.58	3.58	6.00	0.59
0.60	2.67	8.87	3.11	5.77	0.54
0.67	2.77	8.66	2.99	5.72	0.52
0.74	2.87	8.37	3.25	6.12	0.53
0.79	2.96	8.65	3.35	6.31	0.53
0.87	3.06	9.70	3.32	6.38	0.52
0.93	3.15	10.88	3.87	7.00	0.55

Table 4 continued

Relative displacement cm	σ_1 kb	σ_3 kb	τ kb	σ_n kb	μ
Test No. 11/24 $\alpha = 45°$					
0.005	0.70	4.74	2.02	2.72	0.74
0.04	0.66	6.03	2.68	3.34	0.80
0.25	0.66	4.51	1.93	2.58	0.74
0.46	0.66	3.23	1.28	1.94	0.66
0.55	0.66	3.80	1.57	2.22	0.70
0.66	0.66	3.74	1.54	2.20	0.70
0.76	0.64	4.53	1.94	2.58	0.75
Test No. 12/24 $\alpha = 45°$					
0.005	0.71	5.67	2.48	3.19	0.78
0.08	0.65	5.98	2.67	3.31	0.80
0.39	0.66	4.09	1.72	2.38	0.72
0.47	0.65	4.25	1.81	2.45	0.73
0.55	0.65	4.66	1.98	2.62	0.75
0.64	0.65	4.51	1.93	2.58	0.75
0.71	0.65	4.56	1.96	2.60	0.75
0.80	0.65	4.80	2.07	2.72	0.76

Table 4 continued

Relative displacement cm	σ_1 kb	σ_3 kb	τ kb	σ_n kb	μ
Test No. 13/24 $\alpha = 45°$					
0.05	2.17	7.11	2.47	4.64	0.53
0.11	2.19	13.19	5.50	7.69	0.71
0.56	2.21	12.64	4.91	7.12	0.69
0.91	2.59	9.61	3.51	6.11	0.57
0.96	2.70	10.00	3.65	6.35	0.57
0.102	2.83	11.45	4.31	7.14	0.60
Test No. 14/24 $\alpha = 45°$					
0.005	2.23	10.41	4.09	6.32	0.65
0.08	2.23	13.26	5.51	7.75	0.71
0.60	2.17	10.83	4.33	6.55	0.66
0.89	2.21	9.83	3.81	6.02	0.63
1.03	2.19	10.29	4.56	6.74	0.67
Test No. 16/24 $\alpha = 45°$					
0.005	1.28	4.54	1.63	2.91	0.56
0.03	1.30	6.59	2.64	3.79	0.69
0.16	1.30	6.95	2.82	4.12	0.68
0.67	1.32	4.12	1.401	2.72	0.51
0.79	1.32	3.95	1.32	2.63	0.50
0.85	1.30	4.41	1.56	2.85	0.54
0.91	1.30	4.50	1.60	2.89	0.55
0.99	1.28	4.68	1.70	2.98	0.57

Table 4 continued

Relative displacement cm	σ_1 kb	σ_3 kb	τ kb	σ_n kb	μ
Test No. 17/24 $\alpha = 45^\circ$					
0.005	2.59	8.24	2.82	5.42	0.52
0.46	2.62	15.36	6.37	8.98	0.71
0.53	2.66	13.87	5.60	8.26	0.69
1.03	2.64	12.53	4.95	7.58	0.65
Test No. 1/100 $\alpha = 45^\circ$					
0.002	0.66	3.38	1.36	2.02	0.67
0.03	0.68	4.26	1.79	2.47	0.72
0.06	0.72	6.02	2.65	3.37	0.78
0.14	0.79	6.65	2.93	3.72	0.79
0.34	0.97	6.38	2.71	3.67	0.74
0.54	1.22	5.59	2.18	3.40	0.64
0.64	1.36	6.31	2.47	3.83	0.64
0.74	1.53	6.17	2.32	3.85	0.60
0.79	1.64	6.96	2.66	3.80	0.70
Test No. 2/100 $\alpha = 45^\circ$					
0.01	1.08	4.38	1.64	2.73	0.60
0.04	1.15	6.60	2.73	3.87	0.70
0.08	1.21	8.60	3.69	4.91	0.75
0.31	1.47	8.48	3.51	4.97	0.70
0.59	1.79	8.88	3.05	4.83	0.63
0.71	1.94	7.84	2.95	4.89	0.60
0.76	2.00	8.17	3.08	5.08	0.61

Table 4 continued

Relative displacement cm	σ_1 kb	σ_3 kb	τ kb	σ_n kb	μ
Test No. 3/100 $\alpha = 45°$					
0.005	1.70	5.55	1.92	3.62	0.53
0.04	1.79	10.15	4.18	5.97	0.70
0.27	2.13	12.17	5.02	7.15	0.70
0.63	2.62	10.26	3.82	6.43	0.59
0.70	2.72	10.52	3.89	6.62	0.59
0.78	2.83	10.77	3.97	6.80	0.58
0.86	2.94	11.66	4.36	7.29	0.58
Test No. 4/100 $\alpha = 45°$					
0.005	2.17	6.00	1.91	4.08	0.47
0.04	2.21	10.59	4.19	6.40	0.65
0.23	2.21	12.00	4.89	7.11	0.69
0.53	2.21	9.41	3.60	5.81	0.62
0.70	2.21	9.78	3.78	5.49	0.63
0.77	2.21	8.39	3.09	5.30	0.53
0.84	2.21	8.69	3.24	5.95	0.54
Test No. 11/100 $\alpha = 45°$					
0.03	0.66	4.48	1.91	2.57	0.74
Test No. 12/100 $\alpha = 45°$					
0.005	0.70	4.96	2.13	2.83	0.75
0.05	0.66	6.12	2.73	3.39	0.80

Table 4 continued

Relative displacement cm	σ_1 kb	σ_3 kb	τ kb	σ_n kb	μ
Test No. 13/100 $\alpha = 45°$					
0.02	0.70	4.74	2.02	2.72	0.74
0.14	0.65	4.48	1.92	2.57	0.75
0.33	0.66	3.38	1.36	2.02	0.67
Test No. 14/100 $\alpha = 45°$					
0.01	0.68	5.24	2.27	2.95	0.77
0.07	0.66	6.44	2.89	3.55	0.81
0.36	0.66	3.83	1.58	2.25	0.69
0.49	0.66	3.56	1.45	2.11	0.69
Test No. 15/100 $\alpha = 45°$					
0.02	0.70	5.84	2.57	3.27	0.78
0.10	0.66	6.63	2.99	3.64	0.82
0.42	0.67	4.00	1.66	2.33	0.71
0.53	0.65	3.64	1.50	2.14	0.70
0.59	0.65	3.69	1.52	2.17	0.70
Test No. 16/100 $\alpha = 45°$					
0.015	0.70	5.76	2.53	3.23	0.78
0.11	0.65	5.89	2.62	3.26	0.80
0.37	0.67	3.88	1.60	2.27	0.70
0.49	0.66	3.88	1.61	2.27	0.71
0.55	0.65	4.07	1.71	2.36	0.72
0.63	0.65	4.13	1.74	2.39	0.73

Table 4 continued

Relative displacement cm	σ_1 kb	σ_3 kb	τ kb	σ_n kb	μ
Test No. 17/100 $\alpha = 45°$					
0.015	2.26	13.35	5.55	7.80	0.71
0.47	2.23	13.45	5.61	7.84	0.72
0.90	2.23	10.32	4.04	6.27	0.64
Test No. 18/100 $\alpha = 45°$					
0.025	2.19	11.66	4.73	6.92	0.68
0.10	2.23	11.16	4.46	6.69	0.66
0.87	2.23	10.98	4.37	6.60	0.66
1.05	2.19	9.57	3.69	5.88	0.62
Test No. 19/100 $\alpha = 45°$					
0.01	1.30	4.97	1.84	3.13	0.59
0.06	1.32	9.26	3.97	5.29	0.75
0.26	1.32	10.58	4.63	5.95	0.78
0.43	1.32	7.35	3.30	4.62	0.71
0.68	1.32	6.94	2.81	4.12	0.68
0.81	1.30	6.38	2.54	3.83	0.68
0.89	1.29	6.94	2.82	4.12	0.68
0.98	1.30	7.91	3.31	4.60	0.72
Test No. 20/100 $\alpha = 45°$					
0.001	2.57	6.77	2.10	4.67	0.45
0.06	2.64	12.05	4.70	7.34	0.64
0.37	2.66	14.79	6.07	8.73	0.69
0.91	2.66	13.79	5.57	8.22	0.67

Table 4 continued

Relative displacement cm	σ_1 kb	σ_3 kb	τ kb	σ_n kb	μ
Test No. 1/400 $\alpha = 45°$					
0.015	0.67	4.75	2.04	2.71	0.75
0.05	0.67	6.33	2.83	3.49	0.81
0.20	0.67	5.54	2.43	3.10	0.78
0.47	0.66	3.78	1.56	2.22	0.70
0.55	0.65	3.67	1.81	2.16	0.70
0.61	0.64	3.97	1.66	2.30	0.72
0.68	0.64	3.80	1.58	2.22	0.71
Test No. 2/400 $\alpha = 45°$					
0.02	1.36	8.31	3.47	4.83	0.72
0.20	1.35	10.68	4.66	6.02	0.77
0.59	1.35	11.40	5.02	6.37	0.79
0.94	1.30	8.90	3.79	5.10	0.74
1.06	1.31	9.19	3.94	5.25	0.75
Test No. 3/400 $\alpha = 45°$					
0.03	1.77	9.32	3.78	5.54	0.68
0.09	1.81	11.78	4.98	6.79	0.73
0.34	1.76	9.87	4.05	5.82	0.70
0.60	1.74	7.91	3.08	4.82	0.64
0.74	1.74	8.22	3.24	4.98	0.65
0.96	1.74	9.11	3.68	5.42	0.68
0.99	1.72	9.10	3.68	5.41	0.68

Table 4 continued

Relative displacement cm	σ_1 kb	σ_3 kb	τ kb	σ_n kb	μ
Test No. 4/400 $\alpha = 45°$					
0.025	2.19	7.23	2.25	4.71	0.53
0.16	2.21	9.19	3.54	5.75	0.61
0.12	2.19	10.73	4.27	6.46	0.66
0.30	2.21	11.34	4.56	6.77	0.67
0.59	2.17	8.33	3.08	5.25	0.58
0.73	2.17	8.20	3.01	5.18	0.58
0.80	2.17	8.30	3.06	5.23	0.58
0.87	2.17	8.26	3.04	5.21	0.58
Test No. 5/400 $\alpha = 45°$					
0.01	2.57	6.15	1.78	4.36	0.41
0.02	2.62	9.50	3.44	6.06	0.57
0.08	2.64	11.56	4.46	7.10	0.63
0.17	2.66	14.36	5.85	8.51	0.69
0.49	2.62	12.16	4.77	7.38	0.64
0.76	2.62	8.64	3.01	5.63	0.63
Test No. 11/400 $\alpha = 45°$					
0.025	0.70	5.46	2.38	3.08	0.77
Test No. 12/400 $\alpha = 45°$					
0.005	0.69	5.05	2.18	2.87	0.76
0.07	0.66	6.27	2.80	3.46	0.81

Table 4 continued

Relative displacement cm	σ_1 kb	σ_3 kb	τ kb	σ_n kb	μ
Test No. 13/400 $\alpha = 45°$					
0.005	0.66	4.69	2.02	2.67	0.75
0.05	0.66	5.64	2.49	3.15	0.79
0.21	0.66	3.49	1.42	2.08	0.68
Test No. 14/400 $\alpha = 45°$					
0.015	0.68	3.87	1.59	2.27	0.70
0.17	0.66	5.83	2.58	3.24	0.78
0.40	0.65	3.91	1.63	2.27	0.71
Test No. 15/400 $\alpha = 45°$					
0.005	0.66	4.71	2.02	2.68	0.75
0.04	0.66	6.17	2.75	3.42	0.81
0.20	0.66	5.86	2.60	3.26	0.80
0.49	0.66	4.06	1.69	2.35	0.72
0.56	0.64	3.99	1.67	2.31	0.72
Test No. 16/400 $\alpha = 45°$					
0.025	0.68	5.23	2.27	2.95	0.77
0.09	0.68	6.57	2.94	3.62	0.81
0.33	0.68	6.34	2.83	3.51	0.80
0.55	0.66	6.35	1.84	2.51	0.74
0.64	0.66	4.20	1.77	2.43	0.73
0.72	0.66	4.22	1.78	2.44	0.73

Table 4 continued

Relative displacement cm	σ_1 kb	σ_3 kb	τ kb	σ_n kb	μ
Test No. 17/400 $\alpha = 45°$					
0.005	2.17	7.55	2.69	4.86	0.55
0.05	2.21	12.79	5.28	7.50	0.70
0.38	2.21	11.53	4.65	6.86	0.68
0.76	2.23	9.51	3.64	5.87	0.62
0.91	2.17	8.46	3.14	5.32	0.59
0.97	2.17	9.25	3.58	5.71	0.62
1.03	2.17	9.78	3.80	5.97	0.64
Test No. 18/400 $\alpha = 45°$					
0.005	2.17	6.99	2.41	4.58	0.53
0.05	2.15	9.14	3.49	5.64	0.62
0.08	2.15	9.75	3.80	5.94	0.64
0.33	2.21	10.51	4.10	6.36	0.64
0.56	2.19	8.49	3.15	5.34	0.59
0.69	2.17	7.91	2.96	5.04	0.57
0.76	2.17	8.54	3.18	5.35	0.59
0.84	2.17	9.04	3.43	5.60	0.61
0.93	2.19	9.91	3.86	6.05	0.64

Table 4 continued

Relative displacement cm	σ_1 kb	σ_3 kb	τ kb	σ_n kb	μ
Test No. 20/400 $\alpha = 45^\circ$					
0.02	1.11	4.90	1.89	3.00	0.63
0.04	1.08	7.21	3.06	4.15	0.74
0.08	1.08	8.26	3.58	4.67	0.77
0.36	1.13	8.38	3.62	4.75	0.76
0.70	1.08	6.58	2.74	3.83	0.71
0.81	1.07	6.20	2.56	3.63	0.70
0.86	1.08	7.64	3.28	4.35	0.75
1.01	1.09	7.30	3.10	4.19	0.74
Test No. 21/400 $\alpha = 45^\circ$					
0.005	1.08	4.85	1.88	2.96	0.63
0.06	1.11	8.10	3.49	4.60	0.76
0.35	1.13	10.12	4.49	5.62	0.80
0.81	1.11	8.74	3.81	4.92	0.77
1.00	1.11	8.14	3.51	4.62	0.76
1.13	1.09	8.51	3.71	4.94	0.75

Table 5

STRESSES AND COEFFICIENT OF FRICTION FOR SLIDING ON MATED SURFACES

(Stresses corrected for change in area)

Relative displacement cm	σ_1 kb	σ_3 kb	τ kb	σ_n kb	μ
Test No. B12 $\alpha = 28^\circ$					
0	3.15	12.13	3.72	5.13	0.72
0.20	3.19	10.61	3.07	4.83	0.64
0.25	3.15	10.70	3.13	4.81	0.65
0.31	3.12	11.38	3.38	5.03	0.67
0.36	3.32	11.05	3.20	5.02	0.64
0.40	3.40	11.97	3.55	5.23	0.67
0.46	3.51	12.31	3.65	5.45	0.67
0.52	3.62	12.67	3.75	5.61	0.67

Table 5 continued

Relative displacement cm	σ_1 kb	σ_3 kb	τ kb	σ_n kb	μ
Test No. B12 $\alpha = 28^\circ$					
0	3.11	12.47	3.88	5.17	0.75
0.23	3.08	10.00	2.87	4.61	0.62
0.28	3.06	10.63	3.13	4.73	0.66
0.34	30.6	10.99	3.28	4.79	0.68
0.39	3.02	10.63	3.15	4.70	0.67
0.45	3.02	10.78	3.21	4.73	0.68
0.53	3.06	11.00	3.29	4.81	0.68
0.56	3.04	11.32	3.43	4.87	0.70
Test No. B13 $\alpha = 29^\circ$					
0	4.00	14.25	14.35	6.41	0.68
0.18	3.83	12.28	3.58	5.81	0.62
0.23	3.87	12.67	3.73	5.94	0.63
0.28	3.83	12.09	3.50	5.77	0.61
0.33	3.87	12.76	3.77	5.96	0.63
0.38	3.91	13.21	3.94	6.12	0.64
0.44	3.94	13.38	4.00	6.15	0.65
0.54	3.91	12.67	3.71	5.97	0.62
0.58	3.87	12.91	3.83	5.99	0.64
0.63	3.83	12.30	3.59	5.82	0.62

Table 5 continued

Relative displacement cm	σ_1 kb	σ_3 kb	τ kb	σ_n kb	μ
Test No. B14 $\alpha = 28^\circ$					
0	3.96	13.92	4.13	6.15	0.67
0.13	3.91	13.42	3.94	6.01	0.65
0.30	3.91	13.30	3.89	5.98	0.65
0.41	3.83	12.52	3.60	5.75	0.63
0.47	3.83	12.88	3.75	5.82	0.64
0.52	3.83	12.82	3.72	5.81	0.64
0.58	3.87	12.94	3.76	5.87	0.64
0.60	3.87	13.09	3.82	5.90	0.65
Test No. B16 $\alpha = 28^\circ$					
0	1.06	6.34	2.19	2.23	0.98
0.18	1.10	5.14	1.67	1.99	0.84
0.38	1.15	4.68	1.46	1.93	0.76
0.40	1.13	4.76	1.50	1.93	0.78
0.46	1.13	4.91	1.57	1.96	0.80
0.50	1.08	4.94	1.60	1.93	0.82
0.53	1.11	5.01	1.62	1.97	0.82
0.56	1.11	5.00	1.62	1.97	0.82
0.59	1.09	5.03	1.64	0.95	0.84

Table 5 continued

Relative displacement cm	σ_1 kb	σ_3 kb	τ kb	σ_n kb	μ
Test No. B16 (continued)					
0.61	1.09	5.06	1.65	1.96	0.84
0.64	1.11	4.59	1.45	1.87	0.77
0.67	1.11	4.71	1.49	1.90	0.78
0.70	1.11	4.59	1.44	1.87	0.77
0.73	1.11	4.56	1.43	1.87	0.76
0.75	1.09	4.50	1.42	1.84	0.77
0.78	1.11	4.50	1.41	1.85	0.76
0.81	1.09	4.51	1.42	1.84	0.77
0.84	1.09	4.67	1.48	1.87	0.79
0.87	1.09	4.68	1.49	1.88	0.79
0.90	1.09	4.72	1.51	1.89	0.80
0.93	1.11	4.78	1.52	1.92	0.80
0.96	1.09	4.88	1.57	1.92	0.82

Table 5 continued

Relative displacement cm	σ_1 kb	σ_3 kb	τ kb	σ_n kb	μ
Test No. B17 $\alpha = 29^\circ$					
0	2.64	10.37	3.28	4.46	0.74
0.20	2.64	9.03	2.71	4.14	0.654
0.28	2.62	9.04	2.72	4.13	0.66
0.35	2.57	8.84	2.65	4.05	0.65
0.41	2.57	8.95	2.70	4.07	0.66
0.47	2.57	8.74	2.62	4.02	0.65
0.59	2.55	8.56	2.54	3.96	0.64
0.64	2.59	8.71	2.59	4.03	0.64
0.69	2.57	8.58	2.55	3.99	0.64
0.74	2.59	8.80	2.63	4.05	0.65
0.78	2.55	8.52	2.53	3.96	0.64
0.80	2.57	8.71	2.60	4.02	0.65
0.87	2.55	8.44	2.49	3.94	0.63
0.91	2.55	8.33	2.45	3.91	0.63
0.95	2.57	8.69	2.59	4.01	0.65

Table 5 continued

Relative displacement cm	σ_1 kb	σ_3 kb	τ kb	σ_n kb	μ
Test No. B18 $\alpha = 28^\circ$					
0	2.64	10.18	3.12	4.30	0.73
0.20	2.59	9.15	2.72	4.04	0.67
0.25	2.55	9.20	2.75	4.02	0.68
0.31	2.57	9.08	2.70	4.01	0.67
0.36	2.57	9.23	2.76	4.04	0.68
0.45	2.57	9.22	2.76	4.04	0.68
0.50	2.59	9.42	2.83	4.10	0.69
0.55	2.57	9.17	2.73	4.03	0.69
0.59	2.57	9.24	2.76	4.00	0.69
0.64	2.59	9.43	2.83	4.10	0.69
0.69	2.59	9.58	2.89	4.13	0.70
0.73	2.59	9.64	2.92	4.15	0.70
0.78	2.55	9.23	2.76	4.02	0.68
0.83	2.57	9.55	2.89	4.11	0.70
0.87	2.55	9.66	2.95	4.12	0.71
0.90	2.55	9.54	2.90	4.09	0.71
0.94	2.57	9.80	2.99	4.17	0.71
0.98	2.55	9.54	2.89	4.09	0.71

Table 5 continued

Relative displacement cm	σ_1 kb	σ_3 kb	τ kb	σ_n kb	μ
Test No. B21 $\alpha = 30^\circ$					
0	5.08	17.11	5.20	8.08	0.64
0.08	5.08	16.12	4.78	7.84	0.60
0.13	5.08	16.43	4.91	7.92	0.61
0.20	5.08	16.95	5.13	8.05	0.63
0.27	4.95	15.50	4.56	7.59	0.60
0.32	4.95	16.37	4.94	7.81	0.63
Test No. B22 $\alpha = 30^\circ$					
0	6.20	19.38	5.70	9.50	0.60
0.08	6.16	18.39	5.39	9.21	0.57
0.14	6.16	20.13	6.04	9.65	0.62
0.23	6.12	18.02	5.15	9.10	0.56
0.29	6.12	19.32	5.71	9.42	0.60
0.36	6.07	20.44	6.21	9.67	0.64
0.44	6.07	20.13	6.08	9.58	0.63
0.51	6.03	19.01	5.62	9.28	0.60
0.58	5.99	21.35	6.65	9.83	0.67
0.66	5.94	20.18	6.16	9.50	0.64
0.72	5.99	19.74	5.94	9.43	0.62

Table 5 continued

Relative displacement cm	σ_1 kb	σ_3 kb	τ kb	σ_n kb	μ
Test No. B23 $\alpha = 30^\circ$					
0	6.85	20.65	5.97	10.30	0.58
0.09	6.83	21.49	6.34	10.50	0.60
0.17	6.87	21.78	6.45	10.60	0.60
0.26	6.85	23.33	7.13	10.97	0.64
0.36	6.83	21.77	6.46	10.57	0.61
0.41	6.87	23.15	7.04	10.94	0.64
0.50	6.78	23.77	7.36	11.02	0.66
0.56	6.76	24.37	7.62	11.16	0.68
0.62	6.74	22.80	6.95	10.76	0.64
0.68	6.72	24.32	7.62	11.12	0.68
0.75	6.70	23.89	7.43	11.00	0.67
Test No. B25 $\alpha = 32^\circ$					
0	9.65	31.37	9.76	16.96	0.57
0.07	9.57	32.23	10.63	16.22	0.65
0.15	9.65	34.36	11.10	16.59	0.66
Test No. B26 $\alpha = 29^\circ$					
0	10.77	33.78	9.75	16.18	0.60
0.08	10.86	35.34	10.38	16.62	0.62
0.18	10.86	34.91	10.19	16.51	0.61

Table 5 continued

Relative displacement cm	σ_1 kb	σ_3 kb	τ kb	σ_n kb	μ
Test No. B27 $\alpha = 34^\circ$					
0	8.19	23.00	8.86	11.82	0.58
0.07	8.10	23.57	7.16	12.94	0.55
0.15	8.10	26.04	8.31	13.71	0.61
0.24	8.19	26.21	8.35	13.83	0.60
0.33	8.10	24.26	7.49	13.16	0.57
0.37	7.93	27.55	9.09	14.07	0.65
Test No. B28 $\alpha = 28^\circ$					
0	6.38	24.43	7.47	10.36	0.72
0.08	6.29	24.28	7.45	10.26	0.72
0.17	6.25	25.10	7.81	10.41	0.75
0.25	6.16	25.16	7.87	10.35	0.76
0.26	6.20	25.83	8.13	10.53	0.77
0.34	6.12	24.63	7.66	10.20	0.75
0.40	6.08	25.35	7.98	10.33	0.77
0.48	6.03	25.52	8.07	10.34	0.78

Table 5 continued

Relative displacement cm	σ_1 kb	σ_3 kb	τ kb	σ_n kb	μ
Test No. B29 $\alpha = 30^\circ$					
0	7.06	25.94	8.17	11.78	0.69
0.08	6.98	27.87	9.04	12.20	0.74
0.16	6.81	24.92	7.83	11.34	0.69
0.24	6.63	25.54	8.18	11.36	0.72
0.31	6.63	26.70	8.68	11.65	0.74
0.38	6.72	26.23	8.44	11.60	0.72
0.46	6.55	25.54	8.21	11.30	0.71
0.52	6.46	26.91	8.85	11.57	0.76
Test No. B30 $\alpha = 28^\circ$					
0	8.27	30.20	9.08	13.11	0.69
0.08	8.27	29.07	8.62	12.86	0.67
0.15	8.36	31.19	9.45	13.40	0.70

Table 5 continued

Relative displacement	σ_1 kb	σ_3 kb	τ kb	σ_n kb	μ
Test No. B32 $\alpha = 28^\circ$					
0	10.17	34.89	10.24	15.62	0.65
0.02	10.17	35.15	10.35	15.67	0.66
0.10	10.26	36.45	10.85	16.05	0.67
0.19	10.26	36.55	10.89	16.06	0.67
0.27	10.26	37.69	10.91	16.31	0.66
Test No. B33 $\alpha = 28^\circ$					
0	10.69	36.42	10.66	16.37	0.65
0.06	10.69	36.90	10.03	17.03	0.59
0.17	10.51	37.52	11.19	16.47	0.67

Table 6

STRESSES FOR INITIAL MOVEMENT ON MATED SURFACE

Test no	σ_1 kb	σ_3 kb	α degrees	τ kb	σ_n kb
B1C	0.63	4.29	29	1.55	1.49
B2D	1.09	5.48	26	1.73	1.93
B2C	1.15	6.10	31	2.18	2.46
B3D	1.75	7.39	26	2.23	2.83
B3C	1.75	7.87	33	2.80	3.56
B4D	2.04	7.90	27	2.37	3.25
B4C	2.02	7.19	28	2.14	3.16
B5D	2.62	10.50	25	3.02	4.03
B5C	2.60	9.55	28	2.88	4.13
B11C	3.15	12.13	28	3.72	5.13
B12C	3.11	12.47	28	3.88	5.17
B13C	4.00	14.25	29	4.35	6.41
B14C	3.96	13.92	28	4.13	6.15
B15C	1.11	5.63	30	1.96	2.24
B16C	1.06	6.34	28	2.19	2.23
B17C	2.64	10.37	29	3.28	4.46
B18C	2.64	10.18	28	3.12	4.30

Table 6 continued

Test No	σ_1 kb	σ_3 kb	α degrees	τ kb	σ_n kb
B21	5.08	17.11	30	5.20	8.08
B22	6.20	19.38	30	5.70	9.50
B23	6.85	20.65	30	5.97	10.30
B25	9.65	31,78	32	9.76	16.96
B26	10.77	33.78	29	9.75	16.18
B27	8.19	23.00	34	6.86	11.82
B28	6.38	24.43	28	7.47	10.36
B29	7.06	25.94	30	8.17	11.78
B30	8.27	30.20	28	9.08	13.11
B31	9.14	32.10	30	9.94	14.88
B32	10.17	34.89	28	10.24	15.62
B33	10.69	36.42	28	10.66	16.37

Table 7

STRESSES AT FRACTURE FOR VIRGIN ROCK

(Stresses corrected for change in area)

Test No	σ_1 kb	σ_3 kb	α degrees	τ kb	σ_n kb
UB1D	0.57	6.70	25	2.35	1.67
UB2D	1.13	9.72	25	3.29	2.66
UB2C	1.13	10.14	24	3.35	2.26
UB3D	1.87	13.23	27	4.59	4.21
UB3C	1.85	13.47	27	4.70	4.25
UB4D	2.15	13.51	29	4.88	4.69
4B4C	2.04	13.32	29	4.78	4.69
UB5D	2.68	15.48	28	5.30	5.50
UB5C	2.66	15.78	26	5.17	5.19
UB11C	0.58	7.42	20	2.20	1.39
UB12C	1.38	11.31	25	3.80	3.15
UB13C	1.34	11.50	28	4.21	3.58
UB14C	3.19	17.88	28	6.09	6.43
UB15C	3.19	17.80	28	6.05	6.41
UB16C	4.51	22.32	28	7.38	8.44

Table 7 continued

Test No	σ_1 kb	σ_3 kb	α degrees	τ kb	σ_n kb
UB21C	9.48	30.19	35	9.72	16.34
UB22C	10.77	34.11	37	11.21	19.23
UB23C	6.59	27.67	34	9.77	13.19
UB25C	9.65	30.12	32	9.19	15.40
UB26C	6.71	29.42	29	9.62	12.06
UB27C	10.08	37.17	34	12.55	18.56
UB28C	9.91	35.06	38	12.19	19.44
UB29C	5.69	24.35	35	8.77	11.83
UB30C	5.69	23.32	31	7.77	10.37
UB31C	8.45	30.11	31	9.56	14.20
UB32C	9.48	32.01	38	10.92	18.03
UB33C	10.25	34.37	38	11.70	19.40
UB34C	10.86	35.28	38	11.84	20.12
UB35D	10.34	32.15	28	9.03	15.15
UB36D	10.64	33.61	30	10.48	17.46

Table 8

STRESSES FOR FRACTURE AND SLIDING FOR INITIALLY VIRGIN ROCK

(Stresses corrected for change in area)

Strain percent	σ_1 kb	σ_3 kb	$\sigma_3-\sigma_1$ kb	$\sigma_3-\sigma_1$ kb after slip
Test No. UB23 $\alpha = 34°$				
2.5	6.59	27.67	21.08	12.04
4.6	6.42	25.18	18.76	13.39
6.1	6.42	24.57	18.15	13.11
7.7	6.38	25.56	19.18	12.42
9.2	6.25	25.23	18.98	9.18
11.0	6.08	22.86	16.78	10.94

Table 8 continued

Strain percent	σ_1 kb	σ_3 kb	$\sigma_3-\sigma_1$ kb	$\sigma_3-\sigma_1$ kb after slip
Test No. UB35 $\alpha = 28°$				
2.7	10.34	32.15	21.81	8.72
5.6	10.08	30.68	20.00	10.76
7.3	10.08	31.24	21.16	12.27
9.0	10.17	31.69	21.52	12.41
10.5	10.08	32.17	22.09	13.62
Test No. UB36 $\alpha = 33°$				
3.5	10.64	33.61	22.97	11.48
5.6	10.69	33.63	22.94	11.70
7.3	10.60	33.39	22.79	15.56
8.6	10.69	34.13	23.44	14.38
9.8	10.69	33.47	22.78	14.80
11.1	10.69	36.41	25.72	

PART IV

APPLICATIONS

Summary

Results of the theoretical and both the low and high pressure experimental studies are correlated and applied to a number of geologic and geophysical problems.

For sliding on fracture and possibly joint surfaces in granite, μ may be as high as 1.3 and as low as 0.1 for polished fault surfaces. For small shear displacements between the walls of Griffith cracks μ should be about 0.1, but for large displacements μ may reach values as high as 1.0 or greater. Up to very high confining pressures it is easier to slide on old faults than to create new ones, so that in active tectonic regions movement within the crust should be confined to pre-existing faults. Stick-slip motion along a pre-existing fault may be a simple explanation for the seismic source mechanism of crustal earthquakes. The "brittle-ductile" transition pressure in rocks may simply be the pressure at which the frictional shear strength is equal to the fracture shear strength. In the Coulomb-Navier theory it is assumed that the strength of a rock is determined by μ and the cohesive strength. The theory does not hold for Westerly granite.

Roughness

It has been found in this study that the coefficient of friction of Westerly granite increases with the roughness of the surfaces in contact. The increase in friction with roughness is not a characteristic of Westerly granite alone. Other brittle materials behave in a similar way. For example in Part I it was shown that rough surfaces of quartz have a high friction in contrast to the low value found for polished surfaces. This increase in friction with roughness for quartz was also observed by Tschebotarioff and Welch (1948) and Horne and Deere (1962). Rae (1963) obtained a high coefficient of friction with rough surfaces of limestone. But when the surfaces were ground smooth the friction fell to a low value. At a high confining pressure Jaeger (1959) found that the friction of ground surfaces was less than the friction of rough shear fracture surfaces of quartz prophyry. Maurer (1965) obtained high coefficients of friction for rough fracture surfaces of limestone, shale, sandstone, dolomite, basalt and granite, but noted that the friction decreased as the surfaces were ground smooth.

Because the configuration of the surfaces strongly influences the friction, any study of the frictional characteristics of brittle materials must take into account the roughness, flatness and apparent area of contact of the surfaces.

The measured values of the coefficient of friction of single crystals reported in the literature is approximately 0.1 whereas the friction coefficient of rocks has been found to be approximately 0.8. In the past this has been somewhat puzzling because rocks are aggregates of single crystals. The apparent anomaly can be explained by the fact that the low coefficient of friction of single crystals is usually obtained with polished surfaces whereas the high coefficient of friction of rocks was found from rough surfaces.

The friction of rocks sliding on joint, fracture or fault surfaces is of considerable importance to mining and civil engineers. The results from this study show that the coefficient of friction is not a material constant but depends on the configuration of the surfaces in contact. It can reach values as high as 1.3 for surfaces with complete interlocking of the irregularities such as fracture surfaces and possibly joints and it may be as low as 0.1 for polished fault surfaces.

Walsh (1965a, 1965b, 1966) has made theoretical investigations of the effect of cracks on the physical properties of rocks and an important parameter in his equations is the coefficient of friction for sliding on the crack surfaces. The equations derived by Walsh may be difficult to evaluate

because the friction will depend on the microstructure of the crack surfaces. There are however two limiting cases which may be explained.

If the rock has undergone repeated non-elastic deformation during its past history, the irregularities on the crack surfaces will, over the distance that movement has occurred, become ground down and in the limiting case the coefficient of friction will approach that found for polished surfaces. This may be the explanation for the fact that a coefficient of friction of 0.1 is necessary to account for the observed attenuation of seismic waves of small amplitude at low confining pressures, (Walsh, 1966). On the other hand if the movement along the crack surfaces is greater than experienced during the past history of the rock, the irregularities on the surfaces will interlock and the coefficient of friction may reach a value of 1.0 or greater. This would explain why a coefficient of friction of 0.7 is necessary to account for the observed elastic modulus of rocks under a high uniaxial compressive stress (Walsh, 1965a).

Grain boundaries and cleavage surfaces in rocks would be expected to have nearly perfect interlocking of the irregularities provided that they had experienced no movement in their past history. The coefficient of friction

for sliding should be high and would decrease with an increase in the normal stress across the surfaces.

Displacement

It was found for ground surfaces at high normal stresses that the friction increased with displacement until a maximum was reached after approximately 0.1 cm of sliding and then it decreased to a constant value after about 0.5 cm of relative displacement between the surfaces. Examination of the surfaces suggested that the increase in friction was caused by a change in the true area of contact as the out-of-flatness across the surfaces was eliminated by wear with a maximum in friction being reached when intimate contact was established over the entire surface. Jaeger (1959) found an increase in friction with displacement for quartz porphyry sliding on ground surfaces. He also suggested that the increase in friction was caused by an increase in the area of contact.

To test the hypothesis, surfaces were prepared that initially had complete interlocking of the irregularities over the whole of the surface and it was found that the initial friction was the same as the maximum friction observed with ground surfaces. This confirmed the correctness of the original assumption. After the maximum, there is an accumulation of loose wear particles on the surfaces

so that it is now no longer necessary to break through virgin material to cause sliding and the coefficient of friction is reduced.

The friction of perfectly mating surfaces decreased from an initial high value to a constant value after about 0.1 cm of sliding had occurred. The same phenomena was found by Maurer for sandstone, shale, limestone, dolomite, basalt and granite sliding on fracture surfaces. He suggested that the decrease in friction was caused by a decrease in the roughness of the surfaces with sliding but he also noted that the surfaces were covered with crushed material after sliding.

A consequence of geophysical importance from the experiments is that the coefficient of friction for sliding along fault surfaces is reduced by the presence of fault gouge and that it is easier to reactivate old faults than to create new ones so that in active tectonic regions the movement should be confined to pre-existing faults.

Load Dependence

At low normal loads it was found that the coefficient of friction was independent of the normal load. However, at high pressures it was found that the coefficient of friction was dependent on the normal stress across the surfaces.

Handin and Stearns (1964) found the same effect with limestone dolomite and sandstone. They suggested that the lower friction coefficient at high normal stresses was

because the surfaces became smoother. They did not give any explanation of why this should be so. Raleigh and Paterson (1965) found that the coefficient of friction of peridotite sliding on shear surfaces decreased with the confining pressure. Their explanation for the phenomena was that at high confining pressure plasticity of the crystals may play an important role in the sliding process. Maurer (1965) found that the friction coefficient of limestone, dolomite, sandstone, shale, basalt and granite decreased with an increase in the normal stress across the sliding surfaces, but he offered no physical explanation for the phenomena.

The results from this study show that when the shear stress required to cause sliding is plotted against the normal stress across the surfaces then all the points fall along a straight line with an intercept on the shear stress axis. The zero intercept represents the shear strength of the interlocking irregularities on the surface at zero normal load and the slope of the straight line represents the rate of change in the shear strength as the normal load is increased. There is no discontinuity in the data as would be expected if the physical processes involved during sliding changed from brittle to plastic behavior. The evidence is clear that the reason for the decrease in the coefficient of friction is because the interlocking

irregularities on the surfaces have a finite shear strength with no normal load across the sliding plane and the functional relationship for the friction coefficient is given by

$$\mu = A + B/\sigma_n \qquad (51)$$

where A is the rate of change in the strength of the material with an increase in the normal stress and B is the shear strength when the normal stress is zero.

Griggs and Handin (1960), Orowan (1960), Chinnery (1965), when considering the friction for sliding along fault planes have assumed that the coefficient of friction is approximately 1.0 and is independent of the normal stress across the surfaces. The results from this study show that the assumption is incorrect for Westerly granite up to a confining pressure of 10 kb.

Another point that is widely overlooked is that if faulting is to occur then the frictional stress cannot exceed the shear strength of the rock regardless of the physical process involved in the faulting.

Stick-slip

In the experiments on the frictional sliding of Westerly granite the movement between the surfaces took place in a jerky manner and when movement ceased the shear stress

across the sliding surfaces was in most cases approximately 2/3 of the shear stress required to initiate movement. This jerky movement occurred even at a confining pressure of 11 kb, the highest pressure used in the experiments. Jaeger (1959) observed the same phenomenon in his friction experiments on rocks at confining pressure of 200 to 1000 bars and Bridgman (1936) found that shearing of brittle materials at normal stresses up to 50 kb was accompanied by sudden shear stress drops. On the other hand, the shearing of metals took place smoothly.

The phenomenon is well known to workers in the field of friction and is commonly called stick-slip motion. It has been studied extensively by Rabinowicz (1965, p. 94) who found that the magnitude of the force drop during slip could be controlled by the stiffness, inertia and damping of the loading system.

Stick-slip motion along a pre-existing fault may be a simple explanation of the seismic source mechanism for crustal earthquakes. This possibility seems to have been overlooked by geophysicists.

It has been generally assumed by workers in the field of seismology [for example, Chinnery (1964), Byerly and de Noyer (1958), Benioff (1951) and Orowan (1960)] that during faulting all the tectonic stresses are relieved and

that the shear stress drop during an earthquake represents the entire shear stress across the fault plane. Calculations of the shear stress drop during major earthquakes yields a value of approximately 100 bars. This value is far below the shear strength of rocks and so other mechanisms than brittle fracture, which was originally proposed by Reid (1908, 1933), have been suggested for the earthquake source mechanism.

Orowan (1960) has proposed hot creep, Griggs and Handin (1960) have suggested phase transformations or melting and Frank (1965) favored mechanical instability of the material with pore fluids.

The writer suggests that earthquakes in the crust may be caused by stick-slip motion along a pre-existing fault. The observed shear stress drop of 100 bars during the movement on the fault may be because the stiffness, damping and inertia of the moving fault block limits the stress drops during slip to this value.

Physical Processes

Many metals deform plastically when the maximum shear stress reaches a critical value equal to half the yield strength in uniaxial tension. This criterion is known as the Tresca, the Guest or the maximum shear stress criterion (Crandall and Dahl, 1959, p. 200). This yield criterion is

very closely followed. For example (Bridgman, 1952, p. 199) found that the yield strength of steel at a confining pressure of 170,000 psi was within 5 percent of the yield strength at atmospheric pressure. In the experiments on the frictional sliding of Westerly granite with complete interlocking of the asperities, if the material deformed in a ductile manner, sliding would commence when the shear stress reached a critical value independent of the confining pressure of the experiment. The results show that this is not the case. The frictional force increases with confining pressure. For brittle materials confining pressure has a very strong influence on the strength of the material (Brace, 1964). The results for Westerly granite are consistent with the assumption that brittle fracture rather than plasticity is the controlling mechanism during frictional sliding.

Extrapolation of the results found for completely interlocking asperities to zero normal stress gives an intercept of 0.5 kb. The physical significance of this number is that it represents the shear strength of the asperities with zero normal stress across the surfaces. At low normal loads however it is easier for the surfaces to ride over rather than shear through the asperities and this is most probably the explanation for the low frictional force found for interlocking surfaces in the low load experiments described in Part I.

The friction of metals is almost independent of surface roughness (Rabinowicz, 1965, p. 62). But for brittle materials it has been established in this study that the roughness of the surfaces has a very strong influence on the coefficient of friction. This is put forward as further evidence that brittle materials may not deform in the same way as metals during sliding.

Stick-slip during frictional sliding is almost universal with brittle material (Bridgman, 1936), but it only occurs under special circumstances with metals (Rabinowicz, 1959). This further suggests that the physical processes involved in the frictional sliding of brittle materials are different from metals.

The loose wear particles on the surfaces of granite after sliding are angular in shape and are consistent with the concept that they were produced by brittle fracture of the material.

In contrast to what has been generally assumed in the past, namely that all materials deform plastically during frictional sliding, the conclusion reached from this study is that brittle fracture rather than plasticity is more likely the controlling mechanism during the frictional sliding of materials such as granite and quartz.

Theory

In the second section a theory was developed for the friction of polished surfaces of brittle materials. In the mathematical model it was assumed that when surfaces are placed together they make contact over a number of asperities. It was further assumed that for sliding to take place the asperities must break off at a height from their apex equal to the depth of interlocking. For polished surfaces this depth was assumed to be vanishingly small. It was assumed in one model that the asperities were wedged shaped and in another model that they were cone shaped. The theoretical values for the coefficient of friction for the two models were approximately 0.1 and 0.15. This value is close to the values found experimentally for polished surfaces of brittle materials (Table 2). The mathematical models also predicted that the coefficient of friction of polished surfaces of brittle materials would be independent of the strength of the material. Experimentally this has been found to be correct. For example the strength of quartz is far greater than the strength of calcite. But the coefficient of friction for polished surfaces of both these minerals is approximately 0.1 (Table 2).

The effect of surface forces on the friction of

polished surfaces of brittle materials was also analyzed. Theoretically it was predicted that the friction should decrease with an increase in the normal load. In addition μ should increase with an increase in the surface energy of the material. Both these effects have been observed with diamond by Bowden and Young (1951).

If two surfaces are placed together in the presence of a fluid there is an attractive force between the surfaces caused by the surface tension forces of the liquid. The effect of these forces was examined. The theoretical relationship showed that the friction of polished surfaces of brittle materials should increase in the presence of a liquid. But the magnitude of the increase is determined by the area of the surfaces in contact. This could explain why Penman (1953) found a large coefficient of friction with large surfaces of quartz in the presence of water. But the Norwegian Geotechnical Institute (1959) found that the friction of quartz with a very small contact area was almost unaffected by the presence of water.

At high confining pressure the surface tension forces can be neglected. Under a pressure of up to one kilobar Jaeger (1959) found that the friction of rocks is decreased in the presence of water. This can be explained by considering the environmental effects on the strength of

brittle materials.

The increase in friction with roughness of brittle materials is an experimental fact but an analytical solution to the problem has not been derived. Further work on this problem is necessary.

Coulomb-Navier Theory

The Coulomb-Navier criterion of rock fracture states that fracture takes place across a plane on which the shear stress τ first becomes equal to a constant τ_o, plus a constant μ times the normal pressure σ_n across the plane (Jaeger, 1962, p. 76).

$$\tau = \tau_o + \mu \sigma_n \tag{52}$$

τ_o is known as the cohesive shear strength and μ is the coefficient of internal friction.

A consequence of the theory is that at any given normal stress, the difference between the shear stress for sliding along a fracture surface and the shear stress along a fracture surface produced in virgin material at failure would be a constant which would represent the cohesive strength τ_o of the material.

Figure 35 gives a plot of the difference between the shear stress along the fault plane at fracture and the frictional shear stress for sliding along a surface with interlocking asperities over the range of normal stresses

investigated in this study. The results show that the difference is not a constant and so the Coulomb Navier criterion of rock fracture does not hold for this rock.

"Brittle-Ductile" Transition

Figure 36 shows the shear fracture strength of Westerly granite and the frictional shear stress for sliding on surfaces with complete interlocking of the asperities as a function of the normal stress across the sliding plane. The two curves cross when the normal stress is about 17.5 kb. This corresponds to a confining pressure of approximately 10 kb. This indicates that at about 10 kb pressure the axial stress required to create a fracture surface in Westerly granite is equal to the axial stress required to cause sliding on the newly created surface and the envelope of the stress strain curves should resemble those obtained with a ductile material. That this is indeed so is illustrated in Figure 28 and 29 which show the stress strain curve for Westerly granite at 6.6 and 10.1 kb confining pressure. Movement on the shear surface took place by stick-slip but it may be possible to eliminate this by increasing the stiffness, damping and mass of the loading system (Rabinowicz, 1965, p. 99). If this is so then the only significant feature is the stress at which movement occurs. It can be seen in Figure 28 that at 6.6 kb,

once non-elastic deformation takes place the strength of the rock is decreased. At 10.1 kb (Figure 29) the strength is independent of the magnitude of the strain. The criteria for ductility used by Handin and Hager (1957), Mogi (1965), Heard (1960) and others is that the material deforms without loss of strength. In Westerly granite this occurs at 10 kb confining pressure if we accept the assumption that stick-slip motion can be eliminated by increasing the stiffness, inertia and damping of the loading system.

It was originally proposed by Orowan (1960) that the apparent ductility of brittle materials may be caused by the frictional strength being equal or greater than the fracture strength and in this work experimental evidence for the validity of the hypothesis has been obtained.

Maurer (1965) also suggested that this may be the reason for the "apparent" ductility of rocks but he did not obtain experimental evidence to support the hypothesis. To metallurgists and mechanical engineers a ductile material is one that deforms by plastic deformation. In the interest of communication between scientific disciplines it is strongly recommended that in rock mechanics ductility of rocks should not be determined by the characteristics of stress-strain curves. The terms should be restricted to mean permanent deformation of the material caused by the propagation of dislocations.

FIGURE CAPTIONS

Figure

34 "Cohesive strength" versus normal stress for Westerly granite

35 Fracture shear strength and frictional shear strength versus normal stress for Westerly granite

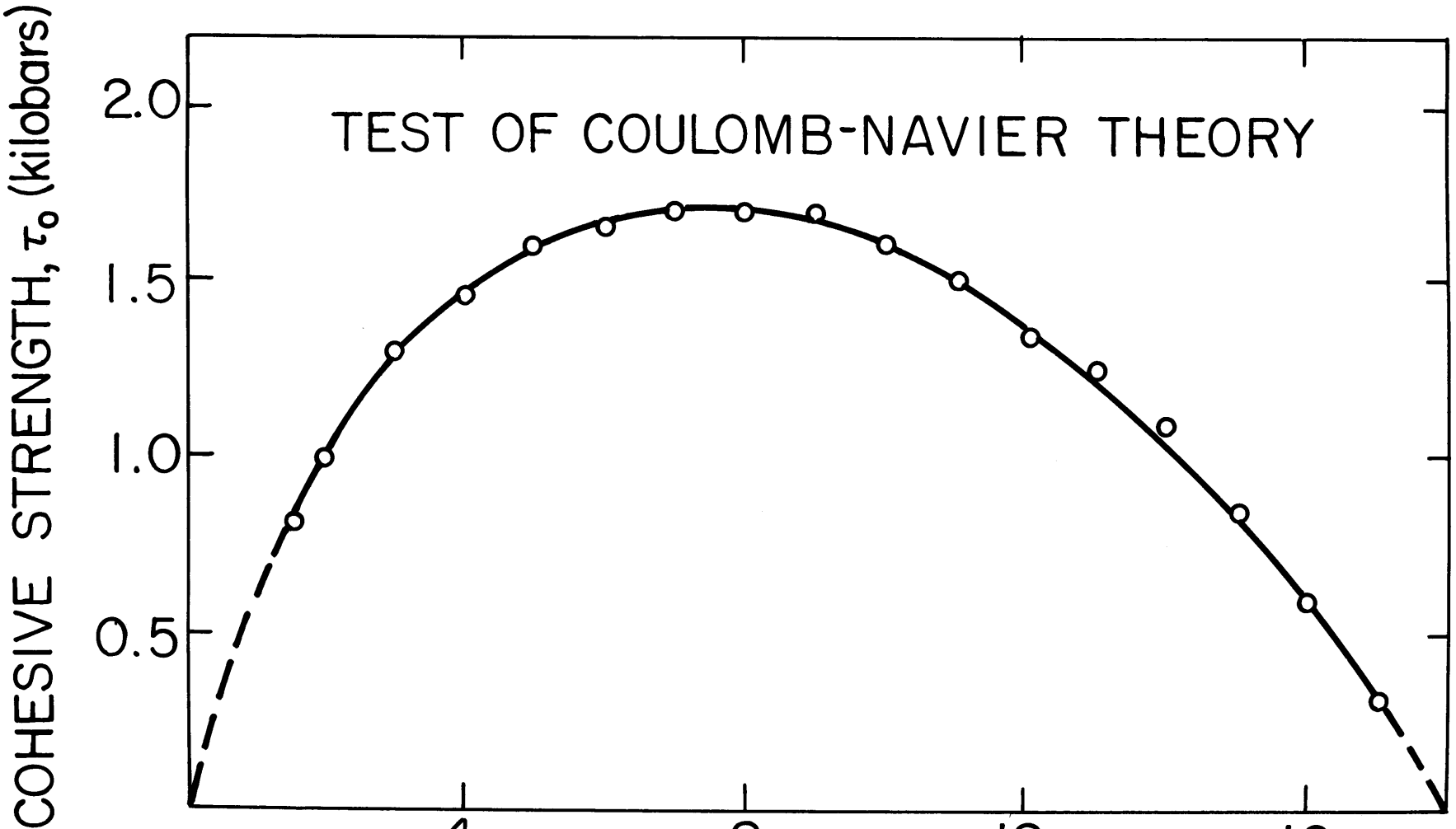
TEST OF COULOMB-NAVIER THEORY
COHESIVE STRENGTH, τ_o (kilobars)
2.0
1.5
1.0
0.5
4
8
12
16
NORMAL STRESS, σ_n (kilobars)

FIG. 35

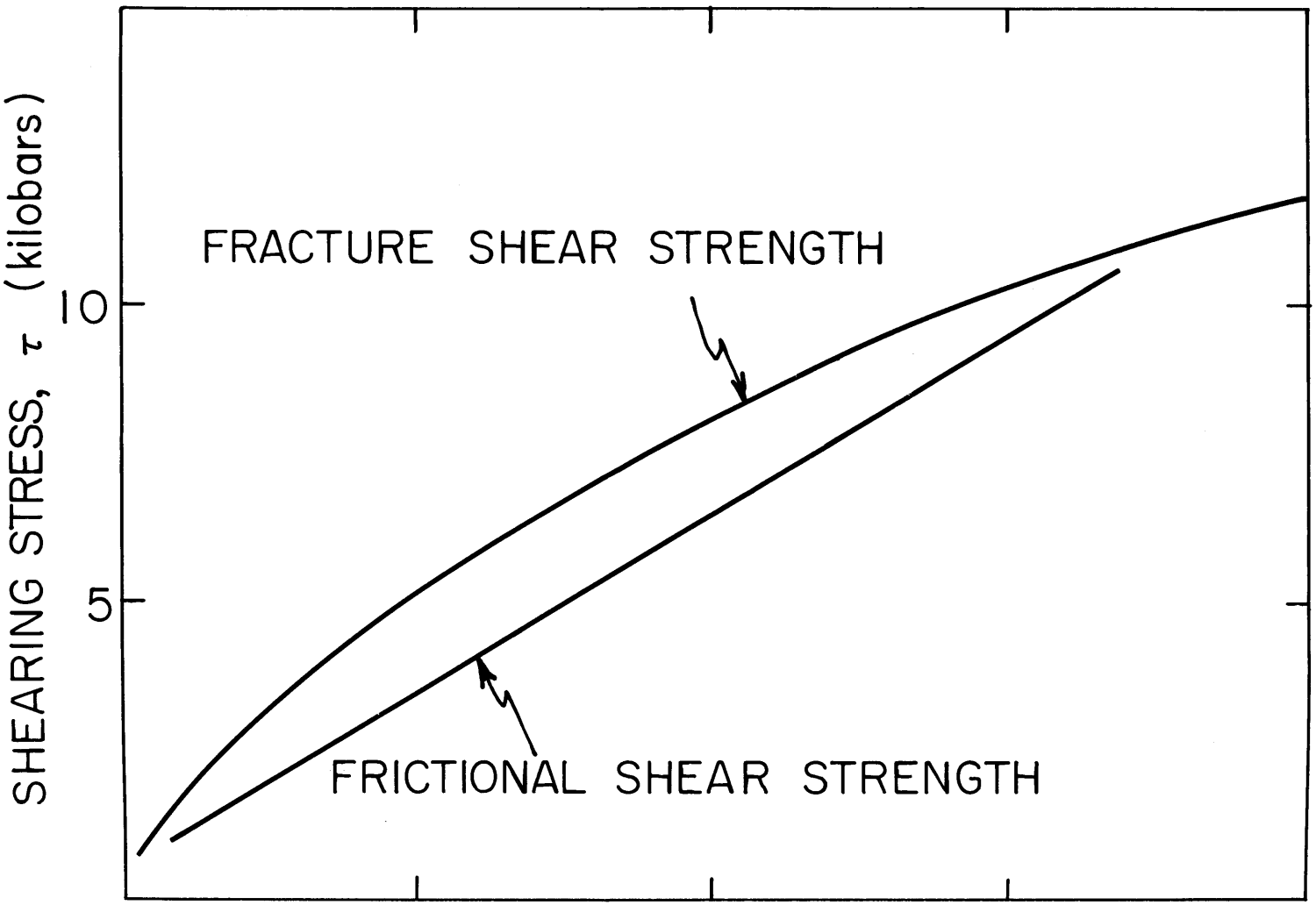
FRACTURE SHEAR STRENGTH
FRICTIONAL SHEAR STRENGTH
SHEARING STRESS, τ (kilobars)
NORMAL STRESS, σn (kilobars)
5
10
15
5
10

FIG. 36

PART V

SUGGESTIONS FOR FURTHER WORK

It has been established that μ is strongly dependent on roughness for Westerly granite and quartz but experiments should be carried out to determine whether this is also true for all the common rock forming minerals. It would also be important to find out if μ for rough surfaces of brittle materials is a function of the strength of the material.

The theory of friction developed here only applies to polished surfaces. But most sliding surfaces of geological interest are rough. Therefore, from a practical standpoint it would be an important contribution if the theory could be extended to include surface roughness.

It has been suggested that water should reduce μ for rocks at high confining pressure. The work of Jaeger (1959) shows that this is correct for gneiss and sandstone. Experiments should be carried out to determine if the reduction in friction is due solely to the reduction in the shear strength of the material.

Magnitude of the stress drops across faults involved in major earthquakes is about 100 bars. In this study the

stress drops during slip of Westerly granite under a confining pressure was found to be 1 kb or greater. It has been suggested that the magnitude of the stress drop during slip is not a property of the material but is a function of the stiffness and damping of the loading system. This possibility should be investigated experimentally.

Granite, although a common rock, may not be typical of the rocks present in active tectonic regions. Experiments should be carried out on peridotite under confining pressure and temperatures typical of the earthquake zones to determine if frictional sliding of this rock also takes place by a stick-slip motion under these conditions.

Limestone, sandstone and shale are common rocks involved in folding and it would be important to determine whether the so-called "brittle-ductile transition" of these rocks is caused by the equality of the fracture and frictional strength.

ACKNOWLEDGEMENTS

These studies were supported by Air Force Cambridge Research Laboratories, Office of Aerospace Research, U.S. Air Force, Bedford, Mass., under contract AF 19(628)-3298.

I am grateful to Mr. F. Gripper for his assistance in the preparation of the specimens and in the construction of the experimental apparatus. I also wish to thank my fellow students who made valuable contributions during discussions of the results.

I wish to thank Professor E. Rabinowicz for his courtesy in making available the Talysurf 4 Profilometer and Dr. P. Gould and Mr. R. J. Bowley who made the roughness measurements.

Special thanks must go to Professor W. F. Brace and Dr. J. B. Walsh who assisted and guided me throughout the research and who were a constant source of encouragement.

I am indebted to my wife Merle for typing and manuscript and also to my family for their patience and understanding.

BIBLIOGRAPHY

Benioff, H., Mechanism of earthquake generation, Geol. Soc. America Bull., 62, p. 1526.

Bowden F.P., Brookes, C.A., and Hanwell, A.E., 1964, Anistropy of friction in crystals, Nature, No. 4940, pp. 27-30.

Bowden, F.P., and Tabor, D., 1942, The theory of metallic friction and the role of shearing and ploughing, Bulletin 145, Comm. of Australia, Council Sci. and Ind. Research.

Bowden, F.P., and Tabor, D., 1958, The friction and lubrication of solids: Oxford, Clarendon Press.

Bowden, F.P., and Tabor, D., 1960, Friction and lubrication, New York, John Wiley.

Bowden, F.P., and Tabor, D., 1964, The friction and lubrication of solids, II, Oxford, Clarendon Press.

Bowden, F.P., and Young, J.E., 1951, Friction of diamond, graphite, and carbon and the influence of surface films, Proc. Roy. Soc., A., 208, pp. 444-455.

Brace, W.F., 1960, Behavior of rock salt, limestone, and anhydrite during indentation, Jour. Geop. Res., 65, No. 6, pp. 1773-1788.

Brace, W.F., 1960, Behavior of quartz during indentation, J. Geology, 71, No. 5, pp. 581-595.

Brace, W.F., 1964, Brittle fracture of rocks: in State of stress in the earth's crust, Ed. W.R. Judd, New York, American Elsevier Pub. Co., pp. 110-178.

Brace, W.F., 1965, Some new measurements on linear compressibility of rocks, Jour. Geop. Res., 70, No. 2, pp. 391-398.

Brace, W.F., Orange, A.S., and Madden, T.R., 1965, The effect of pressure on the electrical resistivity of water-saturated crystalline rocks, Jour. Geop. Res., 70, No. 22, pp. 5669-5678.

Brace, W.F., Paulding, B.W., and Scholz, C., (in press) Dilatency in the fracture of crystalline rocks.

Bridgman, P.W., 1935, Effect of high shearing stress combined with a high hydrostatic pressure, Phys. Rev., 48, pp. 825-847.

Bridgman, P.W., 1936, Shearing phenomenon at high pressure of possible importance to geology, Jour. Geology, 44, pp. 653-669.

Bridgman, P.W., 1937, Shearing phenomena at high pressures, particularly in inorganic compounds, Am. Acad. Arts Sciences Proc., 71, pp. 387-460.

Bridgman, P.W., 1946, Recent work in the field of high pressure, Rev. Modern Phys., 18, pp. 1-93.

Bridgman, P.W., 1952, Studies in large plastic flow and fracture, New York, McGraw-Hill.

Byerly, P., and de Noyer, J., 1958, Energy in earthquakes as computed from geodetic observations, Chapter 2, Contributions in geophysics in honour of Beno Gutenberg, New York, Pergamon Press.

Chinnery, M.A., 1964, The strength of the earth's crust under horizontal shear stress, Jour. Geop. Res., 49 No. 10, pp. 2085-2089.

Colback, P.S.B., and Wiid, B.L., 1965, The influence of moisture content and the compressive strength of rock, Third Canadian Symposium on Rock Mechanics, Toronto.

Crandall, S.H., and Dahl, N.C., 1959, An introduction to the mechanics of solids, New York, McGraw-Hill.

Fairbairn, H.W., et. al., 1951, A cooperative investigation of precision and accuracy in chemical, spectrochemical and modal analysis of silicate rocks, U.S. Geol. Survey Bull. 980, p. 71.

Flom, D.G., 1964, Discussion, A.S.L.E. Transactions, 7, pp. 106-107.

Frank, F.C., 1966, On dilatancy in relation to seismic sources, Reviews of Geophys., 3, No. 4, pp. 485-503.

Griggs, D., and Handin, J., 1960, Observations on fracture and a hybothesis of earthquakes, Geol. Soc. Am. Mem. 79, pp. 347-364.

Griggs, D.T., Turner, F.J., and Heard, H.C., 1960, Deformation of rocks at 500° to 800° C, Geol. Soc. Am. Mem., 79, pp. 39-104.

Handin, J., and Hager, R.V., 1957, Experimental deformation of sedimentary rocks under confining pressure: tests at room temperature on dry samples, Bull. A.A.P.G., 41, p. 1.

Handin, J., and Stearns, D.W., 1964, Sliding friction of rock, Trans. Am. Geophys. Union, 45, p. 103.

Heard, H.C., 1960, Transition from brittle to ductile flow in solenhofen limestone as a function of temperature, confining pressure, and interstitial fluid pressure, Bull. Geol. Soc. Am., 89, pp. 193-226.

Horn, H.M., and Deere, D.U., 1962, Frictional characteristics of minerals, Geotechnique, 12, pp. 319-335.

Jaeger, J.C., 1959, The frictional properties of joints in rocks, Geofisica pure e applicata, 43, pp. 148-158.

Jaeger, J.C., 1962, Elasticity, fracture and flow, London, Methuen.

Lubkin, J.L., 1962, Contact problems, Chapter 42, in Handbook of Engineering Mechanics. Ed. by W. Flugge, New York, McGraw-Hill.

Marsh, P.M., 1964a, Plastic flow and fracture in glass, Proc. Roy. Soc. A., 282, pp. 33-43.

Marsh, D.M., 1964b, Plastic flow in glass, Proc. Roy. Soc. A., 279, pp. 420-435.

Maurer, W.C., 1965, Shear failure of rock under compression, Soc. Pet. Eng. Jour., 5, pp. 167-175.

McClintock, F.A., and Walsh, J.B., 1962, Friction on Griffith cracks in rocks under pressure, Proc. 4th Nat. Cong. Appl. Mech., pp. 1015-1021.

Michell, J.H., 1900, Some elementary distributions of stress in three dimensions, London Math. Soc. Proc., 32, pp. 23-35.

Mogi, K., 1965, Deformation and fracture of rocks under confining pressure (2) elasticity and plasticity of some rocks, Bull. Earthq. Res. Inst., 43, pp. 349-379.

Mogi, K., (in press) Some precise measurements of fracture strength of rocks under uniform compressive stress.

Mügge, O., 1898, Über translation U.S.W. Neues. Jahrb., 1. p. 71.

Norwegian Geotechnical Institute, 1959, Friction tests, Interim Report, 11 pp.

Orowan, E., 1960, Mechanism of seismic faulting, Geol. Soc. Am. Mem. 79, pp. 232-345

Orowan, E., 1965, Physics of the seismic source, Boeing Scientific Research Laboratories, Seattle, Washington.

Paterson, M.S., 1964, Effect of pressure on Young's modulus and the glass transition in rubbers, Jour. App., Phys., 35, No. 1, pp. 176-179.

Paulding, B.W., 1965, Crack growth during brittle fracture in compression, Ph.D. Thesis, M.I.T.

Penman, A.D.M., 1953, Shear characteristics of a saturated silt, measured in triaxial compression, Geotechnique, 3, pp. 312-328.

Rabinowicz, E., 1959, A study of the stick-slip process in Friction and wear, Ed. by Robert Davies, New York Elsevier Publishing Co.

Rabinowicz, E., 1965, Friction and wear of materials, New York, John Wiley.

Rae, D., 1963, The measurements of the coefficient of friction of some rocks during continuous rubbing, J. Sci. Instrum., 40, pp. 438-440.

Raleigh, C.B., and Paterson, M.S., 1965, Experimental deformation of serpentinite and its tectonic implication, Jour. Geop. Res., 70, No. 16, pp. 3965-3985.

Reid, H.F., et.al., 1908, Report, State Earthquake Institution Commission, The California earthquake of April 18th, 1906, Carnegie Institute of Washington.

Reid, H.F., 1933, The mechanics of earthquakes, in Physics of the Earth, Washington, National Research Council, pp. 87-103.

Riesz, C.H., and Weber, H.S., 1964, Friction and wear of sapphire, Wear, 7, pp. 67-81.

Seal, M., 1958, The abrasion of diamond, Proc. Roy. Soc. (London) A 248, pp. 379-393.

Smith, H.I., and Gussenhoven, M.S., 1965, Adhesion of polished quartz crystals under ultra high vacuum, Jour. App., Phys. 36 No. 7, pp. 2327-2328.

Timoshenko, S., and Goodier, J.N., 1951, Theory of elasticity, New York, McGraw-Hill.

Tschebotarioff, G.P., and Welch, J.D., 1948, Lateral earth pressures and friction between soil minerals, Proc. 2nd. Int. Conf. Soil Mech. and Fdn. Eng., 7, pp. 135-138.

Walsh, J.B., 1965a, The effect of cracks on the uniaxial elastic compression of rocks, Jour. Geop. Res., 70, No. 2, pp. 399-411.

Walsh, J.B., 1965b, The effect of cracks in rocks on Poisson's ratio, Jour. Geop. Res., 70, No. 20, pp. 5249-5257.

Walsh, J.B., 1966, Seismic wave attenuation in rock due to friction (in press).

BIOGRAPHY OF THE AUTHOR

Name: James Douglas Byerlee

Born: August 12, 1927, Cairns, Queensland, Australia.

Education:

Secondary Education: Evening Tutorial, Brisbane, Q'ld.

Feb. 1958 to Nov. 1962: University of Queensland

Feb. 1963 to present: Massachusetts Institute of Technology

Received the degree of Bachelor of Science (Hons. Geol.) from the Queensland University in June, 1963.

Unpublished Reports

"A Geophysical and Geological Study of Part of the Kilkivan District, South East Queensland," University of Queensland Honours Thesis.

"Report of a Magnetic Survey over the Mt. Biggenden Magnetite Deposit," Written in conjunction with Dr. J. P. Webb for David Leitch and Associates, Gympie, Queensland, Australia.

"Report of a Magnetic Survey over a Magnetite Deposit south of Mt. Biggenden," written in conjunction with Dr. J. P. Webb for Bonell Brothers, Maryborough, Queensland.

Professional Experience:

In addition to research and teaching assistantships at M.I.T., the author's experience includes the following:

Nov. 1959-Feb. 1960: Field Geologist with Mt. Isa Mines, Queensland. Mapping in the Mt. Isa district.

Nov. 1960-Feb. 1961: Conorada Exploration Co. Queensland. Geologist, contour mapping of the base of the marine cretaceous in Queensland from Artesian bore logs.

Feb. 1961-Nov. 1962: Teaching Fellow, University of Queensland.

In December, 1954 I married Merle A.F. Pittendreigh and now have three children:

David James	born	19th March, 1956
Ian Bruce	born	30th May, 1957
Madonna Ann-Marie	born	13th September, 1961.